THREE-DIMENSIONAL VORTICITY-INDUCED FLOW EFFECTS IN HIGHLY-LOADED AXIAL COMPRESSORS

by

C. S. Tan

GT&PDL Report No. 131 January, 1980

GAS TURBINE & PLASMA DYNAMICS LABORATORY
MASSACHUSETTS INSTITUTE OF TECHNOLOGY
CAMBRIDGE, MASSACHUSETTS

THREE-DIMENSIONAL VORTICITY-INDUCED FLOW EFFECTS IN HIGHLY-LOADED AXIAL COMPRESSORS

by

C. S. Tan

GT&PDL Report No. 131 January, 1980

This work, carried out in the Gas Turbine and Plasma Dynamics Laboratory, was supported by AFOSR Contract F49620-78-C-0084.

PART I - "THREE-DIMENSIONAL VORTICITY-INDUCED FLOW EFFECTS IN HIGHLY-LOADED AXIAL COMPRESSORS"
GT&PDL REPORT NUMBER 141

PART II - "ASYMMETRIC INLET FLOWS THROUGH AXIAL COMPRESSORS"
GT&PDL REPORT NUMBER 151

ABSTRACT

A new analytical method is proposed for the study of flow through highly-loaded turbomachine stages. The technique is used in the present study in order to: (i) analyze the three-dimensional induced effects of the viscous blade wakes in an isolated rotor; and (ii) to study the effects of the passage of distorted flow through an axial compressor rotor or stator. In Part I (GT&PDL Report Number 141), it is found, in contrast with the more familiar situation behind aircraft wings, that the induced effects of the vorticity in the (viscous) wakes are important in practical axial turbomachinery; for example, the flow angles through highly-loaded rotors are modified to a significant extent by such wake effects. The induced disturbances grow in strength within a certain distance downstream of the blade row before beginning to decay inversely with such axial distance. In agreement with earlier predictions, pressure disturbances and vorticity disturbances cannot be decoupled in swirling flow. Similarly, in part II (GT&PDL Report Number 151), it is found that major differences arise on comparing two-dimensional with three-dimensional analyses, both for rectilinear and for annular configurations. Further, only the last of these three-dimensional analyses can adequately describe the true flow phenomena in highly-loaded turbomachines. This is because such a description properly includes both centrifugal effects together with two important distinct types of vorticity: the trailing vorticity and the vorticity associated with any stagnation pressure gradients present. Such an analysis predicts, a strongly persisting downstream pressure field which in many cases increases before again beginning to decay inversely with the axial distance downstream, both for free-vortex stators and rotors. By contrast, three-dimensional wheel flow analysis predicts indefinitely persisting downstream disturbances. Further, a purely two-dimensional theory indicates for a stator, the downstream static pressure to be uniform, while even a three-dimensional rectilinear cascade theory would predict only an exponentially decaying pressure field. The amplitude of the above persistent downstream disturbances decreases for free-vortex downstream flow as the number of significant circumferential harmonics of the inlet distortion increases. These analytical results agree well with available experimental data recently obtained in annular cascades.

ACKNOWLEDGEMENTS

It has been very fortunate and a great privilege for the author to have had the opportunity to carry out the research described in this thesis under Professor James E. McCune, the Chairman of the author's Doctoral Committee, and Professor Sir William R. Hawthorne, Master of Churchill College, Cambridge University, whose stimulating questions have helped the author to further understand flows in turbomachinery. Hardly any paragraph in this thesis can the author claim to be entirely his; any valuable idea in this thesis is a result of the constant discussion with them and their critical comments. In addition, their advice, their constant encouragement, and personal warmth have made the author's association with them over the past two years a very special and memorable one.

Further he would also like to express his sincere gratitude to:

Professor Sir William R. Hawthorne for making arrangements for the author to be at Cambridge University on three occasions, and for making it possible for the author to have fruitful and useful discussions on distorted inlet flows with Mr. N. A. Mitchell of Cambridge University.

Professor James E. McCune, among other things, for editing the major portion of the thesis with patience and meticulosity.

Professor Jack L. Kerrebrock for his thoughtful and critical comments and for the valuable discussions with him.

Professor E. M. Greitzer for making available the experimental data on distorted flow through annular cascades, and for the elucidating discussions on flow through turbomachines.

Professor M. Finston for the useful discussions.

Professor T. H. Dupree for being on the author's Doctoral Committee.

Gayle Ivey for her constant availability and help when needed.

Holly Rathbun for accepting the tedious task of typing this thesis.

Mr. W. K. Cheng for permitting me to use the subroutines he developed for generating Bessel Functions of high orders.

Throughout his Doctoral Study, the author is supported by a Research Assistanship made available through the Gas Turbine and Plasma Dynamics Laboratory which, besides providing competent scientific and technical education, has an internationally cosmopolitan atmosphere. Undoubtedly, in the course of pursuing scientific and technical knowledge, students from many lands, besides interacting academically, have also interacted culturally; this in itself is an invaluable education.

Finally, the author dedicates this thesis to his beloved Father and his late beloved Mother who, in spite of their illiteracy, insisted on his acquiring a higher education.

TABLE OF CONTENTS

TABLE OF CONTENTS (CONTINUED)

TABLE OF CONTENTS (CONTINUED)

TABLE OF CONTENTS (CONTINUED)

OVERALL SUMMARY

An analytical technique, based in part on the Clebsch-Hawthorne formulation, is proposed for use in the predictions of the nature of steady flows through axial turbomachines. Essentially, the method describes the internal aerodynamics of the flow in such machines in terms of any vorticity field present or, as in the case of non-homentropic flow, the reduced vorticity field. The usefulness and simplicity of this approach emerges especially clearly in the particular case of three-dimensional flows, although two-dimensional flows can be similarly analyzed. The basic formulation is exact, but realistic simplifying assumptions are made to keep the problem tractable as well as practical. For example, three-dimensional aspects of the flow resulting from the finite number of blades or inlet maldistribution are treated as perturbations about the mean streamlines derived exactly from the available (non-linear) axisymmetric throughflow-treatments.

In Part I, the proposed method is used to analyze the three-dimensional induced effects of the viscous wakes flowing downstream from the blades on an isolated rotor (or stator) producing free-vortex mean downstream flows encased in an infinite cylindrical annulus. This swirling downstream flow field is then pictured as being threaded with vortex filaments representing the blade-wakes. Because the vorticity field can be related to the variation of the thermodynamical properties of the fluid, the presence of such viscous wakes necessarily implies a variation of entropy from streamline to streamline, or, in the incompressible limit, a corresponding variation of stagnation pressure. Linearization of the analysis is achieved by expanding about an axisymmetric throughflow;

free-vortex mean flow is assumed in the example in Part I. In contrast to external aerodynamics about wings, the blade wakes so described modify the flow angles through highly-loaded rotors significantly. This is in agreement with earlier predictions that pressure disturbances, vorticity disturbances, and entropy disturbances cannot be decoupled in compressible swirling flows.

In Part II, this technique is further applied to analyze the passage of distorted flow through an axial compressor rotor or stator. In this portion of the work, the actuator-disc limit is taken; this concept is introduced in order to suppress the individual identity of the blades. Thus the description of the flow can be taken as steady in absolute coordinates. The flow field is again pictured as being threaded with vortex filaments; in this case the vorticity is either introduced far upstream or can be considered to spring from the solid surfaces of the blades represented by the disc. The resulting linearized analysis yields an overall description of the blade row performance in the presence of inlet flow distortions. It is found that major differences arise on comparing two-dimensional with three-dimensional analyses, both for rectilinear and for annular configurations. In fact, only the last analysis can adequately describe the flow phenomena in highly-loaded turbomachines, because it includes the centrifugal effects together with two important distinct types of vorticity. One of these is the trailing vorticity associated with any spanwise variation of blade loading which may result; the other is associated directly with the inlet distortion. The latter vorticity develops a streamwise component as it swirls downstream, becoming superimposed on any shed circulation already present. This

produces important three-dimensional effects for practical loading. The result again demonstrates that pressure disturbances and vorticity disturbances are not separable in swirling flow. The results are compared successfully not only with earlier three-dimensional analyses but also with recent experimental data.

INTRODUCTION

Axial-flow compressors are the principal type of compressor used in aircraft gas-turbine power plants, primarily because of their unique match with many of the basic requirements of aircraft power-plants. For example, such requirements include high efficiency, high-air-flow rate per unit frontal area and high pressure ratio per stage. In addition, an aircraft engine must be as compact as possible. Engineers in this field attempt to design compressors which meet as many of these basic requirements as possible. In the process, the designer hopes to use a scheme which is accurate enough so that the cost and time involved in the development of the device can be minimized. In any case, the design of an axial-flow compressor ultimately requires the most accurate available calculation of the flow through such compressor blade-rows.

Flow through the blading of an axial-compressor is extremely complex, beginning with the fact that it is inherently three-dimensional in nature. Moreover, not only does the flow have gradients in the axial, radial and circumferential directions, it is time dependent as well. In addition, viscous effects must be taken into consideration in practical compressor studies. Thus, the complete governing equations of fluid flow through turbomachines have not yet been solved. In particular, strictly numerical efforts to represent the flow through the flow passages formed by the blades, the hub, and the casing (especially in the full three-dimensional case) are still in a rapidly developing stage. One thus sees that the fluid mechanical problem in axial compressors continues to present an extremely challenging problem in the field of applied fluid mechanics,

both theoretically and experimentally.

In an effort to provide an increasingly effective basis for designing and understanding axial compressors, research in this field has been quite extensive. Even so, there remains a formidable gap between the information predictable on purely theoretical grounds and that required for the actual production of an efficient, practical machine of this type. In an attempt to close this gap, various empirical techniques have been devised that combine comparatively simplified theories with available experimental data. Even the use of these empirical techniques, however, often requires a considerable investment of time and effort. Often, for developmental purposes, whole series of costly tests requiring continued trial and error become necessary. Consequently, there remains strong motivation for the search for increasingly efficient and accurate ways of predicting the fluid behavior within a "turbomachine"*. In the process continued experimental studies are crucial in establishing improved understanding of the fluid behavior within a turbomachine.

As a comparison, workers studying the air flow past an isolated wing are often faced with a somewhat easier task compared with those involved in the analysis of internal flows of the type just described. Even though the primary problem of both can be described in terms of the determination of the velocity arising at an arbitrary point on an airfoil surface by the overall flow fields (pressure, vorticity, ...) associated with all other confining surfaces present, the geometrical complexity in turbomachines is frequently more difficult. Further, unlike incoming flow over an isolated

---

* In the following, "turbomachine" will be used to refer to the axial type, unless stated otherwise.

wing, the flow in many regions of a turbomachine is necessarily swirling in nature. As already mentioned, an important consequence is that the behavior of the working fluid can be modified considerably. Furthermore, the actual flow through a rotor is always unsteady with respect to uniform flow in a stator, and vice versa. That is, for example, circumferential variations (for instance, those brought about by rotor blade wakes), even though time-independent with respect to the rotor, will inevitably give rise to unsteady flow in the preceding and succeeding stators. Because of the arrangement of blade rows, a stator or a rotor almost always encounters a stream of wakes which have left their generating surfaces only a short distance ahead. An analogous situation is not usually the case for an isolated aircraft wing flying through the free air. In addition to the above complexities, inlet distortions involving variations in both the stagnation pressure and stagnation temperature arise; frequently the phenomena of rotating stall and surge occur as well in axial compressors under certain operating conditions.

The drive towards a compact and light weight design of an engine for aircraft application has resulted in an increase of stage pressure ratio and high mass flow rate per unit frontal area. This certainly requires that each element of the turbomachine be operating near its aerodynamic limit. Therefore, the compressor blades must tolerate large relative Mach numbers so that high mass flow rate and high relative speeds can be achieved. Investigations on free-vortex rotors have indicated the feasibility of obtaining high efficiency from rotors in which the Mach numbers at the tips are as high as 1.35, while those near the hub remain subsonic (transonic rotors). Because the flow is supersonic relative to the rotor

near the tip, the complexity of the flow has further been increased by the presence of shock waves (which lead to shock-wave boundary-layer interaction) in the blade passage. In the transonic regime, the working fluid has to be considered as compressible. This implies, from a mathematical point of view, that the aerodynamic and the thermodynamic equations which govern the fluid flow are strongly coupled and highly non-linear. Very often, no known exact non-trivial solution exists and a linearized perturbation technique is used to obtain solutions.

The work described in Part I deals only with one aspect of the fluid flow through a blade row encased in an infinite cylindrical annulus; namely, the three-dimensional behavior of the viscous blade wakes in the downstream swirling flow and their effect on the performance of the blade row. It is hoped that this work can in someway aid in the eventual closing of the "gap" mentioned earlier.

In Part II, an analytical investigation regarding the three-dimensional aspects of asymmetric inlet flows on the performance of turbomachines is presented; its results are compared with those of two-dimensional theory and three-dimensional theory neglecting the centrifugal effects (i.e., distorted flows through rectilinear cascades) to show the important differences. The theoretical predictions are compared with a set of available experimental data. The performance of axial compressors operating under distorted inlet flows has been widely studied because of the effect of inlet flow distortion on compressor stall, mechanical reliability and efficiency.

The theoretical work is considered entirely from the point of view of the fluid flow through the blade row. Both the incompressible flow

and the compressible flow (except for the inlet distortion problem) are considered but the working fluid is assumed to be inviscid outside the blading. The equations of motion for the flow of a real fluid in an axial flow compressor are nonlinear three-dimensioned equations. Accordingly, realistic simplifying assumptions are made so that fruitful and tractable analysis is possible. For instance, linearizing approximations are introduced to keep the mathematical problems tractable. Such procedures are necessarily conditional upon obtaining physically valid flow descriptions even though the problem may remain very complex. Since solutions of aerothermodynamic equations for the flow with small deviation from free-vortex motion often provide a useful basis for turbomachine design (even though compressors have for some time been designed on other bases), attention is focused here on obtaining solutions for nearly free-vortex motion. Extension to more general mean flows is feasible and underway in a separate study.

PART I

VORTICITY MODELLING OF BLADE WAKES IN TURBOMACHINERY

CHAPTER 1 - SURVEY OF PREVIOUS WORKS; OUTLINE OF THE PRESENT STUDY

1.1 Previous Works

Many theoretical investigations of varying degrees of precision have been made over the past several years regarding the behavior of fluid flow in axial turbomachinery. The difficulties in obtaining solutions from the equations of fluid motion which describe the full three-dimensional flow pattern have required most workers in the field to seek a simpler, less general, but still physically adequate description of the flow. This search has led to the development of several classes of simplified theories; here they are classified according to the essential assumptions on which they are based.

One of these is the so-called two-dimensional strip-theory, which ignores the aerodynamic interference between different radii along the blading; this implies that the flow field at each radius can be considered as virtually the same as that through a two-dimensional cascade.

Another useful approach is that of radial equilibrium theory[1], which assumes that the radial movement of the fluid particles occurs only on passage through the blades and not in the spaces between the blade rows. Experimental investigations have shown that this is frequently not a sufficiently accurate description. Since radial equilibrium theory does not permit any change of velocity distribution in the immediate neighborhood of the blades, one is led to alternative analyses.

Among these alternative analyses are those which treat three-dimensional effects on a circumferentially-averaged or axi-symmetric flow basis[1]. Phsycially, this implies that the blade-row is made up

essentially of an infinite number of infinitesimally thin blades, the chordwise loading of which may be given but must be averaged circumferentially. Further "actuator-disc" theories assume that the blade row can be thought of as having been shrunk axially into a discontinuity, and the flow deflection achieved in an infinitesimal axial distance. This assumption of axial symmetry, also implies that the trailing vortex field is similarly circumferentially uniform and not (as is actually the case) in the form of discrete wakes. Thus, axially-symmetric "throughflow theories" provide the incoming stream direction, and its magnitude, over the blade span. With this information an appropriate blade form may be designed; in this process it is often assumed that the flow about the blade at one radius does not interfere with the flow about the blade at another radius (analogous with strip-theory). Hence, this class of theories not only neglects the circumferential non-uniformities, but also assumes quasi-two-dimensionality at each radius (in that the relation between the cascade geometry and aerodynamic parameters such as lift and turning angles are taken from cascade data and correlation analyses).

The mathematical difficulties involved in the inclusive treatment of the true three-dimensional effects (including discreteness of the actual blading and their wakes) has led many researchers to analyze exclusively some particular aspects of three-dimensional flow effects. These analyses include the so-called secondary flow theories and various shear-flow theories[2,3,4,5]. Some of these studies have been quite successful in describing and predicting certain three-dimensional flow phenomenon due to spanwise non-uniformites in incoming stagnation pressure (or axial velocity), spanwse variation of blade loading[2] and finite blade spacing[3].

However, most of these theories are based on a rectilinear cascade model and have not previously been modified for application in an actual annular cascade situation.

The discrepancies observed between the actual flows in axial turbomachines and those predicted by the above simplified theoretical models increase in magnitude with the existing trend toward more compact and efficient compressors. Consequently, relaxation of some of these simplifying assumptions is necessary, in spite of the resulting increase in analytical complexity, in order to improve the accuracy of flow predictions.

Wu[6] developed a "three-dimensional", inviscid, compressible flow theory for subsonic and supersonic turbomachines with finite numbers of blades of finite thickness. His theory is applicable to axial-, radial-, or mixed-flow turbomachines for both the direct and inverse problems. However, the computational method of his theory, which consists essentially of an iterative solution for the flows on two intersecting families of stream surfaces, seems to be relatively demanding in terms of actual analysis. Furthermore, Wu's approach suffers from considerable difficulty in making clear the essential physical features of the flow.

The relaxation of the assumption of axial symmetry requires the replacing of actuator disc model cascades of blades with infinitesimal spacing by blade rows with finite spacing. The first consequence of this, of course, is that the flow can no longer be considered as circumferentially uniform and with this fact a marked increase in mathematical difficulty arises. Physically one expects that the fact the trailing vorticity is concentrated in the discrete blade wakes would become

significant for practical as well as for large spanwise variation of blade loadings. The resulting class of new three-dimensional theories has adopted a concept of small perturbation about exact (non-linear) axisymmetric throughflow theories. One of the earlies theories of this type (which, however, did not use exact axisymmetric throughflow theories as the base flow) was that developed by McCune[7,8] for non-lifting rotors in the subsonic, transonic, and supersonic regimes. The blades were assumed to be thin so that only weak disturbances are induced in the oncoming flow. That theory establishes the validity of applying two-dimensional strip theory and cascade data to the design of three-dimensional rotors and stators in the purely subsonic and supersonic regimes; however, for transonic rotors, McCune's theory indicates that the aerodynamic interference between different radii is indeed so large that the cascade theory may no longer be applicable.

Davidson[9] derived the velocity potential for rotating lifting-spokes and attempted to describe the subsonic, transonic and supersonic flows through a rotating propeller in a cylindrical duct. Okuroumu and McCune[10] developed a linearized three-dimensional theory for a lifting transonic rotor which induces slight turning of the flow and low pressure ratios using a velocity potential similar to Davidson. In all these cases, the trailing vorticity emanating from each blade was assumed to be convected by the unperturbed flow. Again, it was found that this theory for transonic rotor did not correspond to the cascade theory. This lifting line theory still retains some elements of the assumption of local two-dimensionality regarding the blade geometry and the lift force at each radius, due to the use of lifting line concept. Because of this, its use for a

transonic rotor becomes limited due to the strong three-dimensional effects already mentioned. In consequence, Okuroumu and McCune[11,12] developed a linearized lifting surface theory for a lifting rotor in the subsonic and transonic regimes by an appropriate chordwise distribution of lifting lines. Okuroumu's and McCune's theories[10,11,12] are limited to the design problem. To eliminate this limitation, a Prandtl-type of lifting line theory was developed by McCune and Dharwadkar[13] for subsonic lifting rotors, permitting treatment of both the "design" and "off-design" problems; it is also shown there that whenever there is a spanwise variation of loading, solution is obtainable only if the spanwise derivative of the loading vanishes at the hub and the tip. This is also in agreement with Falc̃ao's result[14].

Namba[15] developed a lifting surface theory for axial compressor blades. The theory treats the design and off-design problems, even in the transonic regimes. He also emphasized the conclusion that cascade theory is only questionally applicable in the transonic regime.

The above class of three-dimensional theories only admits treatment of very weak disturbance of the far upstream flow; consequently, it is restricted to the case of lightly-loaded rotors, a fact which restricts their usefulness in practical compressor design.

Quite recently, a relaxation of this limitation has been made. McCune and Hawthorne[16] have developed a "quasi-linear" theory for the three-dimensional inviscid flow through a highly-loaded turbomachinery cascade of lifting lines using a rectilinear model; this would correspond to flow through practical rotors which induce large turning angles and large pressure ratio. Analysis is limited to the case of incompressible

flow, and to the case for which the spanwise variation of blade loading is small. Morton[17] extended the analysis for this model to compressible flow. The resulting trailing vorticity, being concentrated in the discrete blade wakes and the induced disturbances are convected by the mean flow. Cheng[18] further extended their analysis to incompressible flow through a highly loaded annular cascade which induces a nearly free vortex flow in the mean downstream of the blade row. More recently, Adebayo and McCune[19] have developed a theory which removes the limitation of small variation in spanwise blade-loading; there the parameter, the inverse of the blade number, must be small. Recently, Cheng[20] has extended his annular analysis to the case of a transonic rotor.

This latest class of three-dimensional theories removes the restriction of small disturbance in the incoming flow of the earlier theories; but it is limited to the so-called Beltrami flows in which the trailing vorticity is in alignment with the mean streamlines. Furthermore, the flow field is assumed to be inviscid and homentropic throughout, i.e., the flow is irrotational except in the discrete blade wakes. Therefore, it does not include any of the real flow effects, specifically, the circumferential non-uniformity resulting from the effects of losses at the blades. These losses are usually a result of viscous interaction between the working fluid and the solid surfaces in the thin boundary layers over the blade surfaces; another source of such losses could be due to shock-wave boundary layer interaction in transonic rotors. Exclusion of such "boundary-layer" wake effects, which can dominate† the three-dimensional effects in turbomachines, in some regimes, may lead to an erroneous estimate of local flow angles at and near the blades.

Recently, Kerrebrock[21] has examined the general problem of the behavior of small disturbances in a strongly swirling compressible flow. He showed that pressure disturbances can originate from any of a number of disturbances such as vorticity and entropy disturbances.

1.2 Present Study

In the work described here, an attempt is made to construct an analytical model to consider the effects of the "boundary-layer" wakes on the performance of blades in practical turbomachinery. As such, it attempts to provide a necessary generalization of the works cited above in References 16 to 20. As in an isolated airfoil, in consequence of the action of viscosity, vortices with axes parallel to the direction of the span are produced continuously in the boundary layers on both sides of the blades. At the termination of the boundary layers (close to the trailing egde of the blade unless large scale separation occurs beforehand), these spanwise vorticies become free and are carried along by the general motion of the fluid, forming what will be termed here vortical viscous wakes or, "blade-wakes". It is well known that in non-steady motion, another class of spanwise vorticies, related to the rate of change of circulation on the blade, appears in the wake. Under steady motion, which we will be mainly concerned with here, this class of spanwise vortices can be neglected; consequently the vortex strength at the trailing edge must vanish in order to satisfy the Kutta condition of the continuity of pressure at the trailing edge. By Kelvin's theorm, of course, the net rate of vorticity flux from boundary layers on either side of the blades into the wake must be zero (even though blades in turbomachinery which induce flow angles of practical interest generate thicker boundary layer on the suction side

than on the pressure side). In the external aerodynamics of an isolated airfoil, only the spanwise vorticity resulting from the rate of change of circulation in unsteady motion together with any possible shed circulation[16-20] are of importance, while those originating from the boundary layers on the airfoil surfaces are of relatively small significance. Such a conclusion cannot be carried over into the internal aerodynamics of the axial turbomachinery; this is in fact one of the consequences of Kerrebrock's analysis[21]. Indeed, the two may be of equal significance. This is a result of the fact that the corresponding inertia force field, set up by the highly swirling flow through turbomachines, can significantly modify the behavior of such wakes. As already emphasized, such modifications of wake behavior can bring about a significant change of flow angle at the blades.

In the analytical model that is to be developed here, the effects of losses within the blade row are included through the variation of entropy across the stream surfaces as obtained directly from available data. Hence, the presence of the blade-wakes makes the flow field downstream of the blade row non-homentropic. For the range of Reynold numbers encountered in flow through turbomachines, departure of flow-field from complete homentropy is small. Consequently, the small disturbance of the flow introduced by this departure from complete homentropy can again be described in terms of a linearized perturbation analysis about the axisymmetric throughflow (as in References 16 to 20). Furthermore, the present analysis is confined to the case of blade row which induces a free-vortex flow in the mean, although this restriction can be relaxed[19]. It is argued that the formulation can properly neglect the viscous forces

away from the blades; i.e., it can neglect the resulting diffusion of the wakes in the downstream flow field.

When compressibility effects are negligible, the viscous interaction between the working fluid and the blade surfaces may be considered to result in a loss of stagnation pressure. Consequently, the blade wakes may be considered to be regions of low stagnation pressure.

In essence, the strategy used in the present formulation involves the description of the internal aerodynamics of the turbomachines in terms of an appropriate vorticity field. Once this is done, the resulting flow will simply take care of itself.

† In many cases Beltrami effects and those discussed in this page 23 are actually competitive in practical machines.

CHAPTER 2 - THE BASIC EQUATIONS GOVERNING INCOMPRESSIBLE FLUID FLOW

2.1 Forms of Equations of Motion

The appropriate forms of the equations governing fluid flow are dependent upon the kind of assumptions made in the course of practical analysis. Three-dimensional flow of a non viscous, incompressible fluid through a turbomachine is governed by the following set of basic laws of fluid flow. We start with the case of flow through a blade row rotating at a constant angular velocity, ω, about its own axis. The coordinate system used is a right-handed cylindrical one, (r,θ,z) as shown in Fig. 1a; in this system, the axis of a turbomachine coincides with the z-axis. From the principle of conservation of matter, the equation of continuity is

$$\nabla \cdot \underset{\sim}{W} = 0, \tag{2.1}$$

where $\underset{\sim}{W}$ is the velocity of the fluid relative to the blades.

Newton's second law of motion gives, for a rotating fluid

$$\frac{D\underset{\sim}{W}}{Dt} - \omega^2 \underset{\sim}{r} + 2\underset{\sim}{\omega} \times \underset{\sim}{W} = -\frac{1}{\rho}\nabla p \quad , \tag{2.2}$$

where ρ is the density of the working fluid, p is the static pressure, and the operator D/Dt refers to differentiation with respect to time following the relative motion of each fluid particle. We note at this point that the boundary walls in an axial turbomachine are generally surfaces of revolution and the relative flow may in many cases be approximated as being steady. Therefore it is convenient here to use a relative cylindrical coordinate system (r,θ,z) with θ measured with respect to the rotating

blade (Fig. 1b). By the use of the identity

$$\frac{D\underset{\sim}{W}}{Dt} = \frac{\partial \underset{\sim}{W}}{\partial t} + (\underset{\sim}{W}\cdot\nabla)\underset{\sim}{W} = \frac{\partial \underset{\sim}{W}}{\partial t} + \frac{1}{2}\nabla W^2 - \underset{\sim}{W}\times(\nabla\times\underset{\sim}{W}) \,, \tag{2.3}$$

and the definitions [note also, Eq. (2.6), given below]

$$\frac{P_t^*}{\rho} \equiv \frac{P}{\rho} + \frac{W^2}{2} - \frac{\omega^2 r^2}{2} = \frac{P_t}{\rho} - (\underset{\sim}{W} + \underset{\sim}{\omega}\times\underset{\sim}{r})\cdot(\underset{\sim}{\omega}\times\underset{\sim}{r})$$

$$\equiv \frac{P_t}{\rho} - \underset{\sim}{V}\cdot(\underset{\sim}{\omega}\times\underset{\sim}{r}) = \frac{P_t}{\rho} - V_\theta\,\omega r \,. \tag{2.4}$$

Eq. (2.2) can be rewritten in the form

$$\frac{\partial \underset{\sim}{W}}{\partial t} - \underset{\sim}{W}\times(\nabla\times\underset{\sim}{W}) + 2\,\underset{\sim}{\omega}\times\underset{\sim}{W} = -\nabla\frac{P_t^*}{\rho} \,. \tag{2.5}$$

The quantities P_t and P_t^* are the stagnation pressure and the "rotary stagnation pressure", respectively. An alternative form of these dynamical equations, explicitly involving $\underset{\sim}{\Omega}$, the vorticity of the absolute motion, can be obtained as follows.

With the z-axis parallel to $\underset{\sim}{\omega}$, we have

$$\underset{\sim}{V} \equiv \underset{\sim}{W} + \underset{\sim}{\omega}\times\underset{\sim}{r} = \underset{\sim}{W} + \omega r\,\hat{e}_\theta \,, \tag{2.6}$$

where $\underset{\sim}{V}$ is the absolute velocity of the fluid, and e_θ a unit vector along θ. Hence,

$$\nabla\times\underset{\sim}{V} = \nabla\times\underset{\sim}{W} + \nabla\times(\underset{\sim}{\omega}\times\underset{\sim}{r}) \,.$$

But

$$\nabla\times(\underset{\sim}{\omega}\times\underset{\sim}{r}) = (\underset{\sim}{r}\cdot\nabla)\underset{\sim}{\omega} - (\underset{\sim}{\omega}\cdot\nabla)\underset{\sim}{r} + \underset{\sim}{\omega}(\nabla\cdot\underset{\sim}{r}) - \underset{\sim}{r}(\nabla\cdot\underset{\sim}{\omega}) = 2\underset{\sim}{\omega} \,,$$

therefore,

$$\underset{\sim}{\Omega} \equiv \nabla \times \underset{\sim}{V} = \nabla \times \underset{\sim}{W} + 2\underset{\sim}{\omega} \ . \tag{2.7}$$

Using Eq. (2.7) in Eq. (2.6) results in an alternative form of the equation of motion,

$$\frac{\partial \underset{\sim}{W}}{\partial t} - \underset{\sim}{W} \times \underset{\sim}{\Omega} = -\nabla \frac{P_t^*}{\rho} \ . \tag{2.8}$$

Upon employing Eq. (2.4) together with the dot product of Eq. (2.8) with $\underset{\sim}{W}$, we obtain

$$\frac{D(P_t^*/\rho)}{Dt} = \frac{\partial}{\partial t}\left(\frac{P}{\rho}\right) \ . \tag{2.9}$$

For an isolated blade row, or if the blade rows are placed far apart and no trailing vorticies are shed from the preceding blade rows (or in cases for which such effects can be neglected), the fluid properties at a particular point relative to the blade can be taken to be essentially invariant with respect to time. In such situations, Eqs. (2.8) and (2.9) become

$$\underset{\sim}{W} \times \underset{\sim}{\Omega} = \nabla \frac{P_t^*}{\rho} \ , \tag{2.10}$$

with

$$\underset{\sim}{W} \cdot \nabla \frac{P_t^*}{\rho} = 0 \ . \tag{2.11}$$

Thus, the quantity (P_t^*/ρ) of the fluid remains constant along the streamlines within the stated limitations. This invariance of (P_t^*/ρ)

along relative streamlines implies that the rate of change of actual stagnation pressure along such streamlines is given by the product of the angular speed of the blade and the rate of change in angular momentum of the fluid element along the streamlines. This is of course the well known Euler turbine equation, applied to incompressible fluids.

For the flow through a stationary blade row $\underset{\sim}{\omega} \equiv 0$ and $\underset{\sim}{W}$ reduces to $\underset{\sim}{V}$ while (P_t^*/ρ) becomes (P_t/ρ). The equation of continuity and motion then take the more familiar forms

$$\nabla \cdot \underset{\sim}{V} = 0 \ , \tag{2.12}$$

$$\frac{\partial \underset{\sim}{V}}{\partial t} - \underset{\sim}{V} \times \underset{\sim}{\Omega} = -\nabla \frac{P_t}{\rho} \ , \tag{2.13}$$

respectively. We further note that Eq. (2.9) reduces to

$$\frac{\partial}{\partial t}\left(\frac{P_t}{\rho}\right) + \underset{\sim}{V} \cdot \nabla\left(\frac{P_t}{\rho}\right) = \frac{\partial}{\partial t}\left(\frac{P}{\rho}\right) \tag{2.14}$$

implying (for the inviscid case discussed here) that the stagnation pressure of the fluid can only be changed along streamlines through an unsteady process; as already suggested, these can often be taken to be small in turbomachine practice.

Thus, for steady absolute flow through a stationary blade-row, Eq. (2.13) becomes simply

$$\underset{\sim}{V} \times \underset{\sim}{\Omega} = \nabla \frac{P_t}{\rho} \ ; \tag{2.15}$$

while Eq. (2.11) becomes

$$\underset{\sim}{V} \cdot \nabla \frac{P_t}{\rho} = 0 \ , \tag{2.16}$$

confirming that the stagnation pressure P_t remains constant along absolute streamlines for the stator cases.

It is evident from Eqs. (2.10) or (2.15) that the vortex filaments and streamlines lie on surfaces of constant (P_t^*/ρ) or $P_t/\rho)$. Such surfaces, so formed by the interweaving of streamlines, and vortex filaments, are the familiar Bernoulli surfaces.

Because of the close similarity between the set of Eqs. (2.1), (2.10), (2.11) and that of Eqs. (2.12), (2.15), (2.16), the following analyses will turn out to be applicable to the flow governed by both sets.

2.2 Irrotational Flow

When the rotary stagnation pressure is constant throughout, we have

$$\underset{\sim}{W} \times \underset{\sim}{\Omega} = 0. \tag{2.17}$$

In particular, if the flow is one in which the vorticity $\underset{\sim}{\Omega} = 0$ everywhere, so that the velocity may be written in terms of a velocity potential ϕ as

$$\underset{\sim}{V} = \nabla\phi \ , \tag{2.18}$$

Eq. (2.17) is automatically satisfied and the continuity condition (2.12) simply yields Laplace's equation

$$\nabla^2\phi = 0. \tag{2.19}$$

The solution of (2.19) simply describes a classical irrotational flow field. Frequently the velocity potential ϕ satisfying Laplace's equation, together with an appropriate set of physical boundary conditions, is sufficient to describe (outside of boundary layers) a uniform flow field

upstream of an isolated blade row. It would also describe the downstream flow field if the isolated blade row imparts a radial variation of tangential velocity of the fluid in a downstream z-plane varying similarly to that of a potential vortex (i.e. inversely with r). This corresponds to constant blade circulation, which is consistent with Kelvin's circulation theorm.

2.3 Beltrami Flow[4,5]

If the vorticity in the flow field is not zero but lies along streamlines, then Eq. (2.17) would still be satisfied. This corresponds to the case of so-called Beltrami flow. Such a flow would exist downstream of a blade row which imparts a radial variation of tangential velocity (swirl) of the fluid at a downstream z-plane which departs from that of the above simple potential vortex. In such cases the blade circulation varies along the span and vorticity is shed from the trailing edge to the fluid downstream in the direction of the exit velocity, again satisfying Kelvin's theorem.

Let us dwell on Beltrami flow further as we will need it in analyzing distorted flow through a blade row in Part II of the present study. The general solution to Eq. (2.17) is given by

$$\nabla \times \underset{\sim}{V} \equiv \underset{\sim}{\Omega} = \lambda \underset{\sim}{W} \tag{2.20}$$

where λ is any scalar function of (r,θ,z). Since $\underset{\sim}{\Omega}$ is always a solenoidal vector, and by virtue of Eq. (2.1), the divergence of Eq. (2.20) yield the restriction

$$\underset{\sim}{W} \cdot \nabla \lambda = 0 , \tag{2.21}$$

implying that λ remains constant along a (relative) streamline. A simple physical interpretation of λ is obtained by integrating Eq. (2.20) over an open surface $\underset{\sim}{S}$ bounded by a stream tube giving

$$\lambda = \oint \underset{\sim}{\Omega} \cdot d\underset{\sim}{S} \Big/ \oint \underset{\sim}{W} \cdot d\underset{\sim}{S}$$

Hence, λ gives the circulation about a stream tube through which the fluid volumetric flow rate is unity.[4]

By virtue of Eq. (2.1), the velocity vector $\underset{\sim}{W}$ is also solenoidal here; thus it can be expressed as

$$\underset{\sim}{W} = \nabla\alpha \times \nabla\beta \ , \tag{2.22}$$

where α, β are scalars. Physically, this means that the intersections of surfaces of constant α and β are the streamlines. Consequently, integration of Eq. (2.20) along such streamlines yeilds the general result

$$\lambda = \lambda(\alpha, \beta) \tag{2.23}$$

Because, by definition, $\underset{\sim}{\Omega}$ is solenoidal, we can also write

$$\underset{\sim}{\Omega} \equiv \nabla S \times \nabla\Gamma \quad (= \lambda \underset{\sim}{W}) \tag{2.24}$$

where s, and Γ are scalar quantities still to be determined. Because of Eqs. (2.22) and (2.23), s and Γ also can depend on α and β only.

Eq. (2.24) shows that a Beltrami flow can be described by a velocity vector $\underset{\sim}{V}$ of the form

$$\underset{\sim}{V} = \nabla\phi_I + S\nabla\Gamma \ , \tag{2.25a}$$

or

$$\underset{\sim}{V} = \nabla\phi_{II} - \Gamma\nabla S \cdot \tag{2.25b}$$

Since $S\nabla\Gamma + \Gamma\nabla S = \nabla(\Gamma S)$, the choice of either (2.25a) or (2.25b) is a simple matter of the differing definitions of ϕ_I and ϕ_{II}. Application of the continuity condition gives

$$\nabla^2\phi_I = -\nabla S\cdot\nabla\Gamma - S\nabla^2\Gamma \,, \tag{2.26a}$$

or, alternatively

$$\nabla^2\phi_{II} = \nabla S\cdot\nabla\Gamma + \Gamma\nabla^2 S \cdot \tag{2.26b}$$

Upon the use of appropriate boundary conditions, the corresponding results obtained from either of these equations, applied to (2.25a) or (2.25b), yield, as required, an identical determination of $\underset{\sim}{V}$.

2.4 Flow with a Gradient in Stagnation Pressure

In general, the rotary stagnation pressure P_t^* is not constant throughout but varies from streamline to streamline so that the vorticity is non-zero [recall Eq. (2.10)]. Even for uniform flow upstream of an isolated blade row, the gradient of stagnation pressure downstream of it is not zero in practice because of the inherent viscous interaction of the working fluid at the blade surfaces. A way of analyzing such rotational flow is by the use of the so-called Clebsch Transformation,[22,4] which expresses the velocity vector $\underset{\sim}{V}$ as

$$\underset{\sim}{V} = \nabla\phi_I + \sigma\nabla\tau \,, \tag{2.27a}$$

or

$$\underset{\sim}{V} = \nabla\phi_{II} - \tau\nabla\sigma \quad . \tag{2.27b}$$

Here, the ϕ's, σ and τ are again scalar functions to be determined. The vorticity $\underset{\sim}{\Omega}$ is given by

$$\underset{\sim}{\Omega} \equiv \nabla \times \underset{\sim}{V} = \nabla\sigma \times \nabla\tau \quad , \tag{2.28}$$

guaranteeing once again that the identity $\nabla \cdot \underset{\sim}{\Omega} = 0$ is satisfied. In this case the intersections of the surfaces of constant σ and τ are the vortex filaments of $\underset{\sim}{\Omega}$. Lamb[22] showed that there are an infinite number of ways of selecting the functions σ and τ. Hawthorne, however, suggested[4] that a useful physical meaning could be attached to the Clebsch Transformation by choosing $\sigma = (P_t^*/\rho)$ so that one of the two surfaces is a Bernoulli surface. Substituting for this choice of σ in Eq. (2.28) and taking advantage of Eq. (2.10), we obtain the result that, for such a choice,

$$\underset{\sim}{\Omega} = (\underset{\sim}{W} \cdot \nabla\tau)\underset{\sim}{\Omega} \quad , \tag{2.29}$$

Here, we have used the fact that the vorticity $\underset{\sim}{\Omega}$ lies on surfaces of constant τ [note that $\underset{\sim}{\Omega} \cdot \nabla\tau = 0$, according to (2.28)]. Hence, from (2.29),

$$\underset{\sim}{W} \cdot \nabla\tau = 1 \quad , \tag{2.30a}$$

or

$$W\frac{\partial\tau}{\partial s} = 1 \quad , \tag{2.30b}$$

where s measures the distance along a particular stream trajectory. Thus,

$$\tau = \int_{s_0}^{s} \frac{ds}{W} \quad , \tag{2.31}$$

where the integral is taken along a stream trajectory. Eq. (2.31) can be interpreted as giving a measure of the time taken by surfaces of constant τ to drift through a distance $(s-s_0)$; consequently, such surfaces are termed drift surfaces (after Darwin[23]) and τ is termed the drift function[4, 24, 25]. Because the fluid particles are frozen on vortex filaments in this flow model, any surface of constant τ can specify a particular reference vortex filament after time τ, upon appropriate choice of τ at s_0.

Upon integrating Eq. (2.28), and substituting the choice $\sigma = P_t^*/\rho$, one obtains

$$\underset{\sim}{V} = \nabla\phi_I + \frac{P_t^*}{\rho}\nabla\tau \quad , \tag{2.32a}$$

or

$$\underset{\sim}{V} = \nabla\phi_{II} - \tau\nabla\frac{P_t^*}{\rho} \quad . \tag{2.32b}$$

These results describe a flow for which the rotary stagnation pressure varies from streamline to streamline, in contrast to Beltrami case discussed earlier. The imposition of the continuity condition gives now

$$\nabla^2\phi_I = -\nabla\frac{P_t^*}{\rho}\cdot\nabla\tau - \frac{P_t^*}{\rho}\nabla^2\tau \quad , \tag{2.33a}$$

or

$$\nabla^2\phi_{II} = \nabla\tau\cdot\nabla\frac{P_t^*}{\rho} + \tau\nabla^2\frac{P_t^*}{\rho}\ , \tag{2.33b}$$

the solution of which together with an appropriate set of physical boundary conditions, give either of the velocity potentials, ϕ_I or ϕ_{II}, and hence $\underset{\sim}{V}$.

2.5 General Case of Steady Rotational Motion[26]

Reviewing Sections 2.2 to 2.4, one sees that the velocity vector $\underset{\sim}{V}$ for the general case of a steady rotational flow may be written usefully in the general form

$$\underset{\sim}{V} = \nabla\phi + \underset{\sim}{A} \tag{2.34}$$

Combining the results of both discussions, we have more generally

$$\underset{\sim}{\Omega} \equiv \nabla\times\underset{\sim}{V} = \nabla\times\underset{\sim}{A} = \lambda\underset{\sim}{W} + \underset{\sim}{\Omega}_\tau$$

$$= \nabla S\times\nabla\Gamma + \nabla\left(\frac{P_t^*}{\rho}\right)\times\nabla\tau\ , \tag{2.35}$$

with

$$\underset{\sim}{W}\times\underset{\sim}{\Omega}_\tau \equiv \nabla\left(\frac{P_t^*}{\rho}\right)\ . \tag{2.36}$$

The vector $\underset{\sim}{A}$ can be written either as

$$\underset{\sim}{A} = \frac{P_t^*}{\rho}\nabla\tau + S\nabla\Gamma\ , \tag{2.37a}$$

or

$$\underset{\sim}{A} = -\tau\nabla\frac{P_t^*}{\rho} - \Gamma\nabla S\ , \tag{2.37b}$$

since the freedom of choice previously discussed still obtains. Both forms

are useful, particularly for physical interpretation of the final results.

The application of the continuity equation gives, in this more general situation,

$$\nabla^2\phi = -\nabla\cdot\underset{\sim}{A} = -\nabla\frac{P_t^*}{\rho}\cdot\nabla\tau - \frac{P_t^*}{\rho}\nabla^2\tau - \nabla S\cdot\nabla\Gamma - S\nabla^2\Gamma \,, \tag{2.38a}$$

or

$$\nabla^2\phi = -\nabla\cdot\underset{\sim}{A} = \nabla\tau\cdot\nabla\frac{P_t^*}{\rho} + \tau\nabla^2\frac{P_t^*}{\rho} + \nabla\Gamma\cdot\nabla S + \Gamma\nabla^2 S \,, \tag{2.38b}$$

the solution of which, together with suitable boundary conditions, gives the velocity potential ϕ. One example of such a flow would be that downstream of an isolated blade row where the flow upstream of it has a gradient in stagnation pressure.

Although these equations are exact formulations of the steady, rotational flow of an incompressible, inviscid fluid with specified boundary conditions, exact solutions of them are problably unattainable on an analytical basis. Appropriate approximations can be made for practical situations when attempting to obtain solutions to describe a variety of flows of engineering interest.

CHAPTER 3 - VISCOUS BLADE WAKES IN INCOMPRESSIBLE FLOW

3.1 Analytical Formulation

Consider the flow through an isolated rotor, encased in an infinite cylindrical annulus, using a right-handed cylindrical coordinate system (r,θ,z) in a duct-fixed system (Fig. I.1a). For upstream of the rotor (rotating at an angular velocity ω) let the flow be uniform and have a purely axial velocity, further, let us specify, in the downstream region, that the rotor has set up a free-vortex mean flow. In this case the fluid properties at a fixed point can be regarded as steady relative to the blades; therefore it is convenient to use a relative cylindrical coordinate system (r,θ,z) with θ measured with respect to the rotating blade (Fig. I.1b). When compressibility effects are negligible, it is appropriate to regard the viscous interaction process between the working fluid and the blade surfaces as one leading to a loss in rotary stagnation pressure P_t^* (corresponding to a loss in stagnation pressure P_t in a stationary blade-row) within the thin regions of boundary layer on the blade surfaces.† Outside this boundary layer, the value of P_t^* is the same as that of the far upstream value. Consequently, downstream of the rotor, the wakes are regions of low rotary stagnation pressure P_t^* and thus P_t^* has a circumfer-

†For a flow through a two-dimensional cascade, it is always true that there is a defect of stagnation pressure (or relative stagnation pressure in rotating cascade) within the wakes. However, in annular cascades, strong radial transport of fluid particle may gain sufficient work (moving along a streamline) to offset the loss due to the viscous interaction on the blades thus resulting in an excess of stagnation pressure within the wakes.

ential variation as shown in Fig. I.2†; in practice, the profile for such variation would change as one proceeds downstream because of viscous diffustion and mixing of the wakes. Such effects are not considered in the theory to be developed here, since they do not materially effect the results in most practical cases.

Further, for the range of Reynolds numbers normally encountered in flow through turbomachines under design conditions, the difference in the values of P_t^* within the wake and outside the wake can be considered to be small in comparison with the incoming dynamic head ($1/2\ \rho W^2$) unless boundary layer separation occurs. An experimental illustration of this type of loss, as a function of Reynolds number, is shown in Fig. I.3. As a result, the vorticity introduced by the presence of the wakes is small and the flow can be separated into a circumferentially averaged irrotational flow of zeroth order, $\overline{\underset{\sim}{V}}$ (or $\overline{\underset{\sim}{W}}$ in the relative frame), and a three-dimensional rotational perturbation flow, $\tilde{\underset{\sim}{V}}$ of order ε, where, for example,

$$\varepsilon \sim O\left(\frac{\tilde{V}}{\overline{V}}\right) \sim O\left(\frac{\Delta P_t^*}{\frac{1}{2}\rho \overline{W}^2}\right) \ll 1 \quad . \tag{3.1}$$

Hence, the three-dimensional aspects of such a flow can readily be considered as a perturbation about the circumferentially-averaged mean flow; the latter, however, can be described as precisely as desired or appropriate. In approximation Eq. (2.10) becomes

$$\overline{\underset{\sim}{W}} \times \underset{\sim}{\Omega} = \nabla \frac{P_t^*}{\rho} \tag{3.2}$$

with

†See footnote on previous page.

$$\underset{\sim}{\Omega} = \nabla \times \tilde{\underset{\sim}{V}} = \nabla \frac{P_t^*}{\rho} \times \nabla \tau \ , \tag{3.3}$$

where we have omitted here the second part of Eq. (2.35)(the Beltrami component of vorticity) since we are concerned in this Section with that part of the vorticity arising only from the gradients in rotary stagnation pressure P_t^* just described. We note that the approximation leading to Eq. (3.2) also results in

$$\overline{\underset{\sim}{W}} \cdot \nabla \frac{P_t^*}{\rho} = 0 \ , \tag{3.4}$$

indicating that P_t^* remains, within this model, constant along a <u>mean</u> streamline of the relative flow. It follows, using Eqs. (2.32a) and (3.3), that

$$\tilde{\underset{\sim}{V}} = \nabla \phi + \frac{P_t^* - \bar{P}_t^*}{\rho} \nabla \tau \ , \tag{3.5}$$

where $\bar{P}_t^*$ is the mean value of the rotary stagnation pressure and is constant throughout for the situation under discussion. As mentioned above, any variation in $(P_t^* - \bar{P}_t^*)/\rho$ will be of the order ε; consequently, consistent with the order of approximation used here, it is justified to replace the drift function τ in Eqs. (3.3) and (3.5) by that of the mean flow $\bar{\tau}$. That is, the perturbed flow field can be evaluated (in part) by the use of the approximate drift function $\bar{\tau}$ obtained from the mean flow. Thus, from Eq. (2.31),

$$\bar{\tau} = \int_0^S \frac{ds}{\bar{W}} \ . \tag{3.6}$$

For free-vortex downstream flow considered here the mean velocity vector $\bar{\underset{\sim}{W}}$ behind the rotor is given by

$$\bar{\underset{\sim}{W}} = (\bar{V}_\theta - \omega r)\,\hat{e}_\theta + \bar{V}_z\,\hat{e}_z \quad , \tag{3.7}$$

where $(\bar{V}_\theta r)$ and $\bar{V}_z$ are constant.[1] It is then obvious that we can now write

$$\bar{\tau} = \int_0^z \frac{dz}{\bar{V}_z} = \frac{z}{\bar{V}_z} \quad , \tag{3.8}$$

or

$$\bar{\tau} = \int_{\theta_0(r,z=0)}^{\theta} \frac{r\,d\theta}{(\bar{V}_\theta - \omega r)} = \frac{r(\theta - \theta_0(r))}{(\bar{V}_\theta - \omega r)} \quad , \tag{3.9}$$

where in the first case we have made a specific choice of the "constant" of integration which corresponds to "beginning $\bar{\tau}$ at the rotor plane, z=0.

Because $(P_t^* - \bar{P}_t^*)$ remains constant on streamlines of the relative mean flow, it can be taken to have an arbitrary dependence on r and $\bar{\alpha}^d$, (but no explicit z-dependence), i.e.,

$$\frac{P_t^* - \bar{P}_t^*}{\rho} = \frac{\delta P_t^*}{\rho} = \frac{\delta P_t^*}{\rho}(r, \bar{\alpha}^d) \tag{3.10}$$

where we have defined the developing downstream "swirl angles"

$$\bar{\alpha}^d \equiv \left[\theta - \left(\frac{K_0}{r^2} - \frac{\omega}{\bar{V}_z}\right) z\right] \quad , \tag{3.11}$$

along which the mean (relative) streamlines lie. In this expression $K_0 = (\bar{V}_\theta r)/\bar{V}_z$ is used to indicate the relative strength of the mean swirl. To assist in the determination of the correct analytical form of $(\delta P_t^*/\rho)\nabla\bar{\tau}$

which will correspond closely to a realistic flow for this case, we first consider the nature of the downstream vorticity field. We have indicated in Chapter 1 that vorticies within the boundary layers on the blades have their axes parallel to the direction of the span [this is true so long as if the boundary layer is in fact two-dimensional]. However, the boundary layers on the blade surfaces are in general three-dimensional (sheared), with varying degrees of flow in the radial direction; this implies among other things, that $(\delta P^*/\rho)$ assumes a complex dependence on radial location. Such shear in turn would give rise to vorticity in the tangential direction. Hence, at the exit plane of the blade row, there will in general exist radial vortex filaments as well as tangential vortex filaments. However, we should not expect axial vortex filaments, as shown below.

In fact, by taking the drift function $\bar{\tau}$ to be given straight forwardly by Eq. (3.8), we obtain the vorticity field, $\underset{\sim}{\Omega} = (\xi,\eta,\zeta)$, downstream of the rotor in the relatively simple form

$$\xi = -\frac{1}{\bar{V}_z}\left(\frac{K_0}{r^2} - \frac{\omega}{\bar{V}_z}\right)\frac{1}{\rho}\frac{\partial}{\partial \bar{\alpha}^d}(\delta P_t^*) , \tag{3.12a}$$

$$\eta = -\frac{1}{\bar{V}_z}\left[\frac{1}{\rho}\frac{\partial}{\partial r}(\delta P_t^*) + \frac{2K_0 z}{r^3}\frac{1}{\rho}\frac{\partial}{\partial \bar{\alpha}^d}(\delta P_t^*)\right] , \tag{3.12b}$$

$$\zeta = \left[\frac{1}{\rho}\frac{\partial}{\partial z}(\delta P_t^*)\,\hat{e}_z \times \frac{\hat{e}_z}{\bar{V}_z}\right] \equiv 0 . \tag{3.12c}$$

Further, at the exit plane of the rotor, z=0, the vorticity field reduces to

$$\underset{\sim}{\Omega}(z=0)=\left\{-\frac{1}{\bar{V}_z}\left(\frac{K_0}{r^2}-\frac{\omega}{\bar{V}_z}\right)\frac{1}{\rho}\frac{\partial}{\partial\bar{\alpha}^d}(\delta P_t^*),-\frac{1}{\bar{V}_z\rho}\frac{\partial}{\partial r}(\delta P_t^*),\ 0\right\} \tag{3.13}$$

Thus, using the drift function $\bar{\tau}$ in this form, we can in fact obtain only radial and tangential vortex filaments at the exit plane of the rotor, as expected.

For more involved blade geometries, by contrast, the vorticity field $\underset{\sim}{\Omega}$ downstream of the rotor could be obtained alternatively by using the drift function $\bar{\tau}$ as given in Eq. (3.9). This "more general" result is

$$\xi=\frac{\left(\frac{K_0}{r^2}-\frac{\omega}{\bar{V}_z}\right)}{(\bar{V}_\theta-\omega r)}\frac{1}{\rho}\frac{\partial}{\partial\bar{\alpha}^d}(\delta P_t^*)\ , \tag{3.14a}$$

$$\eta=-\frac{\left[2\bar{V}_\theta(\theta-\theta_0)-r\frac{\partial\theta_0}{\partial r}(\bar{V}_\theta-\omega r)\right]\left(\frac{K_0}{r^2}-\frac{\omega}{\bar{V}_z}\right)}{(\bar{V}_\theta-\omega r)^2}\frac{1}{\rho}\frac{\partial}{\partial\bar{\alpha}^d}(\delta P_t^*) \tag{3.14b}$$

$$\zeta=\frac{\left[\frac{1}{\rho}\frac{\partial}{\partial r}(\delta P_t^*)+\frac{2K_0z}{r^3\rho}\frac{\partial}{\partial\bar{\alpha}^d}(\delta P_t^*)\right]}{(\bar{V}_\theta-\omega r)}-\frac{2\bar{V}_\theta(\theta-\theta_0)-r\frac{\partial\theta_0}{\partial r}(\bar{V}_\theta-\omega r)}{(\bar{V}_\theta-\omega r)^2}\frac{1}{r\rho}\frac{\partial}{\partial\bar{\alpha}^d}(\delta P_t^*)\ . \tag{3.14c}$$

At a particular circumferential position (r,0,0) in the exit plane of the rotor, the vorticity field there would be, correspondingly,

$$\underset{\sim}{\Omega}(z=0) = \left\{ \frac{\left(\frac{K_0}{r^2} - \frac{\omega}{\bar{V}_z}\right)}{(\bar{V}_\theta - \omega r)} \frac{1}{\rho} \frac{\partial}{\partial \bar{\alpha}^d}(\delta P_t^*) \,,\; \frac{\left(\frac{K_0}{r^2} - \frac{\omega}{\bar{V}_z}\right)\left[2\bar{V}_\theta(\theta-\theta_0) - r\frac{\partial \theta_0}{\partial r}(\bar{V}_\theta - \omega r)\right]}{(\bar{V}_\theta - \omega r)^2} \frac{1}{\rho} \frac{\partial}{\partial \bar{\alpha}^d}(\delta P_t^*) \right.$$

$$\left. - \frac{2\bar{V}_\theta(\theta-\theta_0) - r\frac{\partial \theta_0}{\partial r}(\bar{V}_\theta - \omega r)}{(\bar{V}_\theta - \omega r)^2} \frac{1}{r\rho} \frac{\partial}{\partial \bar{\alpha}^d}(\delta P_t^*) \,,\; \frac{1}{(\bar{V}_\theta - \omega r)} \frac{1}{\rho} \frac{\partial}{\partial r}(\delta P_t^*) \right\} \tag{3.15}$$

We thus see that the use of the drift function $\bar{\tau}$ according to Eq. (3.9) can give radial and axial vortex filaments at the exit plane of the rotor in contrast with the results (3.13). Clearly, this is not the case normally to be expected in axial turbomachinery. We conclude for our present problem that use of the drift function $\bar{\tau}$ as given in Eq. (3.8) in describing the vorticity field introduced by the presence of the blade-wakes is both appropriate and convenient for most axial turbomachines.

It then follows that Eq. (3.5) becomes simply

$$\underset{\sim}{\tilde{V}} = \nabla\phi + \frac{\delta P_t^*}{\rho \bar{V}_z} \hat{e}_z \tag{3.16}$$

This implies that, in conventional configurations, gradients in the rotary stagnation pressure due to the blade wakes can be described in terms of an appropriate distribution of vortex filaments emerging at planes of constant axial location.

Obviously, for any practical configuration the ultimate determination of the three-dimensional perturbed flow requires not only an appropriate choice of $\bar{\tau}$, but also detailed knowledge of $(\delta P_t^*/\rho)$. Within the blade wakes, there is a defect in (P_t^*/ρ); outside of the blade wakes, (P_t^*/ρ)

*Recall that the present discussion is restricted to the incompressible case, see foot note on Page

essentially assumes that of the upstream value. In particular, on surfaces of constant radius r,

$$\frac{\delta P_t^*}{\rho} = \left(\frac{P_t^*}{\rho}\right)_w^d - \left(\frac{P_t^*}{\rho}\right)^u = \left(\frac{P}{\rho} + \frac{1}{2}W^2\right)_w^d - \left(\frac{P}{\rho} + \frac{1}{2}\ W^2\right)^u, \tag{3.17}$$

where the superscripts "u" and "d" refer to an upstream station and a downstream station respectively, while the subscript "w" refers to a point within a particular blade wake region. Eq. (3.17) indicates that the difference in the rotary stagnation pressure caused by the viscous interaction process is precisely the same as that occuring in the relative stagnation pressure. It is conventional and convenient to measure the loss in stagnation pressure in units of the incoming dynamic head $(1/2\ \rho W^2)^u$ since such losses will be dependent on the magnitude of the incoming velocity.

In the experimental cascade data, such losses are conventionally measured by the mean stagnation pressure "loss coefficient", $\bar{\omega}$, defined by

$$\bar{\omega} = \frac{\left(P + \frac{1}{2}\rho W^2\right)^u - \left(P + \frac{1}{2}\rho W^2\right)^d}{\left(\frac{1}{2}\rho W^2\right)^u} \tag{3.18}$$

This quantity is dependent upon the incidence angle, the blade profile and the inlet Mach number. Its typical variation with incidence angle at various inlet Mach numbers is shown in Fig. I.4.[27] These curves show, for low-speed rotors, that the mean loss remains fairly constant over a reasonably wide range of incidence, rising rapidly when the incidence has large positive or negative values. At these extreme incidences, the flow of the air around the blades breaks down in a manner similar to the stalling

of an isolated airfoil.

To an extent, $(\delta P_t^*/\rho)$ is directly related to the negative of $[(1/2\ W^2)^u\ \bar{\omega}]$ and is thus obtainable from available experimental cascade data.[27] Actually, however the variation of $\delta P_t^*/(1/2\ \rho W^2)^u$ can be larger than that which the mean stagnation pressure coefficient $\bar{\omega}$ would suggest. Its typical variation is shown in Fig. I.5. Hence, upon using of experimental data, $\delta P_t^*/\rho$ can be totally prescribed. (A more elaborate procedure would be the use of boundary layer analysis in the blade passages to obtain an estimation of viscous losses within the blade row directly. Such an analysis is not be be attempted here as it is the subject of extensive research elsewhere.)

Because of the circumferential periodicity inherent in the geometry of turbomachinery, we can write in general

$$\frac{\delta P_t^*}{\rho} = \sum_{n=1}^{\infty} P_n(r) e^{inB\bar{\alpha}^d} \quad , \tag{3.19}$$

where B is the number of blades on the rotor and the real part is implied in Eq. (3.19). We also note that Eq. (3.19) guarantees that the integral of vorticity $\underset{\sim}{\Omega}$ from blade to blade is identically zero; this is consistent with the fact, previously mentioned, that no net vorticity flux is shed into the wakes in steady flow (a use of Kelvin's theorem). In fact, this is necessary for the Kutta's condition to be satisfied at the trailing edge of the blade.[28]

Collecting all these results for the downstream flow field, we have an expression for the downstream perturbation velocity of the form

$$\tilde{\underset{\sim}{V}}^{d} = \nabla\phi^{d} + \sum_{n=1}^{\infty} \frac{P_n(r)}{\bar{V}_z} e^{inB\bar{\alpha}^{d}} \hat{e}_z \quad . \tag{3.20}$$

For the present case, upstream of the blade row the perturbation velocity is simply irrotational and is given by

$$\tilde{\underset{\sim}{V}}^{u} = \nabla\phi^{u} \quad . \tag{3.21}$$

Upon application of the continuity condition in Eq. (2.1), we obtain

$$\nabla\cdot\bar{\underset{\sim}{W}} = 0 \quad , \tag{3.22}$$

and

$$\nabla\cdot\tilde{\underset{\sim}{W}} = \nabla\cdot\tilde{\underset{\sim}{V}} = 0 \quad . \tag{2.23}$$

Hence, we find the equations for ϕ^u and ϕ^d are

$$\nabla^2\phi^{u} = 0 \quad , \tag{2.24}$$

and

$$\nabla^2\phi^{d} = -\sum_{n=1}^{\infty} \frac{P_n}{\bar{V}_z} \frac{\partial}{\partial z}\left(e^{inB\bar{\alpha}^{d}}\right) \tag{3.25}$$

$$= \sum_{n=1}^{\infty} i \frac{P_n}{\bar{V}_z} nB\left(\frac{K_0}{r^2} - K_1\right) e^{inB\bar{\alpha}^{d}}$$

where we have used $K_1 = \omega/\bar{V}_z$. Eqs. (3.24) and (3.25) are each to be solved under the boundary conditions at the hub ($r=r_h$) and the tip ($r=r_T$) that the radial velocities vanish there.

3.2 Determination of the Three-Dimensional Perturbed Flow

Before proceding to the complete solution of Eqs. (3.24) and (3.25), we introduce a non-dimensionalizing scheme based on the following characteristic scales: the velocity scale will be that of axial velocity $\bar{V}_z$, the length scale will be the tip radius r_T, the time scale will be $r_T/\bar{V}_z$, and the pressure will be measured in units of $1/2\ \rho\bar{V}_z^2$.

Written in dimensionless form, Eqs. (3.24) and (3.25) then become

$$\frac{\partial^2\phi^u}{\partial r^2} + \frac{1}{r}\frac{\partial\phi^u}{\partial r} + \frac{1}{r^2}\frac{\partial^2\phi^u}{\partial\theta^2} + \frac{\partial^2\phi^u}{\partial z^2} = 0 \quad , \tag{3.26}$$

and

$$\frac{\partial^2\phi^d}{\partial r^2} + \frac{1}{r}\frac{\partial\phi^d}{\partial r} + \frac{1}{r^2}\frac{\partial^2\phi^d}{\partial\theta^2} + \frac{\partial^2\phi^d}{\partial z^2} = -i\sum_{n=1}^{\infty} nB\frac{\bar{\omega}_n}{2}\left(\frac{K_0}{r^2} - K_1\right)e^{inB\bar{\alpha}^d} \quad , \tag{3.27}$$

where we have introduced $\bar{\omega}_n$ as defined by

$$\bar{\omega}_n \equiv -\frac{P_n}{\frac{1}{2}\bar{V}_z^2} \quad ; \tag{3.28}$$

the $\bar{\omega}_n$ are related to the stagnation pressure loss coefficient data previously described. We note that K_0/r is the inverse of the local Rossby number which is a measure of the relative importance of the inertial force due to the throughflow to that due to the swirling flow at a particular radius. K_1 is closely related to the inverse of the flow coefficient.

The solutions of Eqs. (3.26) and (3.27) can be written in the form (real part implied)

$$\phi^d = \sum_{n=1}^{\infty}\sum_{p=1}^{\infty} A_{np}^d\, e^{-\lambda_{np}|z|}\,\Gamma_{np}(r)\,e^{inB\theta} + \phi_I^d(r,\theta,z)\,H(z) \tag{3.29}$$

where H(z) is the Heaviside function defined by

$$H(z) = \begin{cases} 0 & z<0 \\ 1 & z>0 \end{cases} \tag{3.30}$$

The first double sum in Eq. (3.29), obtainable by the method of separation of variables, represents the exponentially decaying homogeneous solution typical of inviscid flow through an annulus. The (normalized) radial eigenfunction $\Gamma np(r)$ is a linear combination of the Bessel functions of the first and second kinds; this quantity is given by

$$\Gamma_{np}(r) = \frac{1}{\sqrt{N_{np}}}\left\{J_{nB}(\lambda_{np} r) - \frac{J'_{nB}(\lambda_{np})}{Y'_{nB}(\lambda_{np})} Y_{nB}(\lambda_{np} r)\right\} \tag{3.31}$$

where $\sqrt{N}np$ is the normalizing factor, given by[7,8]

$$N_{np} = \int_h^1 r\left\{J_{nB}(\lambda_{np} r) - \frac{J'_{nB}(\lambda_{np})}{Y'_{nB}(\lambda_{np})} Y_{nB}(\lambda_{np} r)\right\}^2 dr \tag{3.32}$$

where we have introduced h ($\equiv r_h/r_T$) as the hub-to-tip ratio.

The vanishing of the radial velocities at the shroud and at the hub is guaranteed by taking the characteristic values of λnp to be the roots of

$$J'_{nB}(\lambda_{np} h) Y'_{nB}(\lambda_{np}) - J'_{nB}(\lambda_{np}) Y'_{nB}(\lambda_{np} h) = 0, \tag{3.33}$$

There is a countable infinity of the eigenvalues of λnp, ordered in increasing magnitude; this is guaranteed by the Sturm-Lioville Theorem. In fact, the function $\Gamma np(r)$ satisfies the ordinary differential equation

$$\frac{d^2\Gamma_{np}(r)}{dr} + \frac{1}{r}\frac{d\Gamma_{np}(r)}{dr} + (\lambda_{np}^2 - \frac{n^2\beta^2}{r^2})\Gamma_{np}(r) = 0 \tag{3.34}$$

with the boundary conditions

$$\left.\frac{d\Gamma_{np}(r)}{dr}\right|_h = \left.\frac{d\Gamma_{np}(r)}{dr}\right|_1 = 0 \tag{3.35}$$

Thus the set of radial eigenfunctions $\{\Gamma np(r)\}$ form an orthogonal set, and by virtue of (3.31),

$$\int_h^1 r\Gamma_{np}(r)\Gamma_{nj}(r)dr = \delta_{pj} = \begin{cases} 1 & p=j \\ 0 & p\neq j \end{cases} \tag{3.36}$$

where δpj is the Kronecker delta.

The particular solution ϕ_I^d (r,θ,z) of Eq. (3.27), must necessarily satisfy the boundary conditions of the vanishing of radial velocity at the shroud and the hub. This requires

$$\left.\frac{\partial\phi_I^d}{\partial r}\right|_h = \left.\frac{\partial\phi_I^d}{\partial r}\right|_1 = 0 \tag{3.37}$$

The expression for ϕ_I^d is readily obtained by any of a variety of standard techniques (see, e.g., Ref. 1).

The fact that the normalized radial eigenfunctions $\Gamma np(r)$ in Eq. (3.31) have vanishing derivatives at r=h and r=1 suggests that the radial dependence of ϕ_I^d can itself be expressed conveneintly in terms of the $\Gamma np(r)$. Furthermore, invoking the circumferential periodicity inherent in the geometry of an axial turbomachinery, the azimuthal dependence of ϕ_I^d must necessarily be of the form exp (in $B\theta$). Therefore, the particular

solution ϕ_I^d is conveniently expressible as the sum of a product of three functions, each of which has a well-known radial dependence, a θ-dependence and an axial dependence only. Hence, it is natural (and useful!) to express it as a double sum of the form

$$\phi_I^d(r,\theta,z) = \sum_{n=1}^{\infty}\sum_{p=1}^{\infty} \Gamma_{np}(r)\, e^{inB\theta}\, Z_{np}(z) \quad . \tag{3.38}$$

This, in combination with the homogeneous solution, in fact guarantees the vanishing of the radial velocity at the hub and the shroud. The only remaining unknown in Eq. (3.38) is the functional form of Znp(z), which is to be constructed such that it is bounded far downstream. Substitution of Eq. (3.38) in Eq. (3.37), and application of the hub and tip boundary conditions allows one to determine the Znp(z) (see Appendix IA) in the form

$$Z_{np}(z) = \frac{inB}{2}\int_h^1 \frac{\bar{\omega}_n\left(\frac{K_0}{r^2}-K_1\right) r\,\Gamma_{np}(r)\, e^{-inB\left(\frac{K_0}{r^2}-K_1\right)z}}{\left[\lambda_{np}^2 + n^2B^2\left(\frac{K_0}{r^2}-K_1\right)^2\right]}\, dr \quad . \tag{3.39}$$

The behavior of this integral reveals the behavior of the blade wakes and the induced perturbations. It will be discussed subsequently; its form leads to results such as those illustrated in Fig.s I.9 - I.12).

3.3 Matching at the Blade Row

Inspection of Eq. (3.29) shows that for each circumferential harmonic n and radial harmonic p, the remaining unknowns are the summation coefficients $A_{np}^{u,d}$. Determination of these quantities follows from appropriate matching of the upstream flow and downstream flow at the blade row. The two physical boundary conditions at the blade row required for determination of these quantities are:

(i) The mass flux is continuous. For incompressible flow, the density is constant and since the axial velocity in the free-vortex mean flow is constant throughout; therefore this condition is satisfied (for incompressible flow) by

$$\tilde{V}_z^u\Big|_{z=0^-} = \tilde{V}_z^d\Big|_{z=0^+}$$

i.e.,

$$\frac{\partial \phi^u}{\partial z}\Big|_{z=0^-} = \frac{\partial \phi^d}{\partial z}\Big|_{z=0^+} - \sum_{n=1}^{\infty} \frac{\bar{\omega}_n}{2} e^{inB\theta} \tag{3.40}$$

where $z=0^-$ refers to a station immediately upstream of the blade row, and $z=0^+$ refers to one immediately downstream of the blade row.

(ii) The radial velocity can only change as a result of a concentrated radial force at the blade row. Generally, in axial turbomachinery as a result of the fact that the blade surfaces are almost radial, the exerted radial force can be assumed negligible at the blade row. Consequently, the radial velocity can normally be taken to be the same on either side of the blade row at z=0:

$$\tilde{V}_r^u\Big|_{z=0^-} = \tilde{V}_r^d\Big|_{z=0^+}$$

i.e.,

$$\frac{\partial \phi^u}{\partial r}\Big|_{z=0^-} = \frac{\partial \phi^d}{\partial r}\Big|_{z=0^+} \tag{3.41}$$

We note at this point that Eq. (3.41) may not be exactly true due to radial flow in the boundary layers; that is, the presence affecting the boundary layers may result in a change of radial velocity across the blade

row. This can readily be incorporated into the matching condition, if such a change is appropriate.

Substituting for the perturbed velocities from Eq. (3.29) in Eqs. (3.40) and (3.41) yields the following set of algebraic equations:

$$A^u_{np} + A^d_{np} = Z'_{np}(0) + C_{np} \ , \tag{3.42}$$

$$A^u_{np} - A^d_{np} = Z_{np}(0) \ , \tag{3.43}$$

where we have made use of the orthogonality properties of the normalized radial eigenfunction $\Gamma np(r)$ and the definition

$$C_{np} \equiv -\frac{1}{2}\int_h^1 \bar{\omega}_n(r)\, r\, \Gamma_{np}(r)\, dr \tag{3.44}$$

The solution of Eqs. (3.42) and (3.43) gives readily

$$A^u_{np} = \frac{1}{2}\left[Z'_{np}(0) + Z_{np}(0) + C_{np}\right] \tag{3.45}$$

$$A^d_{np} = \frac{1}{2}\left[Z'_{np}(0) - Z_{np}(0) + C_{np}\right] \tag{3.46}$$

At this point, under the restrictions noted, the perturbed flow field due to the presence of the blade wakes are completely known both for upstream and downstream of the rotor. We have:

(i) Upstream of the rotor,

$$V_z^u = \bar{V}_z + \sum_{n=1}^{\infty}\sum_{p=1}^{\infty} \lambda_{np} A^u_{np} \Gamma_{np}(r)\, e^{\lambda_{np} z} e^{inB\theta}$$

$$V_\theta^u = \frac{1}{r}\sum_{n=1}^{\infty}\sum_{p=1}^{\infty} inB A^u_{np} \Gamma_{np}(r)\, e^{\lambda_{np} z} e^{inB\theta} \qquad (3.47)$$

$$V_r^u = \sum_{n=1}^{\infty}\sum_{p=1}^{\infty} A^u_{np} \Gamma'_{np}(r)\, e^{\lambda_{np} z} e^{inB\theta}$$

(ii) Downstream of the rotor,

$$V_z^d = \bar{V}_z + \sum_{n=1}^{\infty}\sum_{p=1}^{\infty} (-\lambda_{np}) A^d_{np} \Gamma_{np}(r) e^{-\lambda_{np} z} e^{inB\theta} + \sum_{n=1}^{\infty}\sum_{p=1}^{\infty} Z'_{np}(z) \Gamma_{np}(r) e^{inB\theta} - \sum_{n=1}^{\infty} \frac{\bar{\omega}_n}{2} e^{inB\theta}$$

$$V_\theta^d = \bar{V}_\theta^d + \frac{1}{r}\sum_{n=1}^{\infty}\sum_{p=1}^{\infty} inB A^d_{np} \Gamma_{np}(r) e^{-\lambda_{np} z} e^{inB\theta} + \frac{1}{r}\sum_{n=1}^{\infty}\sum_{p=1}^{\infty} inB Z_{np}(z) \Gamma_{np}(r) e^{inB\theta} \qquad (3.48)$$

$$V_r^d = \sum_{n=1}^{\infty}\sum_{p=1}^{\infty} A^d_{np} \Gamma'_{np}(r) e^{-\lambda_{np} z} e^{inB\theta} + \sum_{n=1}^{\infty}\sum_{p=1}^{\infty} Z_{np}(z)\, \Gamma'_{np}(r) e^{inB\theta}$$

Here the primes on the $\Gamma np(r)$ and $Znp(z)$ denote differentiation with respect to the arguments of each, respectively.

3.4 Downstream Development of the Vorticity Field

The behavior of the blade wakes is closely related to the convection of the vortex filaments by the downstream flow. For simplicity, we assume here that the loss in P_t^* is invariant with the radius. Using Eq. (3.19) in Eq. (3.12), we then obtain

$$\xi = -\left(\frac{K_0}{r^2} - K_1\right)\sum_{n=1}^{\infty} inB\frac{\bar{\omega}_n}{2} e^{inB\bar{\alpha}^d} \tag{3.49a}$$

$$\eta = -\frac{2K_0 z}{r^3}\sum_{n=1}^{\infty} inB\frac{\bar{\omega}_n}{2} e^{inB\bar{\alpha}^d} \tag{3.49b}$$

$$\zeta = 0 \tag{3.49c}$$

[compare, Eqs. (3.13)].

At the exit of the blade row (i.e., at z=0), the vortex filaments are purely radial. However, as one moves downstream away from the blade, there develops a tangential component of the vorticity, η, as indicated by Eq. (3.49b)(as previously discussed, the axial component of vorticity remains zero). The strength of this tangential vorticity increases with z. The development of η gives rise to a streamwise component of vorticity Ωs given by

$$\Omega_s = -\frac{\bar{W}_\theta}{\bar{W}}\frac{2K_0 z}{r^3}\sum_{n} inB\frac{\bar{\omega}_n}{2} e^{inB\bar{\alpha}^d} \quad . \tag{3.50}$$

This "secondary vorticity", which changes as the flow proceeds, will induce a secondary flow, leading in turn to radial velocity components. In free vortex mean flow, fluid particles at different radial locations would traverse through different angular distances in a given time, since fluid particles are "frozen" on vorticity lines. Therefore a purely radial vortex filament at the exit of the blade row cannot remain so oriented as it moves downstream with the fluid particles. It will

become distorted and stretched by the mean flow and give rise to a tangential component of vorticity, i.e., "secondary" vorticity. This development of secondary vorticity is analogous to that of the case where a vortex filament, initially perpendicular to the velocity, passes round a bend[4]. However, in the present description the free vortex swirl is always present in the downstream flow since there are no following blade rows to remove the swirl; consequently, one may well expect that the secondary flow will grow without bound, as indicated by the z-dependence in Eq. (3.50). The secondary flow will grow in strength for a certain distance downstream of the blade-row but will eventually decay. At infinity (for downstream), the secondary flow vanishes. This is understood through the recognition of the winding-up (Fig. I.6) of the vortex filaments around the axis as the flow proceeds. Thus, the induced field of the secondary vorticity becomes "self-destructive", leading to the expected downstream decay. It is this behavior of the vortex filaments which dictates the mathematical behavior of the integral in Eq. (3.39). The mathematical behavior of this integral is further discussed in Chapter 6.

3.5 Induction of Downstream Static Pressure Perturbation by the Blade Wakes

For low-speed flow through a blade row which induces a free vortex flow, the mass flux distribution is almost uniform over the entire annulus since the density of the fluid then is very nearly invariant. Consequently, in the absence of blade wakes, the streamlines would be parallel and no static pressure perturbation would arise. (In actuality, there would be an exponentially decaying potential pressure field, associated with the blade thickness; however, this effect is not under

consideration here.) In the presence of the actual blade wakes, however, the above situation does not pertain. In addition to the presence of the usual potential pressure field, which decays exponentially with distance away from the blades, there is another portion of the pressure field induced by the blade wakes as a result of the swirl in the downstream flow field. (See Fig. I.9, for example). The latter part of the pressure field is for practical purposes absent in flow over an isolated airfoil. This fact is shown in the following.

Consistent with the order of approximation use here, Eq. (2.4) becomes

$$\frac{P_t^*}{\rho} = \frac{P}{\rho} + \frac{\overline{W}^2}{2} - \frac{\omega^2 r^2}{2} + \overline{\underline{W}}\cdot\tilde{\underline{W}} \tag{3.51}$$

$$= \frac{P}{\rho} + \frac{\overline{W}^2}{2} - \frac{\omega^2 r^2}{2} + \overline{\underline{W}}\cdot\tilde{\underline{V}}$$

However, in the circumferential mean flow, the rotary stagnation pressure is given by

$$\frac{\overline{P}_t^*}{\rho} = \frac{\overline{P}}{\rho} + \frac{\overline{W}^2}{2} - \frac{\omega^2 r^2}{2}, \tag{3.52}$$

so that the perturbation in static pressure is

$$\frac{\delta P^d}{\rho} = \frac{P^d - \overline{P}^d}{\rho} = -\frac{\delta P_t^*}{\rho} - \overline{\underline{W}}\cdot\tilde{\underline{V}} \tag{3.53}$$

In dimensionless form this perturbation in static pressure is given by

$$\delta P^d = -2\left[\frac{\partial \phi^d}{\partial z} + \left(\frac{K_0}{r} - K_1 r\right)\frac{1}{r}\frac{\partial \phi^d}{\partial \theta}\right] \tag{3.54}$$

where we have taken advantage of Eqs. (3.16) and (3.19) in their appropriate dimensionless forms.

Substituting for $\partial\phi_d/\partial z$ and $\partial\phi_d/\partial\theta$ in Eq. (3.54), we have

$$\delta P^d = \sum_{n=1}^{\infty}\sum_{p=1}^{\infty}\lambda_{np}A^d_{np}\Gamma_{np}(r)e^{-\lambda_{np}z}e^{inB\theta} - \left(\frac{K_0}{r^2}-K_1\right)\sum_{n=1}^{\infty}\sum_{p=1}^{\infty}inBA^d_{np}\Gamma_{np}(r)e^{-\lambda_{np}z}e^{inB\theta}$$

$$-\sum_{n=1}^{\infty}\sum_{p=1}^{\infty}\Gamma_{np}(r)e^{inB\theta}\frac{n^2B^2}{2}\int_h^1\frac{\bar{\omega}_n\left(\frac{K_0}{r^2}-K_1\right)^2 r\Gamma_{np}(r)e^{-inBz\left(\frac{K_0}{r^2}-K_1\right)}}{\left[\lambda_{np}^2+n^2B^2\left(\frac{K_0}{r^2}-K_1\right)^2\right]}dr$$

$$+\left(\frac{K_0}{r^2}-K_1\right)\sum_{n=1}^{\infty}\sum_{p=1}^{\infty}\Gamma_{np}(r)e^{inB\theta}\frac{n^2B^2}{2}\int_h^1\frac{\bar{\omega}_n\left(\frac{K_0}{r^2}-K_1\right) r\Gamma_{np}(r)e^{-inBz\left(\frac{K_0}{r^2}-K_1\right)}}{\left[\lambda_{np}^2+n^2B^2\left(\frac{K_0}{r^2}-K_1\right)^2\right]}dr \quad . \qquad (3.55)$$

The first two double sums, arising from the homogeneous part of the solution, decay exponentially with distance downstream of the blade row. However, the last two double sums do not possess this exponentially decaying behavior; they in fact represent that part of the fluctuating pressure field induced by the presence of the blade wakes. The extent of the downstream distance over which this part of the pressure field will persist is dependent upon the magnitude of (nBK_0). Its amplitude is determined by the value of J, defined by

$$J \equiv \left(\frac{K_0}{r^2}-K_1\right)\int_h^1\frac{\bar{\omega}_n\left(\frac{K_0}{r^2}-K_1\right) r\Gamma_{np}(r)e^{-inBz\left(\frac{K_0}{r^2}-K_1\right)}}{\left[\lambda_{np}^2+n^2B^2\left(\frac{K_0}{r^2}-K_1\right)^2\right]}dr$$

$$-\int_h^1\frac{\bar{\omega}_n\left(\frac{K_0}{r^2}-K_1\right)^2 r\Gamma_{np}(r)e^{-inBz\left(\frac{K_0}{r^2}-K_1\right)}}{\left[\lambda_{np}^2+n^2B^2\left(\frac{K_0}{r^2}-K_1\right)^2\right]}dr \qquad (3.56)$$

This will be discussed further in Chapter 6; there it will be shown that for large argument ($nBK_0 z$) of the exponential in the integrand, the induced pressure field will decay inversely with z and with some power of nBK_0. We note here, however, that in the absence of the downstream swirl, K_0 assumes a zero value so that, for that case, the value of J in Eq. (3.56) becomes identially zero. In such a situation, the blade wakes would not induce a perssure field, apart from the familiar portion which decays exponentially. This arises becuase the wake-induced perturbations are then simply convected by a mean flow without swirl. (This is analogous to the case for flow over an isolated airfoil as well.) Conversely, the fact that there is a pressure field associated with the blade wakes in the presence of the swirl indicates that all perturbations in fluid properties are not simply convected by the mean flow; if that were so, there could not be an induced pressure field.

In the sense that the blade wakes, described here by an appropriate distribution of vortex filaments, induce a pressure field, one can therefore conclude that the fluctuating pressure field is coupled to the vorticity field in the presence of an inertial force field caused by the mean swirl. Consequently, the pressure disturbances and vorticity disturbances are not separable here as would be so in flow over an isolated airfoil; this result is in agreement with the predictions of Kerrebrock[21].

CHAPTER 4 - BASIC AEROTHERMODYNAMIC EQUATIONS, RELATIONS, AND THEIR TRANSFORMATIONS

4.1 Introduction

When the velocity of a fluid in motion becomes comparable with that of sound, effects due to the compressibility of the fluid may become of importance. In the fluid mechanics of low speed flow, thermodynamic consideration are not needed as the heat content of the fluid is then so large compared to the kinetic energy of the flow that the temperature would remain nearly constant even if the whole kinetic energy were to be transformed into heat. However, in high speed flow of gases, the kinetic energy can be comparable with the heat content of the moving fluid, and therefore variations in temperature and density due to compression or expansion of the fluid can become important. In this case, at least at moderately high densities, the motion of the fluid is governed simultaneously by the laws of fluid mechanics and thermodynamics. The equation of continuity is non-linear for a compressible fluid, thereby ruling out Laplace's equation as the governing equation even if the flow is irrotational. Hence the dynamics of compressible fluids is more complicated, and, its analysis more difficult, than that of incompressible fluids.

4.2 Forms of Equation of Motion

The three-dimensional flow of an inviscid compressible fluid through a turbomachine is governed by the following set of basic laws of Aerothermodynamics. For the case of a blade row rotating about its own axis at a constant angular velocity ω, and using the right-handed cylindrical coordinate system (r,θ,z) as defined in Fig. I.1a, the equation of continuity is

$$\frac{\partial \rho}{\partial t} + \nabla\cdot(\rho \underset{\sim}{W}) = 0 \,, \tag{4.1}$$

where the relative velocity $\underset{\sim}{W}$ is related to the absolute velocity $\underset{\sim}{V}$ by equation (2.6).

The equation of motion is

$$\frac{D\underset{\sim}{W}}{Dt} - \omega^2 \underset{\sim}{r} + 2\,\underset{\sim}{\omega} \times \underset{\sim}{W} = -\frac{1}{\rho}\nabla p \,, \tag{4.2}$$

where the operator D/Dt, as defined in Eq. (2.3), refers to differentiation with respect to time following the relative motion of a fluid element. In cases where the relative flow can be approximated as being steady, a relative cylindrical coordinate system (r,θ,z) with θ measured with respect to the rotating blade (Fig. I.1b) will be used (as in Chapters 2 and 3).

For inviscid fluids in which the diffusion and transfer of heat is negligible, the first law of thermodynamics (energy equation) may be written as

$$\frac{De}{Dt} + p\frac{D}{Dt}\left(\frac{1}{\rho}\right) = 0 \,, \tag{4.3}$$

where e is the specific energy related to the temperation T by

$$de = c_v dT \,, \tag{4.4}$$

c_v being the specific heat at constant volume.

For any fluid (sufficiently near equilibrium) there exists an appropriate equation of state; for the ranges of temperature and pressure

encountered in flow through turbomachines, the fluid can be considered essentially as an ideal gas, so that its equation of state is given by

$$P = \rho RT \,, \tag{4.5}$$

where R is the specific gas constant.

It is often convenient to express the state of the fluid in terms of the specific entropy s, and either the rothalpy I or stagnation enthalpy H. The equations governing these quantities are obtained by first using their thermodynamic definitions:

$$TdS = de + Pd\left(\frac{1}{\rho}\right) \,, \tag{4.6}$$

$$H = h + \frac{1}{2}V^2 \,, \tag{4.7}$$

$$I = h + \frac{1}{2}W^2 - \frac{1}{2}\omega^2 r^2 = H - \underset{\sim}{V}\cdot(\underset{\sim}{\omega} \times \underset{\sim}{r}) \,, \tag{4.8}$$

where the specific enthalpy h is

$$h \equiv e + \frac{P}{\rho} \,. \tag{4.9}$$

Equations (4.6) and (4.9) can be combined to give

$$dh = \frac{dP}{\rho} + TdS \tag{4.10}$$

Upon using Eqs. (2.3), (4.8), and (4.10), Eq. (4.2) can be rewritten as

$$\frac{\partial \underset{\sim}{W}}{\partial t} - \underset{\sim}{W} \times (\nabla \times \underset{\sim}{W}) + 2\underset{\sim}{\omega} \times \underset{\sim}{W} = -\nabla I + T\nabla S \ , \tag{4.11}$$

thus giving the dynamical equation in a form conveniently combined with appropriate thermodynamic quantities.

Equations (2.6) and (2.7) can now be used in (4.11) to obtain an alternative form of the equation of motion involving the absolute vorticity $\underset{\sim}{\Omega}$:

$$\frac{\partial \underset{\sim}{W}}{\partial t} - \underset{\sim}{W} \times \underset{\sim}{\Omega} = -\nabla I + T\nabla S \ . \tag{4.12}$$

The rate of change of entropy along a streamline (away from the blades) is

$$\frac{DS}{Dt} = 0 \ , \tag{4.13}$$

where we have combined Eqs. (4.3) with the definition (4.6). This result is expected since the fluid has been assumed to be inviscid and in the absence of heat transfer between fluid particles, each fluid particle will pass through only adiabatic and reversible processes (again: away from the blading)*.

Using Eqs. (4.6), (4.8) in the dot product of Eq. (4.12) with W, and noting that Ds/Dt = 0 (see footnote) we obtain

*Of course, Eq. (4.13) is not expected to hold on passage through shocks, nor in boundary layers; it also holds only approximately (at high Reynolds numbers) in the thin "blade wakes" of concern to us here. However, even for transonic rotors, (4.13) is adequate for our present purposes, especially in the downstream flow.

$$\frac{DI}{Dt} = \frac{1}{\rho}\frac{\partial p}{\partial t} \quad , \tag{4.14}$$

where I is the "rothalpy" defined in Eq. (4.8).

In particular, when the flow relative to the blade row can be considered approximately steady (an example is one with uniform upstream flow passing through an isolated rotating blade row), the continuity equation (4.1) becomes

$$\nabla \cdot \rho \underset{\sim}{W} = 0 \quad , \tag{4.15a}$$

or

$$\nabla \cdot \underset{\sim}{W} + \underset{\sim}{W} \cdot \nabla \ln \rho = 0 \, . \tag{4.15b}$$

Further, the equation of motion (4.12) becomes

$$\underset{\sim}{W} \times \underset{\sim}{\Omega} = \nabla I - T \nabla S \quad , \tag{4.16}$$

Eq. (4.13) reduces to

$$W \cdot \nabla S = 0 \quad ; \tag{4.17}$$

while Eq. (4.14) becomes

$$W \cdot \nabla I = 0 \, . \tag{4.18}$$

Note that Eq. (4.18) is the general form of the Euler turbine equation!

Thus, the entropy s and the rothalpy I remain unchanged along a

relative streamline. We note that in the absolute frame,

$$\left(\frac{\partial S}{\partial t}\right)_{\substack{\text{in absolute}\\ \text{frame}}} = -(\underset{\sim}{\omega}\times\underset{\sim}{r})\cdot\nabla S = -\omega\frac{\partial S}{\partial\theta} \quad . \tag{4.19}$$

For flow through a stationary blade row $\underset{\sim}{\omega} = 0$. In this case there is no longer a need to distinguish between relative and absolute coordinates. The equations of continuity and motion then become

$$\frac{\partial\rho}{\partial t} + \nabla\cdot\rho\underset{\sim}{V} = 0 \tag{4.20}$$

$$\frac{\partial\underset{\sim}{V}}{\partial t} - \underset{\sim}{V}\times\underset{\sim}{\Omega} = -\nabla H + T\nabla S \tag{4.21}$$

while the entropy conservation equation reduces to

$$\frac{\partial S}{\partial t} + \underset{\sim}{V}\cdot\nabla S = 0 \tag{4.22}$$

Further, Eq. (4.14) reduces to

$$\frac{\partial H}{\partial t} + \underset{\sim}{V}\cdot\nabla H = \frac{1}{\rho}\frac{\partial p}{\partial t} \quad , \tag{4.23}$$

showing that the stagnation enthalpy of the fluid can only be changed through an unsteady fluid process.

Finally, for steady absolute flow through a stationary blade row (e.g. flow through an isolated stator), Eqs. (4.20), (4.21), (4.22) and (4.23) become

$$\nabla\cdot(\rho\underset{\sim}{V}) = 0 \, , \tag{4.24a}$$

or

$$\nabla\cdot\underset{\sim}{V} + \underset{\sim}{V}\cdot\nabla \ln\rho = 0 \; ; \tag{4.24b}$$

$$\underset{\sim}{V}\times\underset{\sim}{\Omega} = \nabla H - T\nabla S \; ; \tag{4.25}$$

$$\underset{\sim}{V}\cdot\nabla S = 0 \; ; \tag{4.26}$$

and

$$\underset{\sim}{V}\cdot\nabla H = 0 \; . \tag{4.27}$$

Thus, for steady flow in the absolute frame, the entropy s and the stagnation enthalpy H remain constant along flow streamlines.

Once again, we note the similarity between the set of Eqs. (4.15), (4.16), (4.17), (4.18), with that of Eqs. (4.24), (4.25), (4.26), (4.27). In consequence, the analyses in Sections 4.3, 4.4, 4.5, and 4.6 is applicable in both cases, given appropriate interpretation.

4.3 Irrotational Flow

When the gradient of both the rothalpy I and the entropy s vanish or when they are such that the difference betwen ∇I and $T\nabla s$ vanishes, Eq. (4.16) becomes, once again,

$$\underset{\sim}{W}\times\underset{\sim}{\Omega} = 0 \tag{4.28}$$

Further, if the vorticity $\underset{\sim}{\Omega}$ is zero everywhere [thus satisfying (4.28) for this special case) then the velocity V may be written in terms of a velocity potential ϕ,

$$\underset{\sim}{V} = \nabla\phi \tag{4.29}$$

However, as already mentioned, application of the continuity equation no longer yields simply Laplace's equation for ϕ. In fact, in order to obtain a governing equation for the velocity potential ϕ, we can begin by writing the equation of motion (4.2) in the special form

$$\underset{\sim}{W}\cdot[\underset{\sim}{W}\cdot\nabla\underset{\sim}{W} - \omega^2\underset{\sim}{r} + 2\underset{\sim}{\omega}\times\underset{\sim}{W}] = -\frac{1}{\rho}\underset{\sim}{W}\cdot\nabla p = -\left(\frac{\partial p}{\partial\rho}\right)_s \underset{\sim}{W}\cdot\nabla\rho \ , \tag{4.30}$$

where, on the rhs of (4.30), we have used the restriction, applicable here, that p changes along streamlines only as ρ does, as this process is essentially isentropic [(4.13)]. From the definition of the local velocity of sound,

$$a^2 \equiv \left(\frac{\partial p}{\partial\rho}\right)_s \ ; \tag{4.31}$$

moreover, we can eliminate the remaining term $\underset{\sim}{W}\cdot\nabla\ell n\rho$ through the continuity equation (4.24b). We then obtain,

$$\nabla\cdot\underset{\sim}{W} - \frac{1}{a^2}\underset{\sim}{W}\cdot(\underset{\sim}{W}\cdot\nabla\underset{\sim}{W}) - \frac{1}{a^2}\omega^2\underset{\sim}{W}\cdot\underset{\sim}{r} = 0 \ . \tag{4.32}$$

(Here we have also noted that $\underset{\sim}{W}\cdot(\omega\times\underset{\sim}{W}) \equiv 0$.)

Substitution of $\underset{\sim}{W}$ in Eq. (4.32), with the help of Eqs. (2.6) and (4.29), yields

$$\cdot\nabla^2\phi - \frac{1}{a^2}(\nabla\phi - \underset{\sim}{\omega}\times\underset{\sim}{r})\cdot[(\nabla\phi - \underset{\sim}{\omega}\times\underset{\sim}{r})\cdot\nabla(\nabla\phi - \underset{\sim}{\omega}\times\underset{\sim}{r})] - \frac{1}{a^2}\omega^2\nabla\phi\cdot\underset{\sim}{r} = 0 , \qquad (4.33)$$

the solution of which, with appropriate boundary conditions, determines the irrotational flow under discussion, once $a \equiv (\partial p/\partial\rho)_s$ is found. In particular, one can use (4.33) for study of the uniform flow upstream of a transonic rotor[20,29]. However, this equation is highly non-linear in ϕ, in addition to being coupled with the equation(s) determining a. Often analytic solution is practical only through linearized perturbation techniques.

4.4 Beltrami Flow[4]

If all the vortex filaments of the flow field lie along the streamlines, Eq. (4.28) is again satisfied identically. This is "Beltrami" flow, discussed in Section 2.3 for the incompressible case. Here, we write[20,29]

$$\nabla\times\underset{\sim}{V} \equiv \underset{\sim}{\Omega} = \lambda\underset{\sim}{W} = \left(\frac{\lambda}{\rho}\right)(\rho\underset{\sim}{W}) . \qquad (4.34)$$

Taking the divergence of Eq. (4.34) yields the restraint

$$(\rho\underset{\sim}{W})\cdot\nabla\left(\frac{\lambda}{\rho}\right) = 0 , \qquad (4.35)$$

where we have made use of the continuity equation (4.15a) and the fact that the vorticity vector $\underset{\sim}{\Omega}$ is solenoidal. In fact, because of the latter fact, we can again write (see Section 2.3)

$$\nabla\times\underset{\sim}{V} \equiv \underset{\sim}{\Omega} = \left(\frac{\lambda}{\rho}\right)(\rho\underset{\sim}{W}) = \nabla S\times\nabla\Gamma , \qquad (4.36)$$

While, in this case, applying (4.15a), we also have[11,29]

$$\rho \underset{\sim}{W} = \nabla\alpha \times \nabla\beta . \tag{4.37}$$

Thus, from Eq. (4.35), we obtain, in analogy with Eq. (2.23),

$$\left(\frac{\lambda}{\rho}\right) = \frac{\lambda}{\rho}(\alpha, \beta) , \tag{4.38}$$

Again, we see that the scalar functions S and Γ depends on α and β only; these quantities retain the physical meaning given in Section 2.3. Eq. (4.38) demonstrates that the velocity vector can once more be written as

$$\underset{\sim}{V} = \nabla\phi_I + S\nabla\Gamma , \tag{4.39a}$$

or

$$\underset{\sim}{V} = \nabla\phi_{II} - \Gamma\nabla S . \tag{4.39b}$$

Substitution of $\underset{\sim}{W}$ in Eq. (4.32), using Eqs. (2.6) and (4.39), yeilds the (downstream) equation for the velocity potential ϕ for the compressible, Beltrami-flow case. This velocity potential ϕ can be used to describe the downstream flow of a transonic rotor[20,29], in which the blade loading is of the non-free vortex type, while the upstream flow is uniform.

4.5 Homentropic Rotational Flow with a Rothalpy or Stagnation Enthalpy Gradient

When the entropy is constant throughout but there is a gradient in rothalpy or stagnation enthalpy[29], Eq. (4.16) becomes

$$\underset{\sim}{W} \times \underset{\sim}{\Omega} = \nabla I , \tag{4.40}$$

and the Clebsch-Hawthorne Formulation[4] is particularly useful, as

illustrated in Section 2.4. Upon choosing $\sigma \equiv I$ (or $\sigma \equiv H$ in the case of steady flow in the absolute frame, as for an isolated stator), we obtain the results:

$$\underset{\sim}{V} = \nabla\phi_I - I\nabla\tau \ , \tag{4.41a}$$

or

$$\underset{\sim}{V} = \nabla\phi_{II} - \tau\nabla I \ , \tag{4.41b}$$

with

$$\tau = \int_{S_o}^{S} \frac{dS}{W} \ . \tag{4.42}$$

Again, as discussed earlier for the case of incompressible flow,

$$\underset{\sim}{\Omega} \equiv \nabla \times \underset{\sim}{V} = \nabla I \times \nabla\tau \ . \tag{4.43}$$

On substituting for $\underset{\sim}{W}$ in Eqs. (4.32), using Eqs. (2.4) and (4.41), we obtain once more a governing equation for the velocity potential ϕ, coupled with the appropriate energy relation for this situation.

4.6 General Case of Steady, Homentropic, Rotational Flow.

Collecting the results of Sections 4.4 and 4.6, we write the velocity vector $\underset{\sim}{V}$ for the general case of a steady, homentropic, rotational flow as

$$\underset{\sim}{V} = \nabla\phi + \underset{\sim}{A} \ , \tag{4.44}$$

where the vector $\underset{\sim}{A}$ is given by

$$A = I\nabla\tau + S\nabla\Gamma \ , \tag{4.45a}$$

or

$$\underset{\sim}{A} = -\tau\nabla I - \Gamma\nabla S \,. \tag{4.45b}$$

Thus, the vorticity $\underset{\sim}{\Omega}$ is

$$\underset{\sim}{\Omega} \equiv \nabla \times \underset{\sim}{V} = \nabla \times \underset{\sim}{A} = \lambda \underset{\sim}{W} + \underset{\sim}{\Omega}_\tau = \nabla S \times \nabla \Gamma + \nabla I \times \nabla \tau \tag{4.46}$$

with

$$\underset{\sim}{W} \times \underset{\sim}{\Omega}_\tau = \nabla I \tag{4.47}$$

A governing equation for ϕ is given again obtained through the use of Eq. (4.32).

However, as we shall see, when the flow is non-homentropic, direct application of the Clebsch-Hawthorne Formulation is no longer possible.

4.7 Transformation of Steady Flows

It is well-known that there exist a great many different modes of steady flow of an ideal fluid which have the same streamline pattern[4,27,28]. In the study of steady flows of an ideal fluid, one is therefore interested in finding possible transformations between flows of the same general type, possessing similar streamline patterns. In what follows, we restrict ourselves to the case of steady flows in ideal gases, and in an absolute frame, unless otherwise stated.

Given an "original" flow, governed by Eqs. (4.24) through (4.27), the determination of corresponding (transformed) flows with the same streamline patterns (for which the pressure remains unchanged) involves the determination of a so-called "reduced" velocity field, $\underset{\sim}{V}_R$, together with a reduced density field, ρ_R. These can be determined by writing

$$\underset{\sim}{V}_R = f_1 \underset{\sim}{V} \ , \tag{4.48}$$

and

$$\rho_R = f_2 \rho \ , \tag{4.49}$$

and choosing f_1, f_2 such that one does not violate continuity and momentum conservation.

The continuity condition requires

$$\nabla\cdot(\rho_R \underset{\sim}{V}_R) = \nabla\cdot[(f_1 f_2)(\rho \underset{\sim}{V})] = (f_1 f_2)\nabla\cdot(\rho \underset{\sim}{V}) + \rho \underset{\sim}{V}\cdot\nabla(f_1 f_2) = 0 \ .$$

But, by virtue of Eq. (4.24), the above yields simply

$$\underset{\sim}{V}\cdot\nabla(f_1 f_2) = 0 \ . \tag{4.50}$$

On the other hand, the curl of Eq. (4.25) is

$$\nabla\times(\underset{\sim}{V}\times\underset{\sim}{\Omega}) = -\nabla T \times \nabla S \ . \tag{4.51a}$$

Alternatively, this can be written (directly from the Euler equations) as

$$\nabla\times(\underset{\sim}{V}\cdot\nabla\underset{\sim}{V}) = -\nabla\frac{1}{\rho}\times\nabla p \ . \tag{4.51b}$$

Thus, momentum conservation requires

$$\left(f_1^2 - \frac{1}{f_2}\right)\left(\nabla\frac{1}{\rho}\times\nabla p\right) + \frac{1}{\rho}\nabla\left(f_1^2 - \frac{1}{f_2}\right)\times\nabla p = 0 \ ,$$

i.e.,

$$\nabla\frac{1}{\rho}\left(f_1^2 - \frac{1}{f_2}\right)\times\nabla p = 0 \ . \tag{4.52}$$

Thus, any choice of f_1 and f_2 which simultaneously satisfies conditions (4.50) and (4.52) will give a steady flow with the same streamline pattern and equal pressure fields. Of course, there are many choices of f_1, f_2; here we simply note that a useful form is that given by

$$f_2 = f_1^{-2} \equiv F \tag{4.53}$$

such that

$$\nabla(f_1 f_2) \equiv \nabla(f_2^3) \neq 0 .$$

For this particular choice, the continuity condition simply demands, as we have seen, that the product of f_1 and f_2 be conserved along streamlines. We already know, for this case, that the entropy s, together with the stagnation properties of fluid particles remain unchanged also along such streamlines. Hence, the function F can be taken to be any function of the entropy s or of any of the stagnation properties of the fluid, so long as the values of density and velocity along each streamline of the "reduced" flow are increased respectively by a factor of F and $F^{-1/2}$. (We recall that F may vary from streamline to streamline.)

The choice of f_1 and f_2, given in Eq. (4.53), has the following implications:

(a) We note first that $\rho_R V_R^2 = \rho V^2$. Hence, the force component normal to the streamline due to the centrifugal action of the flow in any "reduced" flow is the same as that in the given "original" flow. Dynamic equilibrium of the flows then requires that this force component be equal to the normal component of the pressure gradient in each case. Hence, the pressure field is the same in the two corresponding flows.

(b) The quantity $(p + 1/2\ \rho V^2)$ [or $(\gamma/\gamma\text{-}1\ p + 1/2\ \rho V^2)$] is constant (and the same) in each flow, implying that there is dynamic equilibrium of force components along the corresponding streamlines (Bernoulli).

(c) For a calorically perfect cas (i.e., one with constant specific heats, c_p and c_v), the velocity of sound a is given by

$$a = \sqrt{\left(\frac{\partial p}{\partial \rho}\right)_s} = \sqrt{\frac{\gamma p}{\rho}} \quad , \tag{4.54}$$

in the original flow, while in the reduced flow it is given by

$$a_R = \sqrt{\left(\frac{\partial p}{\partial \rho_R}\right)_s} = \sqrt{\frac{\gamma p}{\rho_R}} \tag{4.55}$$

where $\gamma = c_p/c_v$ for both cases. The Mach numbers in the original flow and reduced flow, respectively, are given by

$$M \equiv \frac{V}{a} = \sqrt{\frac{\rho V^2}{\gamma p}} \quad , \tag{4.56}$$

and

$$M_R \equiv \frac{V_R}{a_R} = \sqrt{\frac{\rho_R V_R^2}{\gamma p}} \quad . \tag{4.57}$$

By virtue of the consequence (a) stated above,

$$M = M_R \quad . \tag{4.58}$$

Hence, the Mach numbers remain unchanged by the transformation embodied in Eqs. (4.53).

(d) Because the pressures are left unchanged by this transformation, any (pressure) drag and lift force acting on any body in the reduced flow

will be the same as those on a corresponding body in the original flow.

(e) Since the velocity of the reduced flow at any point differs from that of the original flow at the corresponding point by a scalar only, it follows that if the original flow satisfies the kinematic boundary conditions at certain boundaries the reduced flow does so as well at the corresponding boundaries.

In the reduced flow, the continuity equation is

$$\nabla \cdot \rho_R \underset{\sim}{V}_R = 0 , \tag{4.59a}$$

or

$$\nabla \cdot \underset{\sim}{V}_R + \underset{\sim}{V}_R \cdot \nabla \ln \rho_R = 0 , \tag{4.59b}$$

while the equation of motion is given by

$$\underset{\sim}{V}_R \cdot \nabla \underset{\sim}{V}_R = -\frac{1}{\rho_R} \nabla p \quad . \tag{4.60}$$

The curl of equation (4.60) gives the reduced flow Helmhotz equation in the form

$$\underset{\sim}{V}_R \cdot \nabla \left(\frac{\underset{\sim}{\Omega}_R}{\rho_R} \right) - \left(\frac{\underset{\sim}{\Omega}_R}{\rho_R} \right) \cdot \nabla \underset{\sim}{V}_R = -\nabla \left(\frac{1}{\rho_R} \right) \times \nabla p \quad , \tag{4.61}$$

where the vorticity $\underset{\sim}{\Omega}_R$ of the reduced flow is defined by

$$\underset{\sim}{\Omega}_R \equiv \nabla \times \underset{\sim}{V}_R \quad . \tag{4.62}$$

4.8 Yih's Transformation

We note that if the density ρ_R is a unique function of the pressure throughout, then the acceleration field, $- 1/\rho_R \nabla p$, has a potential. This

is necessary (but not sufficient) for irrotationality of the reduced flow [see Eq. (4.61)]. Indeed, if the RHS of Eq. (4.61) vanishes, persistence of irrotationality of the reduced flow, once established, is indicated. We have already noted that a major difficulty in dealing with (untransformed) non-homentropic flow is that the acceleration field $1/\rho\nabla p$ for such cases does not possess a potential. Consequently, the original fluid motion, even when starting uniformly from rest will not continue to be irrotational.

We note that for a calorically perfect gas,

$$\frac{\rho e^{\frac{s}{c_p}}}{p^{1/\gamma}} = \tag{4.63}$$

so that by choosing

$$\rho_R = f_2 \rho = e^{\frac{s}{c_p}} \rho \ , \tag{4.64}$$

we can guarantee that ρ_R be a unique function of the pressure throughout. We then obtain

$$f_2 = F = e^{\frac{s}{c_p}} \ , \tag{4.65}$$

and, by virtue of Eq. (4.53),

$$\cdot\ f_1 = e^{-s/2c_p} \ . \tag{4.66}$$

Finally, we arrive at a transformation between flows, due to Yih[32], given here by

$$\cdot\ \rho_R = \rho e^{s/c_p} \ , \quad \underset{\sim}{V}_R = e^{-s/2c_p} \underset{\sim}{V} \ . \tag{4.67}$$

This implies that for every homentropic flow ($\underset{\sim}{V}_R$, ρ_R), there corresponds a non-homentropic flow (V,ρ), and vice versa.

4.9 The Clebsch-Hawthorne Formulation for Reduced Flow

The momentum equation (4.60) for a reduced flow represented by Eq. (4.67) may be written as

$$\underset{\sim}{V}_R \times \underset{\sim}{\Omega}_R = \nabla H e^{-S/c_p} = c_p \nabla P_t^{\left(\frac{\gamma-1}{\gamma}\right)} \tag{4.68}$$

(see Appendix).

For a flow with uniform stagnation pressure field,

$$\underset{\sim}{V}_R \times \underset{\sim}{\Omega}_R = 0 \quad ; \tag{4.69}$$

so that either the reduced flow is irrotational or has its vortex filaments lying in the direction of its streamlines ("reduced" Beltrami flow). An irrotational reduced flow can be described by

$$\underset{\sim}{V}_R = \nabla \phi_R \quad , \tag{4.70}$$

where ϕ_R is the reduced velocity potential. (It is useful to emphasize, however, that irrotationality of the reduced flow does not imply irrotationality of the original flow.)

By dotting Eq. (4.60) with $\underset{\sim}{V}_R$ [with its RHS written as $-(\partial p/\partial \rho_R)_s \nabla \ell n\ \rho_R$] and elminating $\underset{\sim}{V}_R \cdot \nabla \ell n\ \rho_R$ using the continuity equation (4.59b), we obtain

$$\nabla \cdot \underset{\sim}{V}_R - \frac{1}{Q_R^2} \underset{\sim}{V}_R \cdot (\underset{\sim}{V}_R \cdot \nabla \underset{\sim}{V}_R) = 0, \tag{4.71}$$

where we have used Eq. (4.55). Thus, a governing equation for ϕ_R can be obtained by the substitution of Eqs. (4.70) in (4.71), i.e.,

$$\nabla^2\phi_R - \frac{1}{a_R^2}\nabla\phi_R\cdot[(\nabla\phi_R\cdot\nabla)\nabla\phi_R]=0\ . \tag{4.72}$$

This result is, of course, still non-linear, despite the transformation to the reduced flow. However, it has the great advantage of being treatable as a homentropic flow in terms of the "reduced" variables.

For a reduced Beltrami flow, we can now write, in analogy with (4.34),

$$\nabla\times\underset{\sim}{V}_R \equiv \underset{\sim}{\Omega}_R = \lambda_R\underset{\sim}{V}_R = \left(\frac{\lambda_R}{\rho_R}\right)(\rho_R\underset{\sim}{V}_R) \tag{4.73}$$

Because the vectors $\underset{\sim}{\Omega}_R$ and $(\rho_R\underset{\sim}{V}_R)$ are divergence free, one can write

$$\underset{\sim}{\Omega}_R = \nabla S_R\times\nabla\Gamma_R\ , \tag{4.74}$$

and

$$\rho_R\underset{\sim}{V}_R = \nabla\alpha_R\times\nabla\beta_R \tag{4.75}$$

so that

$$(\rho_R\underset{\sim}{V}_R)\cdot\nabla\left(\frac{\lambda_R}{\rho_R}\right)=0 \tag{4.76}$$

$$\frac{\lambda_R}{\rho_R} = \frac{\lambda_R}{\rho_R}(\alpha_R,\beta_R) \tag{4.77}$$

Again, by virtue of Eqs. (4.75), (4.77), (4.73) and (4.74), S_R and Γ_R are dependent on α_R and β_R only. Moreover,

$$\underset{\sim}{V}_R = \nabla\phi_R^I + S_R\nabla\Gamma_R \ , \tag{4.78a}$$

or

$$\underset{\sim}{V}_R = \nabla\phi_R^{II} - \Gamma_R\nabla S_R \tag{4.78b}$$

A governing equation for ϕ_R^I or ϕ_R^{II} is then obtained (as previously) by substitution of Eq. (4.78) in Eq. (4.71).

The appropriate application of the Clebsch-Hawthorne Formulation for reduced flows with stagnation pressure varying from streamline to streamline is now apparent. By choosing

$$\sigma_R \equiv He^{-S/c_p} = c_p P_t^{\left(\frac{\gamma-1}{\gamma}\right)} \tag{4.79}$$

we obtain the results that:

$$\underset{\sim}{V}_R = \nabla\phi_{R1} + \left[c_p P_t^{\left(\frac{\gamma-1}{\gamma}\right)}\right]\nabla\tau_R \ , \tag{4.80a}$$

or

$$\underset{\sim}{V}_R = \nabla\phi_{R2} - \tau_R\nabla\left[c_p P_t^{\left(\frac{\gamma-1}{\gamma}\right)}\right] \ , \tag{4.80b}$$

while

$$\tau_R = \int_{s_o}^{s} \frac{ds}{V_R} \ . \tag{4.81}$$

As expected, τ_R is the "drift function" of Darwin and others, in the "reduced" flow. Finally

$$\underset{\sim}{\Omega}_R = \nabla\left[C_p P_t^{\left(\frac{\gamma-1}{\gamma}\right)}\right] \times \nabla \tau_R \,. \tag{4.82}$$

Substitution of Eqs. (4.80) in (4.71) yields a governing equation for ϕ_{R1} or ϕ_{R2}, in this case including significant vorticity arising from the variation, from streamline to streamline, of the actual flow entropy (or stagnation pressure).

Collecting the above results, we find that the velocity vector $\underset{\sim}{V}_R$ of the general case of a steady, rotational reduced flow is given in a form by now familiar:

$$\underset{\sim}{V}_R = \nabla \phi_R + \underset{\sim}{A}_R \quad , \tag{4.83}$$

where the vector $\underset{\sim}{A}_R$ is given by

$$\underset{\sim}{A}_R = \left[C_p P_t^{\left(\frac{\gamma-1}{\gamma}\right)}\right] \nabla \tau_R + S_R \nabla \Gamma_R \,, \tag{4.84a}$$

or

$$\underset{\sim}{A}_R = \tau_R \nabla \left[C_p P_t^{\left(\frac{\gamma-1}{\gamma}\right)}\right] - \Gamma_R \nabla S_R \,. \tag{4.84b}$$

Again, the vorticity $\underset{\sim}{\Omega}_R$ is

$$\begin{aligned} \underset{\sim}{\Omega}_R = \nabla \times \underset{\sim}{A}_R &= \lambda_R \underset{\sim}{V}_R + \underset{\sim}{\Omega} \tau_R \\ &= \nabla S_R \times \nabla \Gamma_R + \nabla\left[C_p P_t^{\left(\frac{\gamma-1}{\gamma}\right)}\right] \times \nabla \tau_R \end{aligned} \tag{4.85}$$

with

$$\underset{\sim}{V}_R \times \underset{\sim}{\Omega} \tau_R = \nabla [c_p P_t^{(\frac{\gamma-1}{\gamma})}] \tag{4.86}$$

As before, a governing equation for ϕ_R is obtained through Eq. (4.71).

The above formulation is exact (for a perfect gas in non-homentropic flow) but the resulting equations are highly non-linear. They can be treated analytically only after making appropriate linearizing approximations. Adopting relatively recently developed techniques[26,29] for this purpose, however, we are able to apply such procedures to practical turbomachines.

4.10 Reduced Flow in Rotating Coordinates

Up to this point, we have only considered reduced flows which are steady in the absolute frame. Application of the transformation as defined by Eqs. (4.65) and (4.66) to a flow steady relative to a rotating frame yields

$$\nabla \cdot \rho_R \underset{\sim}{W}_R = 0 \tag{4.87}$$

as the equation of continuity, and

$$\underset{\sim}{W}_R \times \underset{\sim}{\Omega}_R = \nabla I e^{-S/c_p} + \frac{1}{2}(H-I)\nabla e^{-S/c_p} \tag{4.88}$$

as the equation of motion. Hence we have used

$$\underset{\sim}{V}_R \equiv \underset{\sim}{W}_R + \underset{\sim}{\omega}_R \times \underset{\sim}{r} \tag{4.89}$$

and

$$\underset{\sim}{\omega}_R \equiv e^{-S/2c_p} \underset{\sim}{\omega}. \tag{4.90}$$

to obtain Eqs. (4.87) and (4.88).

Thus, extension of the Clebsch-Hawthorne Formulation is possible in its usual form only if the difference between stagnation enthalpy and rothalpy is a constant or a unique function of the entropy s. The physical reason for this complication is that in such a flow, changes in streamline pattern can result from gradients of rothalpy as well as the interaction of Coriolis and centrifugal forces with an entropy gradient. However, as we shall see later, for flows with small deviation from mean free-vortex swirl, extension of the Clebsch formulation is possible in an approximate way.

CHAPTER 5 - VISCOUS BLADE-WAKES IN COMPRESSIBLE FLOW

5.1 Analytical Formulation

As before (see Chapter 2), we consider the flow through an isolated rotor (rotating at an angular velocity ω about its own axis) encased in an infinite cylindrical annulus, again using the right-handed cylindrical coordinate system (r,θ,z) illustrated in Fig. I.1a. Far upstream of the rotor, the flow is assumed uniform with purely axial velocity; while downstream of the rotor, a free-vortex mean flow is once more specified as our "reference" flow. For this example, then, the fluid properties at a particular point can be taken to be steady relative to the (isolated) rotor. It is then once more convenient to use a relative cylindrical coordinate system (r,θ,z) with θ measured with respect to the rotating blade (Fig. I.1b).

The process of viscous interaction between the working fluid and the blade surfaces is an irreversible one; thus, there will result in an inevitable increase in entropy (following the appropriate fluid particles along the blading) in accordance with the Second Law of Thermodyanmics. In this way the effects of viscous losses occurring within the blade row appear downstream as variation of entropy across the stream surfaces. Thus, the blade wakes may be regarded as regions of entropy excess. Consequently, because of real fluid effects, the flow downstream of any blade row is inherently non-homentropic. Analytically, this feature of the flow introduces significant complexity into the aerothermodynamic equations (as is already clear from the development given in Chapter 4). Strictly speaking, analytical modeling of the blade wakes using the concept of entropy is both conveneint and appropriate. Its use, rather, than that of the concept of

stagnation pressure (used above in the case of incompressible flow) is particularly useful for our purposes here because entropy is a thermodynamic property of the fluid and remains invariant in transformation between various velocity frames.

For typical flow conditions occurring in turbomachines, viscous effects in the blade passages are generally confined to thin boundary layers on the blades and the thickness (measured in units of appropriate scale length) is of the order of the inverse of the square root of Reynolds number. In consequence, the deviation of the downstream flow field from homentropy must remain small. (To be precise, the change in specific entropy as a result of viscous interaction within the blade row is small compared to the specific heat content per unit temperature of the incoming fluid). Hence, [see Eq. (4.84)] the vorticity will be small; the three-dimensional aspects of the flow introduced by departure from homentropy can again be considered as a small perturbation of the flow about the mean axisymmetric throughflow. In the analysis to follow, the flow is consequently separated into a circumferentially averaged flow of zeroth order, $\bar{\underset{\sim}{V}}$ (or $\bar{\underset{\sim}{W}}$ in the relative frame), and a three-dimensional perturbation flow, $\tilde{\underset{\sim}{V}}$, of order ε, where

$$\varepsilon \sim \frac{\tilde{V}}{\bar{V}} \sim \frac{T\Delta S}{\frac{1}{2}\bar{V}^2} \ll 1 . \tag{5.1}$$

This idea is, as before, exploited in the development of the three-dimensional theory for the compressible flow including blade wakes in axial turbomachines.

With a rotor of free-vortex design in compressible flow, the axial velocity far upstream and downstream of the blade row approaches a constant (it is such throughout in the incompressible case). Whereas, for

low speed flow through the rotor, the variation of density with radius (associated, for example, with centrifugal effects) may be considered negligible so that the mass flux distribution is almost uniform over the entire annulus. On the other hand, for high speed flow through such machines, the velocities are sufficiently large so that the compressibility of the flow has to be fully considered. Hence, across a blade row the given tangential velocity distribution forces radial density gradients of various quantitites, for example the radial velocity, etc.

The resulting shift of streamlines associated with this radial velocity causes the whole flow to readjust itself in several aspects. This radial shift of streamlines and the corresponding flow disturbances will relax axially. Thus, the circumferentially averaged flow will possess both a radial and an axial dependence which in principle complicates the analytical determination of the three-dimensional perturbations even with respect to the mean streamlines of the circumferentially averaged flow. However, we find that we can take advantage of the fact that this disturbance, which occurs near the blade row, is in fact small (even if not negligible). This occurs in an axial turbomachine because the annular flow region is bounded by walls which tend toward concentric cylinders thus leading not only to a small but also a gradual radial shift of the streamlines as the flow passes through the blade row. As an important result, we are able to neglect this particular effect in so far as it affects the three-dimensional perturbations to be described in the following. However, the three-dimensional perturbations so determined are to be superimposed on the actual mean flow (not, for example, on a simple radial equilibrium flow).

In the approximation just discussed, we can write Eq. (4.84) in the simplified form

$$\underset{\sim}{W}_0 \times \underset{\sim}{\Omega}_R \simeq \nabla(I e^{-S/c_p}) + \frac{1}{2} V_{\theta 0} r \omega \nabla e^{-S/c_p} , \tag{5.2}$$

where subscript "0" refers to that of the simple radial equilibrium flow mentioned above. For free-vortex flow, with the tangential velocity inversely proportional to the radius ($V_{\theta 0} r$ = constant = $V_{z0}^{u} K_0$), Eq. (5.2) assumes the even simpler form

$$\underset{\sim}{W}_0 \times \underset{\sim}{\Omega}_R = \nabla[(I + \frac{1}{2} \omega V_{z0}^{u} k_0) e^{-S/c_p}] , \tag{5.3}$$

with $K_0 = V_{\theta 0}^{d} r / V_{z0}^{u}$.

The approximation leading to Eq. (5.3) also results in

$$\underset{\sim}{W}_0 \cdot \nabla[(I + \frac{1}{2} \omega V_{z0}^{u} K_0) e^{-S/c_p}] = 0 , \tag{5.4}$$

and

$$\underset{\sim}{\Omega}_R \cdot \nabla[(I + \frac{1}{2} \omega V_{z0}^{u} K_0) e^{-S/c_p}] = 0 . \tag{5.5}$$

From (5.4), we note that the quantitiy $(I + 1/2\omega\ V_{z0}^{u}\ K_0)\ e^{-s/p}$ remains constant along the streamlines of the approximate relative flow provided by radial equilibrium theory.

With the above equations taking the present form, we are again able to apply the Clebsch-Hawthorne formulation for the determination of three-dimensional perturbations. We can write, quite generally,

$$\underset{\sim}{\tilde{V}}_R = \nabla \phi_R + \sigma_R \nabla \tau_R , \tag{5.6a}$$

or

$$\tilde{\underset{\sim}{V}}_R = \nabla\phi_R - \tau_R\nabla\sigma_R \ , \tag{5.6b}$$

whence the vorticity $\underset{\sim}{\Omega}_R$ is given by

$$\underset{\sim}{\Omega}_R \equiv \nabla \times \tilde{\underset{\sim}{V}}_R = \nabla\sigma_R \times \nabla\tau_R \ . \tag{5.7}$$

Eq. (5.5) suggests that a suitable choice for σ_R is

$$\sigma_R \equiv -\left(1 + \frac{1}{2}\omega V_{z_0}^4 k_0\right)\frac{s}{c_p} \ , \tag{5.8}$$

where, here, we have made use of the additional approximation

$$e^{-s/c_p} = 1 - \frac{s}{c_p} + \cdots \ , \tag{5.9}$$

and assumed that part of σ_R which is constant can be absorbed in ϕ_R in Eq. (5.6a).

By substituting σ_R as given in (5.8) in Eq. (5.7) and by using Eq. (5.3), we obtain

$$\underset{\sim}{\Omega}_R \simeq \left(\underset{\sim}{W}_0 \cdot \nabla\tau_R\right)\underset{\sim}{\Omega}_R \ ; \tag{5.10}$$

here, we have made use of the fact that $\underset{\sim}{\Omega}_R$ lies on surfaces of constant τ_R. So, in this approximation

$$\underset{\sim}{W}_0 \cdot \nabla\tau_R = 1 , \tag{5.11a}$$

or

$$W_0 \frac{\partial\tau_R}{\partial s} = 1 \ . \tag{5.11b}$$

Thus, the three-dimensional perturbed flow can again be evaluated by using the "drift function" τ_R determined by the above radial equilibrium flow. Integrating Eq. (5.11b) along the relevant streamlines, we obtain

$$\tau_R = \int_0^S \frac{dS}{W_0} \,. \tag{5.12}$$

The relative velocity vector $\underset{\sim}{W}_0$ downstream of the rotor is given by

$$\underset{\sim}{W}_0 = (V_{\theta 0}^d - \omega r)\,\hat{e}_\theta + V_{z0}^d\,\hat{e}_z \,, \tag{5.13}$$

while the axial velocity V_{z0}^d is constant, appropriate to free-vortex flow. Because of Eq. (5.13), we can also write

$$\tau_R = \int_0^z \frac{dz}{V_{z0}} = \frac{z}{V_{z0}} \,, \tag{5.14}$$

or

$$\tau_R = \int_{\theta_0(r)}^{\theta} \frac{r\,d\theta}{(V_{\theta 0} - \omega r)} = \frac{r(\theta - \theta_0(r))}{(V_{\theta 0} - \omega r)} \,. \tag{5.15}$$

As discussed previously (see Chapter 4, pg.65), the entropy remains constant on streamlines of the relative mean radial equilibrium flow within the present approximation. Here this implies

$$\underset{\sim}{W}_0 \cdot \nabla S = 0 \,. \tag{5.16}$$

[This result also follows from Eq. (5.4) since $(I + 1/2\ \omega V_{z0}^u\ K_0)$ is constant.] As a result the entropy has an arbitrary dependence only on r and α_0^d, [compared to Eqs. (3.10), Chapter 3]:

$$\frac{S}{C_p} = \frac{S}{C_p}(r, \alpha_0^d) \,, \tag{5.17}$$

where, here, we have defined

$$\alpha_o^d = \left[\theta - z\left(\frac{V_{zo}^u}{V_{zo}^d}\frac{K_o}{r^2} - \frac{\omega}{V_{zo}^d}\right)\right] \tag{5.18}$$

Guided by the analysis in Chapter 3, we choose to use the drift function τ_R as given in Eq. (5.14) in describing the (reduced) vorticity field introduced by the presence in compressible flow, of the blade wakes. It follows that Eq. (5.6a) becomes

$$\tilde{\underset{\sim}{V}}_R = \nabla\phi_R - \frac{(I+\frac{1}{2}\omega V_{zo}^u K_o)}{V_{zo}^d}\frac{S}{C_p}\hat{e}_z, \tag{5.19}$$

which, in analogy with the case discussed in Chapter 3, implies that any gradient in entropy due to the blade wakes can be described in terms of (reduced) vortex filaments on purely axial planes.

In order to proceed further, we now require the knowlege of entropy production within the blade row. As in Chapter 3, we obtain this information from available data. However, one does not measure entropy directly; rather, losses within the blade row are quoted in terms of measured stagnation pressure defect. Therefore, we need to relate stagnation pressure loss to the entropy production in which we are interested here. For a calorically perfect gas (i.e., one with constant specific heats), the entropy change across the blade row (or equivalently the difference between the entropy of the fluid in the wake and that of the fluid outside of the wake is given by

$$\frac{\Delta S}{C_p} = \ln\frac{T_t^d}{T_t^u} - \frac{\gamma-1}{\gamma}\ln\frac{P_t^d}{P_t^u}, \tag{5.20}$$

where the subscript "t" refers to stagnation property of the fluid.

In the case of a stator, the stagnation temperature is constant throughout so that T_t^d/T_t^u is unity while, for a rotor, the stagnation quantities should appropriately be replaced by those in the rotating coordinate.* Thus, we can simply write,

$$\frac{\Delta S}{C_p} = -\frac{\gamma-1}{\gamma} \ln \frac{P_t^d}{P_t^u} \tag{5.21}$$

except in the special case noted.*

As previously noted, experimental data regarding viscous losses are quoted in terms of a mean stagnation pressure loss coefficient $\bar{\omega}$ [see Eq. (3.18)]. Typical examples of such losses are illustrated in Fig. I.4 for various inlet Mach number as obtained from two-dimensional cascade data. However, we are interested in applying this compressible three-dimensional theory to the case of transonic rotors in which the Mach number in the tip region is supersonic and that in the hub region is subsonic. It is then, however, possible that the loss picture in transonic rotors may be quite different from that of the subsonic blade row[35,36]. Nevertheless, we will use, in the present study, experimental cascade data in order to illustrate the three-dimensional effects of the blade wakes even in transonic annular rotors. Eq. (3.18) for $\bar{\omega}$ can be rewritten as

$$\bar{\omega} = \frac{P_t^u - P_t^d}{P_t^u - P^u} = \frac{-\Delta P_t}{\left(\frac{1}{2}\rho V^2\right)^u} \tag{5.22}$$

upon writing the pressure ratio (P_t^d/P_t^u) as

$$\frac{P_t^d}{P_t^u} = 1 + \frac{P_t^d - P_t^u}{P_t^u - P^u} \cdot \frac{P_t^u - P^u}{P_t^u} = 1 - \bar{\omega}\left(1 - \frac{P^u}{P_t^u}\right), \tag{5.23}$$

*See footnote on Pg. 39

we have the result that

$$\frac{\Delta S}{C_p} = -\frac{\gamma-1}{\gamma}\ln\left\{1-\bar{\omega}\left[1-\left(1+\frac{\gamma-1}{2}M^2\right)^{-\frac{\gamma}{\gamma-1}}\right]\right\}, \tag{5.24}$$

where we have made use of the definition

$$\frac{p^u}{p_t^u} = \left(1+\frac{\gamma-1}{2}M^2\right)^{-\frac{\gamma}{\gamma-1}} . \tag{5.25}$$

Since $\bar{\omega}$ is a small parameter [Eq. (3.1)], in the approximation here, we can expand Eq. (5.24) in a Taylor series, retaining the first term only.

$$\frac{\Delta S}{C_p} = \frac{\gamma-1}{\gamma}\bar{\omega}\left[1-\left(1+\frac{\gamma-1}{2}M^2\right)^{-\frac{\gamma}{\gamma-1}}\right] + O(\varepsilon^2) . \tag{5.26}$$

Though we have derived a relation for the entropy production and stagnation pressure loss coefficient for flow through a stationary blade row, the corresponding relation for flow through a rotating blade row is simply obtained by replacing the inlet Mach number M by that of the relative inlet Mach number.

Because of the near-invariance of entropy along the streamlines of the mean radial equilibrium flow and the circumferential periodicity inherent in the geometry of turbomachinery, we can write to an excellent approximation

$$\frac{S}{C_p} = \sum_{n=1}^{\infty} S_n(r)\, e^{inB\bar{\alpha}_0^d} \tag{5.27}$$

We again note that Eq. (5.27) guarantees that the integral of vorticity from blade-to-blade is identically zero, as required by the fact that no net amount of vorticity flux is shed into the wakes in steady flow (Kelvin's Theorem). Collecting these results for the downstream flow field,

we have an expression for the downstream reduced perturbation velocity in the form

$$\underset{\sim}{V}_R^d = \nabla\phi_R - \frac{(I+\frac{1}{2}\omega V_{\theta 0} r)}{V_{z0}^d}\sum_{n=1}^{\infty} S_n(r) e^{inB\alpha_0^d} \tag{5.28}$$

Since these three-dimensional perturbations are to be added to the circumferentially averaged flow we can write Eq. (4.63) as

$$\overline{\underset{\sim}{V}}_R + \tilde{\underset{\sim}{V}}_R = (\overline{\underset{\sim}{V}} + \tilde{\underset{\sim}{V}}) e^{-s/2c_p} \tag{5.29}$$

To the order of approximation used here, Eq. (5.29) becomes

$$\overline{\underset{\sim}{V}}_R + \tilde{\underset{\sim}{V}}_R = \overline{\underset{\sim}{V}} - \overline{\underset{\sim}{V}}\frac{s}{2c_p} + \tilde{\underset{\sim}{V}} \ , \tag{5.30}$$

so that we have

$$\overline{\underset{\sim}{V}}_R = \overline{\underset{\sim}{V}} \ , \tag{5.31}$$

and

$$\tilde{\underset{\sim}{V}} = \overline{\underset{\sim}{V}}\frac{s}{2c_p} + \tilde{\underset{\sim}{V}}_R \tag{5.32}$$

Similarly, using Eqs. (4.89) and (4.90), we obtain

$$\begin{aligned}\overline{\underset{\sim}{W}} + \tilde{\underset{\sim}{W}} &= (\overline{\underset{\sim}{V}}_R + \tilde{\underset{\sim}{V}}_R - \underset{\sim}{\omega}_R \times \underset{\sim}{r}) e^{s/2c_p} \\ &\simeq (\overline{\underset{\sim}{V}} - \underset{\sim}{\omega}\times\underset{\sim}{r}) + \overline{\underset{\sim}{V}}\frac{s}{2c_p} + \tilde{\underset{\sim}{V}}_R \ .\end{aligned} \tag{5.33}$$

so that

$$\overline{\underset{\sim}{W}} = \overline{\underset{\sim}{V}} - \underset{\sim}{\omega}\times\underset{\sim}{r} \ , \tag{5.34}$$

and

$$\tilde{\underset{\sim}{W}} = \bar{\underset{\sim}{V}} \frac{S}{2C_p} + \tilde{\underset{\sim}{V}}_R \quad . \tag{5.35}$$

In obtaining Eqs. (5.33), (5.34), and (5.35), we have made use of Eq. (5.31). Hence, in the actual ("original", see Chapter 4) flow field, the three-dimensional velocity perturbation is given by either Eq. (5.32) or its equivalent, (5.35). Upon using Eqs. (5.27) and (5.28) in Eqs. (5.32) and (5.35), we obtain the result for the downstream perturbation velocity in the form

$$\tilde{\underset{\sim}{W}}^d = \tilde{\underset{\sim}{V}}^d = \frac{1}{2}\bar{\underset{\sim}{V}} \sum_{n=1}^{\infty} S_n(r)\, e^{inB\alpha_0^d} + \nabla\phi_R - \frac{\left(I + \frac{1}{2}\omega V_{z_0}^u K_0\right)}{V_{z_0}^d} \sum_{n=1}^{\infty} S_n(r)\, e^{inB\alpha_0^d}\, \hat{e}_z \quad . \tag{5.36}$$

Upon writing our result in this way, we can now make use of Eq. (4.32) to obtain a governing equation for the perturbation potential ϕ_R. Making the corresponding approximations in the remaining applicable relations, we obtain the result that

$$\nabla\cdot\tilde{\underset{\sim}{W}} - \frac{1}{a_0^2}\underset{\sim}{W}_0\cdot\left(\underset{\sim}{W}_0\cdot\nabla\tilde{\underset{\sim}{W}} + \tilde{\underset{\sim}{W}}\cdot\nabla\underset{\sim}{W}_0\right) - \frac{1}{a_0^2}\tilde{\underset{\sim}{W}}\cdot\left(\underset{\sim}{W}_0\cdot\nabla\underset{\sim}{W}_0\right) - \frac{1}{a_0^2}\omega^2\tilde{\underset{\sim}{W}}\cdot\tilde{\underset{\sim}{I}} = 0 \quad . \tag{5.37}$$

Substitution of $\bar{\underset{\sim}{W}}$ in Eq. (5.37) leads to a governing equation for ϕ_R

$$\nabla^2\phi_R - \frac{1}{a_0^{d2}}\underset{\sim}{W}_0^d\cdot\left[(\underset{\sim}{W}_0^d\cdot\nabla)\nabla\phi_R + (\nabla\phi_R\cdot\nabla)\underset{\sim}{W}_0^d\right] - \frac{1}{a_0^{d2}}\nabla\phi_R\cdot(\underset{\sim}{W}_0^d\cdot\nabla\underset{\sim}{W}_0^d)$$

$$- \frac{1}{a_0^{d2}}\omega^2(\nabla\phi_R)\cdot\underset{\sim}{r} = -\nabla\cdot\underset{\sim}{L} + \frac{1}{a_0^{d2}}\underset{\sim}{W}_0^d\cdot(W_0^d\cdot\nabla\underset{\sim}{L} + \underset{\sim}{L}\cdot\nabla\underset{\sim}{W}_0^d) \tag{5.38}$$

$$+ \frac{1}{a_0^{d2}}\underset{\sim}{L}\cdot(\underset{\sim}{W}_0^d\cdot\nabla\underset{\sim}{W}_0^d) + \frac{1}{a_0^{d2}}\omega^2\underset{\sim}{L}\cdot\underset{\sim}{r} \quad ,$$

where $\underset{\sim}{L}$ is a vectorial quantity given by

$$\underset{\sim}{L} = \frac{1}{2}\left[\underset{\sim}{V}_0^d - \frac{(I + \frac{1}{2}\omega V_{z0}^u K_0)}{V_{z0}^d}\hat{e}_z\right]\sum_{n=1}^{\infty} S_n(r)\, e^{inB\alpha_0^d} \quad , \tag{5.39}$$

Upstream of the blade row, the flow is simply irrotational so that the perturbation velocity is expressible in terms of a velocity potential,

$$\underset{\sim}{\tilde{W}}^u = \underset{\sim}{\tilde{V}}^u = \nabla\phi^u \tag{5.40}$$

upon substituting Eq. (5.40) in Eq. (5.37), we obtain the result:

$$\nabla^2\phi^u - \frac{1}{a_0^{u2}}\underset{\sim}{W}_0^u\cdot\left[(\underset{\sim}{W}_0^u\cdot\nabla)\nabla\phi^u + (\nabla\phi^u\cdot\nabla)\underset{\sim}{W}_0^u\right] - \frac{1}{a_0^{u2}}\nabla\phi^u\cdot(\underset{\sim}{W}_0^u\cdot\nabla\underset{\sim}{W}_0^u)$$

$$- \frac{1}{a_0^{u2}}\omega^2\nabla\phi^u\cdot\underset{\sim}{r} = 0 \, . \tag{5.41}$$

Before proceeding to the solution of Eqs. (5.38) and (5.41) under the boundary conditions of vanishing radial velocity at the hub ($r = r_h$) and the tip ($r = r_t$), we note that because of compressibility effects, $\underset{\sim}{W}_0^d$ differs from $\underset{\sim}{W}_0^u$ and therefore that there is a small disturbance flow near the blade row due to the radial shaft of streamlines as mentioned earlier. In the next two Sections, we determine W_0^d using the radial equilibrium theory[10]; this is then followed by the determination of the small

disturbance three-dimensional flow.

5.2 The Radial Equilibrium Flow

The basic assumptions of the radial equilibrium theory[1,27] have been mentioned in Chapter 1, especially that the radial velocity is zero at the entry and the exit from a blade row. The velocity and the fluid properties have a radial dependence only. Upon making use of Eqs. (4.7), (4.10) and the equations of motion in the radial direction, we obtain

$$\frac{1}{\rho}\frac{dP}{dr} = \frac{V_{\theta 0}^2}{r} . \tag{5.42}$$

It follows from (4.21) that

$$\frac{dH}{dr} - T\frac{dS}{dr} = V_{z0}\frac{dV_{z0}}{dr} + \frac{V_{\theta 0}}{r}\frac{d}{dr}(rV_{\theta 0}) . \tag{5.43}$$

Upstream of the blade row, the flow is uniform and $V_{\theta 0}$ is zero so that V_{z0}^u is constant. Appropriate to free vortex flow for downstream of the blade row, the product $(rV_{\theta 0})$, the stagnation enthalpy H and the entropy s are invariant with radius so that V_{z0}^d is constant according to Eq. (5.43). Because the upstream flow is uniform, the density ρ_0^u there is constant; however, the density distribution changes across the blade row as a result of compressibility effects so that the downstream density ρ_0^d varies with r. For isentropic flow through a blade row ρ_0^d can be shown to be given by

$$\frac{\rho_o^d}{\rho_o^u} = \left(M_{z0}^{u2}\right)^{\frac{1}{\gamma-1}} \left\{ \frac{\left(\frac{P_{t0}^d}{P_{t0}^u}\right)^{\frac{\gamma-1}{\gamma}} \left(1+\frac{\gamma-1}{2}M_{z0}^{u2}\right)}{M_{z0}^{u2}} - \frac{\gamma-1}{2}\left[V_{z0}^d + \frac{(V_{\theta 0}r)^2}{r^2}\right] \right\}^{\frac{1}{\gamma-1}} \tag{5.44}$$

where M_{z0}^u is the upstream axial Mach number. If the entropy increases by

a constant value Δs_0 across the blade row, then ρ_0^d would be given by

$$\frac{\rho_0^d}{\rho_0^u} = \left(M_{z0}^{u2}\right)^{\frac{1}{\gamma-1}} \left\{ \frac{\left(\frac{P_{t0}^d}{P_{t0}^u}\right)^{\frac{\gamma-1}{\gamma}} \left(1+\frac{\gamma-1}{2}M_{z0}^{u2}\right)}{M_{z0}^{u2}} - \frac{\gamma-1}{2}\left[V_{z0}^{d2} + \frac{(V_{\theta 0} r)^2}{r^2}\right] \right\}^{\frac{1}{\gamma-1}} e^{-\Delta s_0/c_p} . \tag{5.45}$$

The downstream axial velocity V_{z0}^d is determined through the application of continuity of mass flux across the blade row; i.e.,

$$\int_{r_h}^{r_t} \rho_0^u V_{z0}^u r\,dr = \int_{r_h}^{r_t} \rho_0^d V_{z0}^d r\,dr , \tag{5.46}$$

or

$$V_{z0}^d \int_{r_h}^{r_t} \rho_0^d r\,dr = \frac{\rho_0^u V_{z0}^u}{2}\left(r_t^2 - r_h^2\right) . \tag{5.47}$$

In view of the implicit dependence of ρ_0^d on V_{z0}^d as given in Eqs. (5.44) or (5.45), it turns out that V_{z0}^d can be found most conveniently using an iterative process.

5.3 Determination of the Actual Circumferential-Averaged Flow

An improved solution for this part of the flow is provided by an actuator disc approach[23]. Since the flow far from the baldes is irrotational (as appropraite to a free-vortex flow) it follows from Kelvin's Theorem that the mean flow must be irrotational everywhere. Consequently, there exists a potential function $\bar{\phi}(r,z)$ which is sufficient to describe this correction to $(\,)_0$; i.e., we can write

$$\bar{\underset{\sim}{V}} = \underset{\sim}{V}_0 + \nabla\bar{\phi}(r,z) , \tag{5.48}$$

for both the upstream and downstream flow fields.

As in earlier Sections, a governing equation for this perturbation

potential may be derived using the continuity equation

$$\nabla\cdot\bar{\rho}\underset{\sim}{\bar{V}} = 0 \,, \tag{5.49a}$$

or

$$\nabla\cdot\underset{\sim}{\bar{V}} + \underset{\sim}{\bar{V}}\cdot\nabla \ell n\bar{\rho} = 0 \,, \tag{5.49b}$$

combined with the equation of motion for the mean flow

$$\underset{\sim}{\bar{V}}\cdot\nabla\underset{\sim}{\bar{V}} = -\frac{1}{\bar{\rho}}\nabla\bar{p} = -\left(\frac{\partial\bar{p}}{\partial\bar{\rho}}\right)_s \nabla \ell n\bar{\rho} \,. \tag{5.50}$$

Eliminating $\nabla \ell n\bar{\rho}$ in Eq. (5.50) with the help of Eq. (5.49b), we obtain

$$\nabla\cdot\underset{\sim}{\bar{V}} - \frac{1}{\bar{a}_0^2}\underset{\sim}{\bar{V}}\cdot\left(\underset{\sim}{\bar{V}}\cdot\nabla\underset{\sim}{\bar{V}}\right) = 0 \,, \tag{5.51}$$

which is also obtainable from Eq. (5.37) by simply taking $\omega = 0$. Thus,

$$\nabla^2\bar{\Phi} - \frac{1}{a_0^2}\underset{\sim}{V}_0\cdot\left[\left(\underset{\sim}{V}_0\cdot\nabla\right)\nabla\bar{\Phi} + \left(\nabla\bar{\Phi}\cdot\nabla\right)\underset{\sim}{V}_0\right] - \frac{1}{a_0^2}\nabla\bar{\Phi}\cdot\left(\underset{\sim}{V}_0\cdot\nabla\underset{\sim}{V}_0\right) = 0 \,. \tag{5.52}$$

Eq. (5.52) provides a governing equation for both the upstream and downstream potentials for the improved mean flow description.

In what follows, the variables occurring in the analysis will be made dimensionless in terms of the tip radius r_t as the length scale, far upstream axial velocity V_{z0}^u as the velocity scale, r_t/V_{z0}^u as the time scale, the far upstream density ρ_0^u as the density scale, the far upstream dynamic pressure $(1/2\ \rho_0^u\ V_{z0}^{u2})$ as the pressure scale and the specific heat at constant pressure c_p as the entropy scale.

Eq. (5.52) must be solved for the upstream and the downstream

perturbation potentials under the boundary conditions of vanishing radial velocity at the hub and the tip; here,

$$\left.\frac{\partial \bar{\Phi}_d^u}{\partial r}\right|_h = \left.\frac{\partial \bar{\Phi}_d^u}{\partial r}\right|_1 = 0 \cdot \tag{5.53}$$

5.3A The Upstream Mean-Flow Correction

Since the upstream flow is purely axial, upon expanding Eq. (5.52) in cylindrical coordinates we obtain

$$\frac{\partial^2 \bar{\Phi}^u}{\partial r^2} + \frac{1}{r}\frac{\partial \bar{\Phi}^u}{\partial r} + (1 - M_{z0}^{u2})\frac{\partial^2 \bar{\Phi}^u}{\partial z^2} = 0 \quad , \tag{5.54}$$

where M_{z0}^u is the far upstream axial Mach number given by

$$M_{z0}^u = \frac{V_{z0}^u}{a_0^u} \cdot \tag{5.55}$$

The solution for $\bar{\phi}^u(V,z)$, readily obtainable by the method of the separation of variables, can be written in the form,

$$\bar{\Phi}^u = \sum_{p=1}^{\infty} A_p^u e^{\lambda_p^u z} R_p^u(r) \cdot \tag{5.56}$$

The normalized upstream radial eigenfunction $R_p^u(r)$, a linear combination of Bessel Function of the first and second kind with order zero (compare Chapter 3), is given by

$$R_p^u(r) = \frac{1}{\sqrt{N_p}}\left\{J_0(\chi_p^u r) - \frac{J_0'(\chi_p^u)}{Y_0'(\chi_p^u)} Y_0(\chi_p^u r)\right\} , \tag{5.57}$$

where

$$\chi_p^u = \sqrt{(1-M_{z0}^{u2})}\ \lambda_p^u \ . \tag{5.58}$$

Each R_p^u satisfies the differential equation

$$\frac{d^2R_p^u}{dr^2} + \frac{1}{r}\frac{dR_p^u}{dr} + (1-M_{z0}^{u2})\lambda_p^{u2} R_p^u = 0 \ , \tag{5.59}$$

where the λ_p^u are the upstream eigenvalues given for example in Refs. 7 and 10. As before, the normalizing factor $\sqrt{N_p}$ is determined through

$$N_p = \int_h^1 r\left[J_0(\chi_p^u r) - \frac{J_0'(\chi_p^u)}{Y_0'(\chi_p^u)} Y_0(\chi_p^u r)\right]^2 dr \ . \tag{5.60}$$

By taking χ_p^u [from which the eigenvalues λ_p^u are determined (see Eq. (5.58))] to be the roots of the equation

$$J_0'(\chi_p^u) Y_0'(\chi_p^u h) - Y_0'(\chi_p^u) J_0'(\chi_p^u h) = 0, \tag{5.61a}$$

or, equivalently,

$$J_1(\chi_p^u) Y_1(\chi_p^u h) - Y_1(\chi_p^u) J_1(\chi_p^u h) = 0 \ , \tag{5.61b}$$

we are able to guarantee the boundary conditions [Eq. (5.53)] of the vanishing of the radial velocity at the hub and the tip. We note from Eq. (5.58) that compressibility effects have increased the eigenvalues λ_p^u by a factor of $(1-M_{z0}^{u2})^{-1/2}$[1]. Thus, the effect of the finiteness of M_{z0}^u is analogous to the Prandtl-Glauert correction for compressible flow about aerofoils; it has a tendency to crowd the upstream disturbances caused by the presence of the blades into a region closer to the blade row.

We can also write Eq. (5.59) in its self-adjoint form,

$$\frac{d}{dr}\left\{r\frac{dR_p^u}{dr}\right\} + r(1-M_{z0}^{u2})\lambda_p^{u2} R_p^u(r) = 0 \,. \tag{5.62}$$

from which it is readily seen that the set of eigenfunctions $\{R_p^u(r)\}$ is orthogonal with respect to the weighting function r. Furthermore, we note that upon direct integration of Eq. (5.62) over the internal (h,1) we obtain the result

$$\int_h^1 r\, R_p^u(r)dr = 0 \,. \tag{5.63}$$

Here we have used

$$\left.\frac{dR_p^u}{dr}\right|_{r=h} = \left.\frac{dR_p^u}{dr}\right|_{r=1} = 0 \,. \tag{5.64}$$

The result in Eq. (5.63) has the implication that any arbitrary constant function is orthogonal to all the normalized radial eigenfunctions $R_p^u(r)$; consequently, the set $\{R_p^u(r)\}$ is not complete unless a constant $R_0^u(r) = (2/1-h^2)^{1/2}$ is added to it.[10]

By virtue of the orthonormal properties of the eigenfunctions $R_p^u(r)$ the eignen values λ_p^u can be estimated through

$$\lambda_p^{u2} \sim \frac{\int_h^1 r\, R_p^{u/2} dr}{(1-M_{z0}^{u2})} \,. \tag{5.65}$$

5.3B The Downstream Mean Flow Correction.

Downstream of the blade row,

$$\underset{\sim}{V}_o^d = V_{\theta o}^d \hat{e}_\theta + V_{zo}^d \hat{e}_z, \tag{5.66}$$

so that upon expanding Eq. (5.52) in cylindrical coordinates, we obtain

$$\frac{\partial^2\bar{\Phi}^d}{\partial r^2} + \frac{(1+M_{\theta a}^2)}{r}\frac{\partial\bar{\Phi}^d}{\partial r} + (1-M_{z0}^{d2})\frac{\partial^2\bar{\Phi}^d}{\partial z^2} = 0 \ , \tag{5.67}$$

where the downstream axial Mach number M_{z0}^d and the absolute tangential Mach number $M_{\theta a}$ are given by

$$M_{z0}^d = \frac{V_{z0}^d}{a_0^d} \ , \tag{5.68}$$

and

$$M_{\theta a} = \frac{V_{\theta 0}^d}{a_0^d} \ , \tag{5.69}$$

respectively.

Because of compressibility effects, the Mach numbers downstream of the disc vary with radius. As for $\bar{\phi}^u$, the solution for $\bar{\phi}^d(r,z)$ can be expressed in the form of an infinite series of products of functions of each of the independent variables r and z. However, by mere inspection, we note that the most general solution of Eq. (5.67) is of the form

$$\bar{\phi}^d = C_1 + C_2 z + \sum_{p=1}^{\infty} A_p^d R_p^d(r)\, e^{-\lambda_p^d z} \ , \tag{5.70}$$

where the λ_p^d are the downstream axial eigenvalues. The downstream radial eigenfunctions $R_p^d(r)$ satisfy the differential equations

$$\frac{d^2R_p^d}{dr^2} + \frac{(1+M_{\theta a}^2)}{r}\frac{dR_p^d}{dr} + \lambda_p^{d2}(1-M_{z0}^{d2})R_p^d = 0 \ , \tag{5.71}$$

and the boundary conditions that

$$\left.\frac{dR_p^d}{dr}\right|_{r=h} = \left.\frac{dR_p^d}{dr}\right|_{r=1} = 0, \tag{5.72}$$

the latter being required by the vanishing of the radial velocity at the hub and the tip. Because of the radial dependence of the coefficients in the differential Eq. (5.67) no solution in terms of known tabulated functions is available. Therefore we resort to various methods of approximate analysis and numerical techniques for the determination of the radial eigenfunctions $R_p^d(r)$ and their associated eigenvalues λ_p^d. The useful methods of approximate analysis are, in this case, usually based on variational principles. Two examples of these methods are the Rayleigh-Ritz method and the Galerkin Method. We note that in using these techniques computational effort may be minimized and better accuracy also obtained if one is able to choose a function which describes the modal shape as closely as possible to that described by the exact $R_p^d(r)$.

We note that because the radial dependence of the Mach number $M_{\theta a}$ and M_{z0}^d is weak compared to that of 1/r and $R_p^d(r)$. The former can be considered to be almost constant over the annulus (relative to the latter) or assume an average annular value. Such an assumption would permit the solution to be expressed approximately in terms of known tabulated functions[33]

$$R_p^d(r) = r^{-\frac{1}{2}M_{\theta a}^2} \chi_{\frac{1}{2}M_{\theta a}^2}\left(\lambda_p^d \sqrt{(1-M_{z0}^{d2})} \cdot r\right) \tag{5.73}$$

where χ_ν is a linear combination of Bessel functions of the first and second kind of order ν. In physical terms, the radial dependence of the Mach numbers simply creates a distortion, the extent of which depends on

how strong their radial dependence is, to the radial harmonics described in Eq. (5.73); for weak radial dependence, this distortion is slight and appropriate solutions are of the form given in Eq. (5.73). A further simplification results if one uses a mean value (1/r) as the solution would then be expressible in terms of a linear combination of sine and cosine. From such an observation, one may conclude that a linear combination of sinusoidal functions or Bessel functions can give a useful approximate discription of a particular radial mode $R_p^d(r)$; these are also possible choices for use in the Galerkin Method or in the Raleigh-Ritz Method. A brief outline of the Galerkin Method is given in Appendix (I.H)

Eq. (5.71) can also be written in its self-adjoint form

$$\frac{d}{dr}\left\{e^{\int\frac{1+M_{\theta a}^2}{r}dr}\frac{dR_p^d}{dr}\right\}+\lambda_p^{d2}e^{\int\frac{1+M_{\theta a}^2}{r}dr}(1-M_{za}^{d2})R_p^d=0. \tag{5.74}$$

One sees that the set of radial eigenfunctions $\{R_p^d(r)\}$ is orthogonal over the interval (h,1) with respect to the weighting function q(r) given by

$$q(r)=(1-M_{za}^{d2})e^{\int\frac{1+M_{\theta a}^2}{r}dr} \tag{5.75}$$

Once again, direct integration of Eq. (5.74) over the interval (h,1) leads to

$$\int_h^1 q(r)\,R_p^d(r)\,dr=0. \tag{5.76}$$

where we have used the boundary conditions in (5.72). Hence, any arbitrary constant is orthogonal to all the $R_p^d(r)$ with respect to the weighting function in Eq. (5.75). Consequently, as with the $\{R_p^u(r)\}$, a constant must be added to the set $\{R_p^d(r)\}$ to make it complete.

By making use of the orthogonality of $R_p^d(r)$, we obtain from Eq. (5.74) that

$$\lambda_p^{d^2} \sim \frac{\int_h^1 e^{\int \frac{1+M_{\theta q}^2}{r} dr} \left(\frac{dR_p^d}{dr}\right)^2 dr}{\int_h^1 q(r)\, R_p^d(r)^2\, dr} \tag{5.77}$$

Because the blade row ($\omega \neq 0$) adds work to the fluid as it passes through, we must have

$$M_{z_0}^u > M_{z_0}^d \ , \tag{5.78}$$

so that

$$\lambda_p^u > \lambda_p^d \ . \tag{5.79}$$

Hence, the axial "wavelength" of the downstream disturbance is larger than that of the upstream one. In other words, the downstream disturbance field is spread over a larger region than that of the upstream one.

5.3C Matching of the Upstream Flow and the Downstream Flow at the Actuator Disc

Inspection of Eqs. (5.56) and (5.70) shows that the remaining unknowns are C_1, C_2 and the coefficients $A_{np}^{d\,u}$. Determination of these unknowns follows directly from appropriate matching of the upstream and the downstream flows at the actuator disc located at z = 0:

(a) The mass flux is continuous so that

$$\left[\bar{P}\,\bar{V}_z\right]_{z=0^+}^{z=0^-} = 0 \ , \tag{5.80}$$

where $z = 0^-$ and $z = 0^+$ refer to points immediately upstream and downstream

of the disc respectively. Within the present approximation, Eq. (5.80) can be shown to be equivalent to

$$(1-M_{z_0}^{uz})\frac{\partial\bar{\Phi}^u}{\partial z}\bigg|_{z=0^-} - \rho_o^d(1-M_{z_0}^{dz})\frac{\partial\bar{\Phi}^d}{\partial z}\bigg|_{z=0^+} = (\rho_o^d V_{z_0}^d - 1) \quad . \tag{5.81}$$

(See Appendix I.D)

(b) Since the spanwise force on the blades is to be considered negligible in the present work, the radial velocity is the same on either side of the disc, i.e.,

$$\frac{\partial\bar{\Phi}^u}{\partial r}\bigg|_{z=0^-} = \frac{\partial\bar{\Phi}^d}{\partial r}\bigg|_{z=0^+} \quad . \tag{5.82}$$

The use of Eqs. (5.56) and (5.70) in Eqs. (5.81) and (5.82) gives

$$(1-M_{z_0}^{uz})\sum_{p=1}^{\infty}\lambda_p^u A_p^u R_p^u(r) - \rho_o^d(1-M_{z_0}^{dz})\left[C_z - \sum_{p=1}^{\infty}\lambda_p^d A_p^d R_p^d(r)\right] = (\rho_o^d V_{z_0}^d - 1) \quad , \tag{5.83}$$

and

$$\sum_{p=1}^{\infty} A_p^u R_p^{u'}(r) = \sum_{p=1}^{\infty} A_p^d R_p^{d'}(r) \quad . \tag{5.84}$$

respectively.

As noted earlier, the compressibility effects introduced by the strong downstream swirl modify the downstream radial eigenfunctions $R_p^d(r)$ as well as the downstream eigenvalues λ_p^d; the extent of such modification depends on the strength of the downstream swirl. As a result, mode by mode matching of the upstream flow and the downstream flow, which can always be carried out in incompressible flow with uniform inlet conditions, is not possible here. In the limit of zero downstream swirl, however,

both the downstream radial eigenfunctions and the axial eigenvalues revert to those of the upstream ones.

In the determination of these unknowns, use is made of the orthogonal properties of the radial eigenfunctions to minimize any required computational work. On multiplying Eq. (5.83) by r and integrating from r = h to r = 1, we obtain

$$C_2 = -\int_h^1 r(\rho_0^d V_{z0}^d - 1)\,dr \Big/ \int_h^1 r\rho_0^d(1-M_{z0}^{d2})\,dr \,, \tag{5.85}$$

where we have used Eq. (5.63) and (5.76). [Note further that

$$\int_h^1 r\rho_0^d(1-M_{z0}^{d2})R_p^d\,dr \propto \int_h^1 q(r)R_p^d(r) = 0 .$$

However, from the radial equilibrium theory, mass flux continuity at the blade row implies that

$$\int_h^1 r(\rho_0^d V_{z0}^d - 1)\,dr = 0 \,, \tag{5.86}$$

so that C_2 is identically zero.

We now multiply Eq. (5.83) by $rR_p^u(r)$ and then integrate from r = h to 1 so that we obtain, upon using the orthogonality of the normalized eigenfunctions $\{R_p^u(r)\}$,

$$(1-M_{z0}^{u2})\lambda_p^u A_p^u + \sum_{j=1}^{\infty}\lambda_j^d A_j^d \int_h^1 \rho_0^d(1-M_{z0}^{d2})R_j^d(r)\, r R_p^u(r)\,dr = \int_h^1 r R_p^u(r)(\rho_0^d V_{z0}^d - 1)\,dr \,. \tag{5.87}$$

Direct integration of Eq. (5.88) with respect to r leads to

$$\sum_{p=1}^{\infty} A_p^u R_p^u(r) = \sum_{p=1}^{\infty} A_p^d R_p^d(r) + C_1 \,, \tag{5.88}$$

where we have chosen C_1 to be the arbitrary constant of integration. Eq. (5.88) has the implication that the velocity potential (which is unique up to a constant only) is continuous across the actuator disc. Multiplication of Eq. (5.88) by r and integration of the result from r = h to 1 leads to[10]

$$C_1 = -\frac{2}{(1-h^2)}\sum_{j=1}^{\infty} A_j^d \int_h^1 r R_j^d(r)\, dr \,, \tag{5.89a}$$

where use is made of Eq. (5.63). Alternatively, we could have multiplied Eq. (5.88) by q(r) and integrated the result over the interval [h,1] to obtain

$$C_1 = \sum_{j=1}^{\infty} A_j^u \int_h^1 q(r) R_j^u(r)\, dr \Big/ \int_h^1 q(r)\, dr \,, \tag{5.89b}$$

with the use of Eq. (5.76). Analogous with the results discussed in Sections 5.3A and 5.3B the existence of C_1 is a result of the fact that the radial eigenfunctions, $\{R_p^u(r)\}$ and $\{R_p^d(r)\}$, do not form complete sets. Further, on multiplying Eq. (5.88) by $rR_p^u(r)$ and integrating from r = h to r = 1 we obtain, by virtue of the orthogonality of the normalized eigenfunctions $\{R_p^u(r)\}$,

$$A_p^u - \sum_{j=1}^{\infty} A_j^d \int_h^1 r R_j^d(r) R_p^u(r)\, dr = 0 \,, \tag{5.90}$$

where we have made use of Eq. (5.63).

In essence, to obtain Eqs. (5.87) and (5.90), we have expanded the downstream radial eigenfunction $R_p^d(r)$ in terms of the upstream normalized eigenfunctions $R_p^u(r)$ (discussed in Chapter 3) as a Fourier-Bessel Series[15]. We observe that the resulting modification of the downstream radial

harmonics has led to a mutual interference among these harmonics and that they are therefore inseparable a feature which is absent in incompressible flow with uniform inlet conditions. The matching conditions (a) and (b) at the actuator disc z = 0 provide a set of linear equations, embodied in Eqs. (5.87) and (5.90), sufficient for the determination of the sets of unknowns $\{A_p^u\}$ and $\{A_p^d\}$. This set of equations can also be written in a matrix form as follows:

$$\left[\begin{array}{c|c} [\delta_{ij}] & [-\Lambda_{ij}] \\ \hline [(1-M_{z0}^{u2})\lambda_i \delta_{ij}] & [\lambda_j^d \mu_{ij}] \end{array}\right] \left[\begin{array}{c} [A_i^u] \\ \hline [A_i^d] \end{array}\right] = \left[\begin{array}{c} [0] \\ \hline [\varepsilon_i] \end{array}\right] \tag{5.91}$$

where $[a_{ij}]$ is a submatrix with elements a_{ij},

δ_{ij} is the Kronecker delta defined in Eq. (4.36),

$$\Delta_{ij} = \int_h^1 r R_i^u(r) R_j^d(r) dr,$$

$$\mu_{ij} = \int_h^1 \rho_0^d \, (1 - M_{0z}^d) \, r R_i^u(r) \, R_j^d(r) \, dr,$$

and

$$\varepsilon_i = \int_h^1 (\rho_0^d \, V_{z0}^d - 1) \, r R_i^u(r) \, dr,$$

which results from the redistribution of the mass flux as the flow passes through the actuator disc.

Each suffix i and j runs from 1 to p so that each submatrix is either a p by 1 matrix (i.e., a column matrix) or a p by p matrix.

The inversion of matrix Eq. (5.91) gives $\{A_p^u\}$ and $\{A_p^d\}$, from which C_1 can be determined through Eqs. (5.89a) or (5.89b). With their determination, the circumferentially averaged flow field is totally known, it is

given by:

(i) Upstream of the actuator disc,

$$\bar{V}_z^u = V_{z0}^u + \sum_{p=1}^{\infty} \lambda_p^u A_p^u e^{\lambda_p^u z} R_p^u(r) \,.$$

$$\bar{V}_r^u = \sum_{p=1}^{\infty} A_p^u e^{\lambda_p^u z} R_p^{u\prime}(r) \,; \tag{5.92}$$

(ii) Downstream of the actuator disc,

$$\bar{V}_z^d = V_{z0}^d - \sum_{p=1}^{\infty} \lambda_p^d A_p^d e^{-\lambda_p^d z} R_p^d(r) \,.$$

$$\bar{V}_r^d = \sum_{p=1}^{\infty} A_p^d e^{-\lambda_p^d z} R_p^{d\prime}(r) \,. \tag{5.93}$$

5.4 The Three-Dimensional Blade-to-Blade Flow

We can now proceed to determine the three-dimensional perturbations due to the presence of the blade-wakes by solving Eqs. (5.38) and (5.41); as in Chapter 3, these three-dimensional perturbations are to be added to the circumferentially averaged flow determined previously. On expanding these two equations in cylindrical coordinates, we have:

For Eq. (5.41):

$$\frac{\partial^2\phi^u}{\partial r^2} + \frac{1}{r}\frac{\partial\phi^u}{\partial r} + \frac{(1-\omega^2 r^2 M_{z0}^{u2})}{r^2}\frac{\partial^2\phi^u}{\partial\theta^2} + 2\omega M_{z0}^{u2}\frac{\partial^2\phi^u}{\partial\theta\partial z} + (1-M_{z0}^{u2})\frac{\partial^2\phi^u}{\partial z^2} = 0 \,, \tag{5.94}$$

and for Eq. (5.38):

$$\frac{\partial^2\phi^d}{\partial r^2} + \frac{(1+M_{\theta a}^2)}{r}\frac{\partial\phi^d}{\partial r} + \frac{(1-M_{\theta r}^2)}{r^2}\frac{\partial^2\phi^d}{\partial\theta^2} - 2M_{z0}^d M_{\theta r}\frac{1}{r}\frac{\partial^2\phi^d}{\partial\theta\partial z} + (1-M_{z0}^{d2})\frac{\partial^2\phi^d}{\partial z^2}$$
$$= -\sum_{n=1}^{\infty} inBS_n\left\{\frac{(1+\frac{1}{2}\omega K_0)}{V_{z0}^{d2}}\left(\frac{K_0}{r^2}-K_1\right)+K_1\right\}e^{inB\alpha_0^d} \,. \tag{5.95}$$

where we have written ϕ_R^d as ϕ^d, since in the approximation used here, the perturbation potential in the actual flow and in the reduced flow are the same. The relative tangential Mach number $M_{\theta r}$ in Eq. (5.95) is given by

$$M_{\theta r} \equiv \frac{(V_{\theta 0}^d - \omega r)}{a_0^d} \tag{5.96}$$

Once more, the boundary condtions are

$$\left.\frac{\partial \phi_d^u}{\partial r}\right|_h = \left.\frac{\partial \phi_d^u}{\partial r}\right|_1 = 0 \tag{5.97}$$

so that the radial velocity vanishes at the hub and the tip.

The partial differential equations in Eqs. (5.94) and (5.95) are of the form

$$A\frac{\partial^2\phi}{\partial z^2} + 2B\frac{\partial^2\phi}{\partial\theta\partial z} + C\frac{\partial^2\phi}{\partial\theta^2} + D\frac{\partial^2\phi}{\partial r^2} + F\left(\phi, \frac{\partial\phi}{\partial r}, r, \theta, z\right) = 0, \tag{5.98}$$

and the type of PDE (elliptic, parabolic or hyperbolic) to which they belong depends on the eigenvalues of the matrix

$$\begin{bmatrix} D & 0 & 0 \\ 0 & C & 2B \\ 0 & 2B & A \end{bmatrix}.$$

As it turns out, if

(i) $B^2 - AC > 0$ the PDE is of the hyperbolic type with two distinct families of characteristics.

(ii) $B^2 - AC = 0$ the PDE is of the parabolic type with one real family of characteristics

(iii) $B^2 - AC < 0$ the PDE is of the elliptic type in which the "characteristics" are conpigate complex

For Eq. (5.94),

$$B^2 - AC = M_{z0}^{u2}(1+\omega^2 r^2) - 1 \,, \tag{5.99}$$

We note that $M_{z0}^{u}\sqrt{(1+\omega^2 r^2)}$ is the Mach number of the upstream undisturbed fluid relative to the rotor, and it increases with the radius r. It may happen that, as in the case of a transonic axial fan[8,10,11,15] this relative Mach number could vary from subsonic value in the inner annular section to supersonic value in the outer annular section. We therefore find that Eq. (5.94) is of the elliptic type in the inner annular section where $M_{z0}^{u^2}(1+\omega^2 r^2)$ is less than unity while it is of the hyperbolic type in the outer annular section $[M_{z0}^{u^2}(1+\omega^2 r^2) > 1]$. Clearly, the change occurs at the sonic radius r_s given by

$$r_s \equiv \frac{\sqrt{1-M_{z0}^{u2}}}{\omega M_{z0}^{u}} \tag{5.100}$$

However, for Eq. (5.95)

$$B^2 - AC = (M_{z0}^{d2} + M_{\theta r}^{2}) - 1 \,, \tag{5.101}$$

where $\sqrt{M_{z0}^{d^2} + M_{\theta_r}^2}$ is the Mach number of the downstream undisturbed fluid relative to the rotor. Therefore Eq. (5.95) in contrast with (5.99) becomes elliptic or hyperbolic according to whether the relative Mach number $\sqrt{M_{z0}^{d^2} + M_{\theta r}^2}$ is less than or greater than unity. But the rotor is adding work to the fluid as it passes through the blades so that it is highly unlikely that the actual relative mean Mach number of the downstream

undisturbed fluid will ever exceed unity, even though that of the upstream undisturbed fluid does so over the outer portion of the blades.

5.4A The Upstream Three-Dimensional Perturbations

We can write the solution of Eq. (5.98) in the form of

$$\phi^u = \sum_{n=1}^{\infty} \sum_{p=1}^{\infty} A^u_{np} R^u_{np}(r) e^{\lambda^u_{np} z} e^{inB\theta} . \tag{5.102}$$

The normalized upstream radial eigenfunction $R^u_{np}(r)$ is given by

$$R^u_{np}(r) = \frac{1}{\sqrt{N_{np}}} \left\{ J_{nB}(\chi^u_{np} r) - \frac{J'_{nB}(\chi^u_{np})}{Y'_{nB}(\chi^u_{np})} Y_{nB}(\chi^u_{np} r) \right\} \tag{5.103}$$

7,8

where

$$\chi^{u2}_{np} = (1 - M^{u2}_{z0}) \lambda^{u2}_{np} + n^2 B^2 \omega^2 M^{u2}_{z0} + 2inB \lambda^u_{np} \omega M^{u2}_{z0} . \tag{5.104}$$

Each $R^u_{np}(r)$ satisfies the differential equation

$$\frac{d^2 R^u_{np}}{dr^2} + \frac{1}{r} \frac{dR^u_{np}}{dr} + \left\{ \chi^{u2}_{np} - \frac{n^2 B^2}{r^2} \right\} R^u_{np}(r) = 0 , \tag{5.105}$$

where the λ^u_{np} are the upstream axial eigenvalues. Once again, the normalizing facotr $\sqrt{N_{np}}$ can be found from

$$N_{np} = \int_h^1 r \left\{ J_{nB}(\chi^u_{np} r) - \frac{J'_{nB}(\chi^u_{np})}{Y'_{nB}(\chi^u_{np})} Y_{nB}(\chi^u_{np} r) \right\}^2 dr . \tag{5.106}$$

The upstream axial eigenvalues λ^u_{np} are to be found as required by the boundary conditions in Eq. (5.97), as the roots of the following equations [see also Eq. (3.33)]:

$$J'_{nB}(\chi^u_{np}h)Y'_{nB}(\chi^u_{np}) - J'_{nB}(\chi^u_{np})Y'_{nB}(\chi^u_{np}h) = 0, \tag{5.107}$$

and

$$\lambda^u_{np} = \frac{-inBM^{u2}_{zo}\omega \pm \sqrt{(1-M^{u2}_{zo})\chi^{u2}_{np} - n^2B^2\omega^2M^{u2}_{zo}}}{(1-M^{u2}_{zo})} . \tag{5.108}$$

[Eq. (5.108) has been obtained by solving the quadratic Eq. (5.104) for λ^u_{np}]. For each value of χ^u_{np} obtained from Eq. (5.107), there corresponds two values of λ^u_{np}; a choice is made so that a physically valid perturbed flow is realized. If the value of χ_{np} is such that the argument of the square root in Eq. (5.108) is positive, the positive sign is chosen so that all disturbances would die out at large distances upstream from the blade row. This would give a complex eigenvalue λ^u_{np}, corresponding to a disturbance of the subsonic type with an exponentially osciallatory decay[9]. On the other hand, if the value of χ_{np} is such that the arguement of the square root is negative, then the negative sign is chosen so that the upstream propagating disturbances have a finer pitch (the Doppler effect)[8]. Thus the eigenvalue λ^u_{np} is imaginary and it corresponds to a disturbance of the supersonic type which propagates to the far field without any decay. Since χ^u_{np} is at least of the order of nB, the argument of the square root can go negative only if the upstream relative Mach number at the tip ($M^u_{z0}\sqrt{1+\omega^2}$) becomes supersonic[8]. Hence, for transonic rotors, the sonic radius as defined in Eq. (5.104) is within the annulus so that the upstream disturbance field is composed of the components of supersonic modes and those of the subsonic modes.

We further note that if for any particular value of χ_{np} is such that it exactly satisfies

$$\chi_{np}^{u2} = \frac{n^2B^2\omega^2M_{z0}^{u2}}{(1-M_{z0}^{u2})} \tag{5.109}$$

then solution exists only if $(n^2B^2\omega^2\ M_{z0}^{u}/\sqrt{1-M_{z0}^{u2}})$ is a root of Eq. (5.107). This corresponds to the phenomenon of transonic resonance which has been investigated in references 8, 10, and 12.

The radial eigenfunctions $\{R_{np}^{u}(r)\}$ forms an orthonormal set, and by making use of this property, one can readily show that

$$\chi_{np}^{u2} \sim \int_h^1 r\left(\frac{dR_{np}^{u}}{dr}\right)^2 dr\ . \tag{5.110}$$

since

$$\int_h^1 r R_{np}^{u}(r) R_{nq}^{u}(r)\, dr = \delta_{pq}\ . \tag{5.111}$$

5.4B The Downstream Three-Dimensional Perturbations

In general, the solution of the non-homogeneous partial differential equation (5.95) with variable coefficients can be written as

$$\phi^d = \sum_{n=1}^{\infty}\sum_{p=1}^{\infty} A_{np}^{d} R_{np}^{d}(r) e^{i\lambda_{np}^{d}z} e^{inB\theta} + \phi_I^d(r,\theta,z)\ . \tag{5.112}$$

The first double sum in the above equation is the exponentially, oscillatorily decaying homogeneous solution; it is osciallatory because the axial eigenvalues λ_{np}^{d} are invariably complex. As noted earlier, it is highly unlikely that a disturbance of the supersonic type, which propagates far downstream without any decay, will occur here since the rotor is working on the fluid passing through it.

The downstream radial eigenfunctions $R^d_{np}(r)$ satisfys the differential equations

$$\frac{d^2R^d_{np}}{dr^2}+\frac{(1+M^2_{\theta a})}{r}\frac{dR^d_{np}}{dr}+\left[\left(\lambda^d_{np}M_{z0}+\frac{nB}{r}M_{\theta r}\right)^2-\lambda^{d2}_{np}-\frac{n^2B^2}{r^2}\right]R^d_{np}=0. \tag{5.113}$$

which can be rewritten in their self-adjoint form

$$\frac{d}{dr}\left[e^{\int\frac{1+M^2_{\theta a}}{r}dr}\frac{dR^d_{np}}{dr}\right]+e^{\int\frac{1+M^2_{\theta a}}{r}dr}\left[\frac{2M^d_{z0}M_{\theta r}nB}{r}\lambda^d_{np}-(1-M^{d2}_{z0})\lambda^{d2}_{np}-\frac{n^2B^2}{r^2}(1-M^2_{\theta r})\right]R^d_{np}=0. \tag{5.114}$$

Because of Eq. (5.97), we require,

$$\left.\frac{dR^d_{np}(r)}{dr}\right|_h=\left.\frac{dR^d_{np}(r)}{dr}\right|_1=0 \tag{5.115}$$

Thus the inhomogeneous part of the solution, $\phi^d_I(r,\theta,z)$, must again satisfy

$$\left.\frac{\partial\phi^d_I}{\partial r}\right|_h=\left.\frac{\partial\phi^d_I}{\partial r}\right|_1=0\ , \tag{5.116}$$

so that the net radial velocity vanishes at the hub and the tip.

As a result of compressibility effects and the presence of the downstream swirl, the radial dependence of the coefficients in Eqs. (5.113) or (5.114) is such that its solution in terms of known tabulated functions is not available. Various methods of approximate analysis and numerical techniques may be used for determining the radial eigenfunctions $R^d_{np}(r)$ and the associated downstream eigenvalues λ^d_{np}. (In general, it is expected that the eigenvalues λ^d_{np} will occur in complex conjugate pairs so that the choice is to be made such that the perturbation potential is bounded far downstream).

In the limit of vanishing downstream swirl (i.e. for a lightly-loaded rotor), the downstream radial harmonics, and eigenvalues become the same as those of the upstream ones;[7,10,11] in this limit, downstream propagating disturbances of the supersonic type, can occur if the sonic radius lies within the annulus.[8,10,15]

For blade wakes in incompressible flow, we have managed to obtain an exact solution to the corresponding inhomogeneous equation (3.27); however, for blade wakes in compressible flow, because of the radial dependence of various coefficients in Eq. (5.95), is such that it necessitates some sort of approximation in an attempt to obtain $\phi_I^d(r,\theta,z)$ to satisfy the boundary conditions in Eq. (5.116). [One may be tempted to express the radial dependence of $\phi_I^d(r,\theta,z)$ in terms of the $R_{np}^d(r)$, as we have done in the incompressible flow case (see Chapter 3) so that Eq. (5.116) is satisfied. However, this is not convenient in this situation.]

At this point, we note that for a free-vortex flow, the radial dependence of the factors $(1-M_{z0}^{d2})$ and $(M_{z0}^d M_{\theta r}/r)$ is rather weak compared to that of $\phi_I^d(r,\theta,z)$. [Typically, for a transonic rotor with a hub-to-tip ratio of 0.8 with an inlet Mach number of 0.65, a tip Mach number of 1.3, and a pressure ratio of 1.8, the radial dependence of $(1-M_{z0}^{d2})$ and $M_{z0}^d M_{\theta r}/r)$ is as shown in Fig. I.7.] One sees that they are nearly constant over the annulus so that it is quite appropriate to replace $(1-M_{z0}^{d2})$ and $(M_{z0}^d M_{\theta r}/r)$ occurring in Eq. (5.95) by their annularly averaged values.

With these approximations in mind, we can therefore define a set of eigenfunctions $\{R_{np}^I(r)\}$ which is orthogonal with respect to the weighting function

$$y(r) = e^{\int \frac{1+M_{\theta a}^2}{r} dr}, \qquad (5.117)$$

while each member of this set also satisfies the differential equation

$$\frac{d^2R^I_{np}}{dr^2} + \frac{(1+M^2_{\theta a})}{r}\frac{dR^I_{np}}{dr} + \left\{-K^2_{np}(1-M^{d2}_{z0})_{av} + 2nBK_{np}\left(\frac{M^d_{z0}M_{\theta r}}{r}\right)_{av}\right.$$

$$\left. - \frac{n^2B^2}{r^2}(1-M^2_{\theta r})\right\} R^I_{np} = 0 \tag{5.118}$$

which can further be rewritten in its self-adjoint form,

$$\frac{d}{dr}\left[y(r)\frac{dR^I_{np}}{dr}\right] + y(r)\left[-k^2_{np}(1-M^{d2}_{z0})_{av} + 2nBK_{np}\left(\frac{M^d_{z0}M_{\theta r}}{r}\right)_{av}\right.$$

$$\left. - \frac{n^2B^2}{r^2}(1-M^2_{\theta r})\right]R^I_{np} = 0, \tag{5.119}$$

where the K_{np} are the corresponding eigenvalues determined by the radial boundary conditions previously described. The annularly-averaged values of $(1-M^{d^2}_{z0})_{ar}$ and $(M^d_{z0}M_{\ r}/r)_{ar}$ are given by

$$(1-M^{d2}_{z0})_{av} = \frac{1}{(1-h)}\int_h^1 (1-M^{d2}_{z0})\,dr \tag{5.120}$$

and

$$\left(\frac{M^d_{z0}M_{\theta r}}{r}\right)_{av} = \frac{1}{(1-h)}\int_h^1 \left(\frac{M^d_{z0}M_{\theta r}}{r}\right) dr\,. \tag{5.121}$$

The above approximations [which would be especially good for higher modes since then the radial dependence of $(1 - M^{d2}_{z0})$, and $(M^d_{z0}M_{\theta r}/r)$ is very weak compared to that of the $\phi^d_I\ (r,\theta,z)$] allow the radial dependence of $\phi^d_I(r,\theta,z)$ to be expressed in terms of $R^I_{np}(r)$. Hence, we can write the solution $\phi^d_I\ (r,\theta,z)$ as a double sum:

$$\phi_I^d(r,\theta,z) = \sum_{n=1}^{\infty}\sum_{p=1}^{\infty} Z_{np}(z)\, R_{np}^{I}(r)\, e^{inB\theta} \quad . \tag{5.122}$$

Thus Eq. (5.116) is satisfied. It is shown in Appendix I.F that $Z_{np}(z)$ is of the form

$$Z_{np}(z) = \frac{inB}{\Lambda_{np}(1-M_{z_0}^{d2})_{av}} \int_h^1 \frac{G_n(r)\, R_{np}^{I}(r)\, dr}{\left\{\left[\frac{nB\left(\frac{M_{z_0}^{d} M_{\theta r}}{r}\right)_{av}}{(1-M_{z_0}^{d2})_{av}} + \frac{nB}{V_{z_0}^{d}}\left(\frac{K_0}{r^2}-K_1\right)\right]^2 + \left[\frac{\chi_{np}^{I2}(1-M_{z_0}^{d2})_{av} - n^2B^2\left(\frac{M_{z_0}^{d} M_{\theta r}}{r}\right)_{av}^2}{(1-M_{z_0}^{d2})_{av}^2}\right]\right\}} dr \tag{5.123}$$

where

$$\Lambda_{np} = \int_h^1 Y(r)\, R_{np}^{I2}(r)\, dr \, . \tag{5.124}$$

$$\chi_{np}^{I2} = -K_{np}^2(1-M_{z_0}^{d2})_{av} + 2nBK_{np}\left(\frac{M_{z_0}^{d} M_{\theta r}}{r}\right)_{av} , \tag{5.125}$$

and

$$G_n(r) = S_n(r)\left\{\frac{(I+\frac{1}{2}\omega K_0)}{V_{z_0}^{d2}}\left(\frac{K_0}{r^2}-K_1\right) + K_1\right\} \tag{5.126}$$

The analytical behavior of the integral in Eq. (5.123) is closely related to the true nature of the blade wakes and their induced perturbations.

5.4C Matching of the Flow Field at the Blade Row

For each circumferential harmonic n and radial harmonic p, the remaining unknowns are A_{np}^{d} appearing in Eqs. (5.102) and (5.112); their determination follows directly from the matching of the upstream flow, and the downstream flow at the blade row (in the actuator disc limit) using

the following physical boundary conditions:

(a) Mass fux continuity across the blade row requires

$$\left[\rho V_z\right]_{z=0^+}^{z=0^-} = 0 \quad . \tag{5.127}$$

Because of Eq. (5.80), the above equation becomes (in the approximations here)

$$\left[\bar{\rho}\tilde{V}_z + \tilde{\rho}\bar{V}_z\right]_{z=0^+}^{z=0^-} = 0 \tag{5.128}$$

It is shown in Appendix I.G that Eq. (5.128) is equivalent to

$$\rho_0^d(1-M_{z0}^{d2})\frac{\partial\phi^d}{\partial z}\bigg|_{z=0^+} - \rho_0^d\frac{M_{z0}^d M_{\theta r}}{r}\frac{\partial\phi^d}{\partial\theta}\bigg|_{z=0^+} - (1-M_{z0}^{u2})\frac{\partial\phi^u}{\partial z}\bigg|_{z=0^-} - \omega M_{z0}^{u2}\frac{\partial\phi^u}{\partial\theta}\bigg|_{z=0^-} \quad .$$

$$= \left\{\left(\frac{\gamma}{\gamma-1}\right) + \rho_0^d(1-M_{z0}^{u2})\left[\frac{(I+\frac{1}{2}\omega K_0)}{V_{z0}^d} - \frac{V_{z0}^d}{2}\right] + \rho_0^d K_0\frac{M_{z0}^d M_{\theta r}}{2r}\right\} S \quad . \tag{5.129}$$

(b) As before the spanwise force on the blades is to be considered negligible here, the radial velocity is continuous across the blade row; i.e.,

$$V_r^u\big|_{z=0^-} = V_r^d\big|_{z=0^+} \tag{5.130}$$

Because of Eq. (5.82), Eq. (5.130) becomes

$$\tilde{V}_r^u\big|_{z=0^-} = \tilde{V}_r^d\big|_{z=0^+} \tag{5.131}$$

or

$$\frac{\partial\phi^u}{\partial r}\bigg|_{z=0^-} = \frac{\partial\phi^d}{\partial r}\bigg|_{z=0^+} \tag{5.132}$$

The use of Eqs. (5.102) with (5.112) in Eqs. (5.129) and (5.132) results in, for each circumferential harmonic n,

$$\sum_{p=1}^{\infty} i\left[\rho_0^d(1-M_{z0}^{d2})\lambda_{np}^d - nB\rho_0^d\frac{M_{z0}^d M_{\theta r}}{r}\right]A_{np}^d R_{np}^d(r) - \sum_{p=1}^{\infty}\left[(1-M_{z0}^{u2})\lambda_{np}^u + \omega M_{z0}^{u2} inB\right]A_{np}^u R_{np}^u(r)$$

$$= \Delta_n(r) - \rho_0^d(1-M_{z0}^{d2})\sum_{p=1}^{\infty} Z'_{np}(0)R_{np}^I(r) + \rho_0^d\frac{M_{z0}^d M_{\theta r}}{r}\sum_{p=1}^{\infty} inB\,Z_{np}(0)R_{np}^I(0)\,, \tag{5.133}$$

with

$$\Delta_n(r) = \left\{\left(\frac{r}{r-1}\right) + \rho_0^d(1-M_{z0}^{d2})\left[\frac{(I+\frac{1}{2}\omega k_0)}{V_{z0}^d} - \frac{V_{z0}^d}{2}\right] + \frac{\rho_0^d k_0}{2}\frac{M_{z0}^d M_{\theta r}}{r}\right\} S_n(r)\;; \tag{5.134}$$

and

$$\sum_{p=1}^{\infty} A_{np}^u R_{np}^{u'}(r) = \sum_{p=1}^{\infty} A_{np}^d R_{np}^{d'}(r) + \sum_{p=1}^{\infty} Z_{np}(0)\,R_{np}^{I'}(r)\,. \tag{5.135}$$

We can integrate Eq. (5.135) with respect to r to give

$$\sum_{p=1}^{\infty} A_{np}^u R_{np}^u(r) = \sum_{p=1}^{\infty} A_{np}^d R_{np}^d(r) + \sum_{p=1}^{\infty} Z_{np}(0)\,R_{np}^I(r)\,, \tag{5.136}$$

where we have chosen the constant of integration to be zero in order that the velocity potential be the same on either side of the blade row.

We note that the circumferential harmonics n are separable; i.e., we can match each of the downstream circumferential modes to the corresponding upstream one. However, as in the solution for the circumferentially mean flow, the radial harmonics are not separable here because, as already emphasized, these radial harmonics have been modified through the presence of the downtream swirl and compressibility effects. Consequently, mode-by-mode matching is not possible here. However, in order to minimize

computational work, we still make use of the orthogonality properties of the upstream normalized radial eigenfunctions in order to match the flow field at the blade row. This is equivalent to now expanding the downstream eigenfunctions $R^{d}_{np}(r)$ and $R^{I}_{np}(r)$ in terms of the upstream radial eigenfunctions $R^{u}_{np}(r)$ in the form of Fourier Bessel Series[15].

On multiplying Eqs. (5.133) and (5.136) by $r\,R^{u}_{np}(r)$ and integrating from r = h to r = 1 we obtain, by virtue of the orthogonality of the normalized eigenfunctions $\{R^{u}_{np}(r)\}$:

$$-\left[(1-M_{z0}^{u2})\lambda^{u}_{np}+\omega M_{z0}^{u2}inB\right]A^{u}_{np}+\sum_{j=1}^{\infty}\left[\lambda^{d}_{nj}\int_{h}^{1}\rho_{0}^{d}(1-M_{z0}^{d2})\,r\,R^{u}_{np}(r)R^{d}_{np}(r)\,dr-nB\int_{h}^{1}\rho_{0}^{d}M^{d}_{z0}M_{\theta r}R^{u}_{np}(r)R^{d}_{np}(r)\,dr\right]A^{d}_{nj}.$$

$$=\int_{h}^{1}\Delta_{n}(r)\,r\,R^{u}_{np}(r)\,dr-\sum_{j=1}^{\infty}Z'_{nj}(0)\int_{h}^{1}\rho_{0}^{d}(1-M_{z0}^{d2})\,r\,R^{u}_{np}(r)R^{I}_{np}(r)\,dr+\sum_{j=1}^{\infty}inBZ_{nj}(0)\int_{h}^{1}\rho_{0}^{d}M^{d}_{z0}M_{\theta r}R^{u}_{np}(r)R^{I}_{np}(r)\,dr \qquad (5.137)$$

while

$$A^{u}_{np}-\sum_{j=1}^{\infty}A^{d}_{nj}\int_{h}^{1}rR^{u}_{np}(r)R^{d}_{nj}(r)\,dr=\sum_{j=1}^{\infty}Z_{nj}(0)\int_{h}^{1}rR^{u}_{np}(r)\,R^{I}_{nj}(r)\,dr\,. \qquad (5.138)$$

Equations (5.137) and (5.138) show, as before, the mutual interference among the radial harmonics. As noted earlier, in limit of vanishing swirl, the downstream radial eigenfunctions and eigenvalues would revert to the upstream ones so that this mutual interference would disappear, and the earlier more convenient procedures could be employed.

The above two matching conditions, as expressed in Eqs. (5.137) and (5.138), give rise to linear equations sufficient for the determination of the two sets of unknowns, $\{A^{u}_{np}\}$; they can be written as a 2p-by-2p complex matrix equation:

$$\left[\begin{array}{c|c} [\delta_{ij}] & [-\alpha_{nij}] \\ \hline [-\tau_{ni}\delta_{ij}] & [i(\lambda^d_{nj}\gamma_{nij} - nB\eta_{nij})] \end{array}\right] \left[\begin{array}{c} [A^u_{ni}] \\ \hline [A^d_{ni}] \end{array}\right] = \left[\begin{array}{c} [\sum_i] \\ \hline [\psi_{ni} + \sigma_i] \end{array}\right]$$

where

$$\begin{aligned}
\alpha_{nij} &= \int_h^1 r R^u_{ni}(r) R^d_{nj}(r)\, dr, \\
\sum_i &= \sum_J Z_{nj}(0) \int_h^1 r R^u_{ni}(r) R^I_{nj}(r) dr, \\
\gamma_{nij} &= \int_h^1 \rho_0^d (1 - M^{d2}_{z0}) r R^u_{ni}(r) R^d_{nj}(r)\, dr, \\
\eta_{nij} &= \int_h^1 \rho_0^d M^d_{z0} M_{\theta r} R^d_{nj}(r) R^u_{ni}(r)\, dr, \\
\sigma_i &= \sum_j \left\{ inB Z_{nj}(0) \int_h^1 \rho_0^d \frac{M^d_{z0} M_{\theta r}}{r} r R_{ni}(r) R^I_{nj}(r) dr \right. \\
&\qquad \left. - Z'_{nj}(0) \int_h^1 \rho_0^d (1 - M^{d2}_{z0}) r R^u_{ni}(r) R^I_{nj}(r) dr \right\}, \\
\tau_{ni} &= \left[(1 - M^{u2}_{z0}) \lambda^u_{ni} + i\omega M^{u2}_{z0} nB \right],
\end{aligned} \tag{5.139}$$

and

$$\psi_{ni} = \int_h^1 r R^u_{ni}(r) \Delta_n(r)\, dr$$

(Although these expressions may appear complicated, actual computation is direct, standard, and extremely rapid.)

Upon inverting the matrix equations (5.139) to give the $\{A^{u\,d}_{np}\}$, the three-dimensional flow field is completely determined.

Upstream of the blade row, we have

$$V^u_z = \bar{V}^u_z + \sum_{n=1}^{\infty} \sum_{p=1}^{\infty} \lambda^u_{np} A^u_{np} R^u_{np}(r) e^{\lambda^u_{np} z} e^{inB\theta}$$

$$V_\theta^u = \sum_{n=1}^{\infty}\sum_{p=1}^{\infty} inB A_{np}^u R_{np}^u(r) e^{\lambda_{np}^u z} e^{inB\theta},$$

$$V_r^u = \bar{V}_r^u + \sum_{n=1}^{\infty}\sum_{p=1}^{\infty} A_{np}^u R_{np}^{u'}(r) e^{\lambda_{np}^u z} e^{inB\theta} . \tag{5.140}$$

while downstream of the blade row we find

$$V_z^d = \bar{V}_z^d + \frac{V_{z0}^d}{2}\sum_{n=1}^{\infty} S_n(r) e^{inB\alpha_o^d} - \frac{(I+\frac{1}{2}\omega k_o)}{V_{z0}^d}\sum_{n=1}^{\infty} S_n(r) e^{inB\alpha_o^d}$$
$$+ \sum_{n=1}^{\infty}\sum_{p=1}^{\infty} i\lambda_{np}^d A_{np}^d R_{np}^d(r) e^{i\lambda_{np}^d z} e^{inB\theta} + \sum_{n=1}^{\infty}\sum_{p=1}^{\infty} Z'_{np}(z) R_{np}^I(r) e^{inB\theta}$$

$$V_\theta^d = V_{\theta o}^d + \frac{V_{\theta o}^d}{2}\sum_{n=1}^{\infty} S_n(r) e^{inB\alpha_o^d} + \frac{1}{r}\sum_{p=1}^{\infty}\sum_{n=1}^{\infty} inB A_{np}^d R_{np}^d(r) e^{i\lambda_{np}^d z} e^{inB\theta} + \frac{1}{r}\sum_{n=1}^{\infty}\sum_{p=1}^{\infty} inB Z_{np}(z) R_{np}^I(r) e^{inB\theta} \tag{5.141}$$

$$V_r^d = \bar{V}_r^d + \sum_{n=1}^{\infty}\sum_{p=1}^{\infty} A_{np}^d R_{np}^{d'}(r) e^{i\lambda_{np}^d z} e^{inB\theta} + \sum_{n=1}^{\infty}\sum_{p=1}^{\infty} Z_{np}(z) R_{np}^{I'}(r) e^{inB\theta}$$

where $\bar{V}_z^u$, $\bar{V}_z^r$, $\bar{V}_z^d$, and $\bar{V}_r^d$ are given in Eqs. (5.92) and (5.93).

5.5 The Downstream Vorticity Field

As pointed out below Eq. (5.19), gradients in entropy arising in the blade wakes can be described in terms of "reduced" vortex filaments on axial planes. Specifically, the reduced vorticity is given by

$$\xi_R = -\frac{(I+\frac{1}{2}\omega k_o)}{r V_{z0}^d}\sum_{n=1}^{\infty} inB S_n(r) e^{inB\alpha_o^d} , \tag{5.142}$$

$$\eta_R = +\frac{(I+\frac{1}{2}\omega K_0)}{V_{z0}^d}\sum_{n=1}^{\infty}\frac{\partial S_n}{\partial r}e^{inB\alpha_0^d} + \frac{(I+\frac{1}{2}\omega K_0)}{V_{z0}^{d2}}\sum_{n=1}^{\infty}\frac{2inBK_0}{r^3}zS_n(r)e^{inB\alpha_0^d}\,, \tag{5.143}$$

$$\zeta_R = 0\,, \tag{5.144}$$

where we recall (Section 5.2) that V_{z0}^d = constant and

$$V_{\theta 0}^d r = K_0\,.$$

Note that ζ_R remains zero as the flow proceeds downstream; this is consistent with the approximation used here, since the corresponding Helmholtz Equation for the reduced flow is simply

$$\underset{\sim}{W}_R\cdot\nabla\frac{\underset{\approx}{\Omega}_R}{\rho_R} - \frac{\underset{\approx}{\Omega}_R}{\rho_R}\cdot\nabla\underset{\sim}{W}_R = 0 \tag{5.145}$$

(see also the discussion of the reduced flow transformation in Section 4.7).

However, the above result does not necessarily imply that the actual vorticity field in the original flow must have components lying only in such planes. In fact from Eq. (5.32), we find the actual downstream vorticity field to be

$$\xi = \left[\frac{V_{z0}^d}{2r} + \frac{V_{\theta 0}^d}{2V_{z0}^d}\left(\frac{K_0}{r^2}-K_1\right) - \frac{(I+\frac{1}{2}\omega K_0)}{rV_{z0}^d}\right]\sum_{n=1}^{\infty}inBS_n(r)e^{inB\alpha_0^d}\,, \tag{5.146}$$

$$\eta = -\left[\frac{V_{z0}^d}{2} - \frac{(I+\frac{1}{2}\omega K_0)}{rV_{z0}^d}\right]\sum_{n=1}^{\infty}\frac{2inBK_0z}{r^3V_{z0}^d}S_n(r)e^{inB\alpha_0^d}$$

$$-\left[\frac{V_{z0}^d}{2} - \frac{(I+\frac{1}{2}\omega K_0)}{V_{z0}^d}\right]\sum_{n=1}^{\infty}\frac{\partial S_n}{\partial r}e^{inB\alpha_0^d}\,, \tag{5.147}$$

$$\zeta = Z\frac{rV_{\theta_0}^d}{2}\frac{1}{r}\sum_{n=1}^{\infty}\frac{2inBK_0}{V_{z_0}^d r^3}S_n(r)e^{inB\alpha_0^d} + \frac{rV_{\theta_0}^d}{2r}\sum_{n=1}^{\infty}\frac{\partial S_n}{\partial r}e^{inB\alpha_0^d} . \tag{5.148}$$

Thus, in the real flow axial vorticity components, ζ, actually grows with Z (when s_n is independent of r, however, ζ does vanish at the rotor plane).

The full Helmholtz equation for the untransformed flow can be written

$$\underset{\sim}{W}\cdot\nabla\frac{\underset{\approx}{\Omega}}{\rho} - \frac{\underset{\approx}{\Omega}}{\rho}\cdot\nabla\underset{\sim}{W} = \nabla T X \nabla S$$

$$= -\nabla\frac{1}{\rho} X \nabla P \ , \tag{5.149}$$

and this provides a means of interpreting (5.146) to (5.148).
The presence of downstream swirl results in the usual radial pressure gradient, which in turn results in a radial static temperature gradient. Because of the variation of the entropy field in the blade wakes considered here [Eq. (5.3)], surfaces of constant static temperature and entropy do not coincide (i.e., the fluid is non-barotropic). Thus, the RHS of Eq. (5.149) does not vanish. Correspondingly, Kelvin's theorem does not hold here, i.e., the fluid motion is not required to maintain irrotationality in the downstream region! The presence of non-zero ζ for $z > 0$ in the swirling downstream flow is consistent with this observation as well as with the results of Kerrebrock.[21]

[Alternatively, the presence of a growing ζ can be explained in terms of the occurring of secondary fluid motion through "bouyancy" effect (corresponding here to the centrifugal force field), which couples with density stratification in the working fluid introduced by the entropy variation brought in by the blade wakes]. The analysis given in Appendix I.E offers still another way of viewing this result; there it is shown

in particular, that the resulting axial vorticity component vanishes in the incompressible limit.

As mentioned above, if s_n is a constant, then as in our study of blade wakes in incompressible flow (Chapter 3), the vortex filaments are purely radial at the exit of the blade row (i.e., at z = 0). Still, as we have seen, as one moves downstream away from the blades, both tangential and axial components of the actual vorticity develop [Eqs. (5.147) and (5.148)]. This in turn effects the development of the streamwise component of vorticity, Ω_s, given in this case ($ds_n/dr = 0$) by

$$\Omega_S = -\frac{W_{\theta_0}^d}{W_0^d}\left[\frac{V_{z_0}^d}{2} - \frac{(I+\frac{1}{2}\omega K_0)}{V_{z_0}^d}\right]\sum_{n=1}^{\infty}\frac{2inBK_0Z}{V_{z_0}^d r^3} S_n(r)\, e^{inB\alpha_0^d} \cdot$$

$$+ \frac{W_{z_0}^d}{W_0^d}\frac{rV_{\theta_0}^d}{2r}\sum_{n=1}^{\infty}\frac{2inBK_0Z}{V_{z_0}^d r^3} S_n(r)\, e^{inB\alpha_0^d} \cdot \qquad (5.150)$$

Such streamwise vorticity, developing progressively, as the flow proceeds, sets up a "secondary" flow, including in particular radial flow. The flow field therefore must readjust as the result of continuity requirements. This provides an example of a three-dimensional effect analogous in many respects with more familiar types of secondary flow phenomena.

5.6 Induction of the Downstream Perturbation Static Pressure by the Blade Wakes.

As in the case of blade wakes in incompressible flow, a structural (downstream) pressure field is induced by the presence of blade wakes occurring simultaneously with a centrifugal force field.[21] Referring to Eq. (4.8), we have, for a calorically perfect gas,

$$I = H - \underset{\sim}{V}\cdot(\underset{\approx}{\omega}\times\underset{\sim}{r})$$

$$= C_p T_t - \omega r V_\theta ,$$

whence

$$I \cong C_p T_{to} - \omega r V_{\theta o} + C_p \delta T_t - \omega r \delta V_\theta , \tag{5.151}$$

in the approximation used here. In Eq. (5.151), δ denotes the net change in fluid properties as a result of any disturbance with respect to the reference flows, $\underset{\sim}{V}_0$. We have already noted that the rothalpy I remains constant along a relative streamline; because of the uniform inlet conditions assumed for the present case, the rothalpy therefore remains constant throughout. Hence, Eq. (5.151) yeilds

$$C_p \delta T_t - \omega r \delta V_\theta = 0 \tag{5.152}$$

But the stagnation temperature T_t is given in this case by

$$C_p T_t = C_p T + \frac{1}{2}\underset{\sim}{V}\cdot\underset{\sim}{V} , \tag{5.153}$$

so that

$$C_p \delta T_t = C_p \delta T + \underset{\sim}{V}\cdot\delta\underset{\sim}{V}$$

$$\simeq C_p \delta T + V_{zo}\delta V_z + V_{\theta o}\delta V_\theta . \tag{5.154}$$

Thus, Eq. (5.152) and (5.154) leads to

$$C_p \delta T = \omega r \delta V_\theta - V_{\theta o}\delta V_\theta - V_{zo}\delta V_z . \tag{5.155}$$

The specific entropy, s, is given by

$$\frac{\delta S}{C_p} = \ln\frac{T}{T_0} - \left(\frac{\gamma-1}{\gamma}\right)\ln\frac{P}{P_0} \tag{5.156}$$

which can be rewritten here in the form

$$\frac{\delta S}{C_p} = \ln\left(1+\frac{\delta T}{T_0}\right) - \left(\frac{\gamma-1}{\gamma}\right)\ln\left(1+\frac{\delta P}{P_0}\right) \simeq \frac{\delta T}{T_0} - \left(\frac{\gamma-1}{\gamma}\right)\frac{\delta P}{P_0} \,. \tag{5.157}$$

Combining Eqs. (5.155) and (5.157), we obtain finally

$$\frac{\delta P}{P_0} = -\left(\frac{\gamma}{\gamma-1}\right)\left[(V_{\theta 0}-\omega r)\frac{\delta V_\theta}{C_p T_0} + \frac{V_{z0}}{C_p T_0}\delta V_z + \frac{\delta S}{C_p}\right] \tag{5.158}$$

In dimensionless variables (see Section 5.), the upstream static pressure perturbation can be expressed as

$$\delta P^u = 2K_1 r\,\delta V_\theta^u - 2\delta V_z^u \,, \tag{5.159}$$

while the downstream static pressure perturbation, according to (5.158), can be written

$$\delta P^d = -2\left[\left(\frac{K_0}{r}-K_1 r\right)\delta V_\theta^d + V_{z0}^d \delta V_z^d\right](\tau_{du})^{\frac{1}{\gamma-1}} - \left(\frac{2}{\gamma-1}\right)\frac{(\tau_{du})^{\frac{\gamma}{\gamma-1}}}{M_{z0}^{u2}}\delta S \,, \tag{5.160}$$

where M_{z0}^u is the upstream reference Mach number, and τ_{du} is the ratio of downstream to upstream static temperatures. This latter ratio is given here by

$$\tau_{du} = (\pi_{du})^{\frac{\gamma-1}{\gamma}}\left(1+\frac{\gamma-1}{2}M_{z0}^{u2}\right) - \frac{\gamma-1}{2}M_{z0}^{u2}\left(V_{z0}^{d2}+\frac{K_0^2}{r^2}\right) \,, \tag{5.161}$$

where π_{du} is the pressure ratio across the rotor.

We focus our interest in the following downstream static pressure

field only. Substitution of δV_θ^d, δV_z^d, and δs in Eq. (5.161) leads to

$$\delta p^d = 2(\tau_{du})^{\frac{1}{\gamma-1}} V_{z0}^d \sum_{p=1}^{\infty} \lambda_p^d A_p^d e^{-\lambda_p^d z} R_p^d(r)$$

$$-2(\tau_{du})^{\frac{1}{\gamma-1}} \left\{ V_{z0}^d \sum_{n=1}^{\infty}\sum_{p=1}^{\infty} i\lambda_{np}^d A_{np}^d R_{np}^d(r) e^{i\lambda_{np}^d z} e^{inB\theta} + \left(\frac{K_0}{r_2} - K_1\right) \sum_{n=1}^{\infty}\sum_{p=1}^{\infty} inB A_{np}^d R_{np}^d(r) e^{i\lambda_{np}^d z} e^{inB\theta} \right\}$$

$$-2(\tau_{du})^{\frac{1}{\gamma-1}} \left\{ V_{z0}^d \sum_{n=1}^{\infty}\sum_{p=1}^{\infty} Z'_{np}(z) R_{np}^I(r) e^{inB\theta} + \left(\frac{K_0}{r_2} - K_1\right) \sum_{n=1}^{\infty}\sum_{p=1}^{\infty} inB Z_{np}(z) R_{np}^I(r) e^{inB\theta} \right\} . \quad (5.162)$$

The first single sum, arising from the solution to the circumferentially averaged flow, decays exponentially with distance downstream of the blade row. Similarly, the following two double sums, representing the homogeneous part of the solution of the circumferentially non-uniform flow, have an exponentially decaying behavior downstream of the blade row (combined with some osciallatory behaviro). However, the final two double sums doe not process this exponentailly decaying nature; they represent that part of the fluctuating pressure arising from the combined presence of the blade wakes with the centrifugal effects, as previously discussed. Its presistence downstream is dependent (among other parameters) upon the magnitude of nbK_0/V_{z0}^d ; indeed, its amplitude is determined by the value of an integral quite similar to that in Eq. (3.56)(the modification s here arises primarily from compressibility effects). Consequently, as with the effects of blade wakes in incompressible flow previously discussed, the induced pressure field will again decay inversely

with z. The specific dependence on (nBK_0/V^d_{z0}) is discussed in Chapter 6. We note further that, as expected, in the limit of zero swirl (i.e., $K_0 \to 0$), this induced pressure field vanishes identically. Thus, the induction of a persistent pressure field by downstream swirl can also be seen to reflect the fact that the perturbations induced by the wakes are not purely convected by the flow [in agreement with Eq. (5.141) , and the predictions in Reference 21].

In summary, we see that the entropy field produced by the viscous interaction between the working fluid and the blade surfaces is instrumental in determining the nature of the downstream vorticity field. In the presence of a centrifugal force field, this vorticity field in turn induces a static pressure disturbance. In this sense, therefore, the entropy, vorticity, and pressure disturbances are indeed coupled in swirling flows, as predicted in Reference 21.

CHAPTER 6 - BEHAVIOR OF BLADE WAKES

In this chapter we further examine the specific behavior of the blade wakes, together with the perturbations in fluid properties they induce as they are carried downstream (to a good approximation) by the mean fluid motion. We note first that the integrals appearing in the solution [i.e., Eqs. (3.39) and (5.127)], which describe the axial dependence of the waked induced velocity potentials, have in their integrals an exponential factor with an imaginary arguement. This factor can be expressed in the (dimensionless) form exp $\{-\text{inBz}\ (K_0/r^2 - K_1)/V_{z0}^d\}$ (recall here that V_{z0}^d is by definition unity for incompressible flow). Consequently, the integrand becomes increasingly oscillatory as a function of radius as the factor $(nBzK_0/V_{z0}^d)$ increases downstream, and the value of the integral can be expected to decrease as z increases for fixed values of n, B, and K_0/V_{z0}^d. Far downstream (i.e., for sufficiently large value of z) the integrals of this type finally vanish. We therefore conclude that the perturbations in fluid properties induced by the wakes (with the exception of those which are purely convected, such as entropy disturbances) also ultimately vanish at large distances from the blade row. Of course, the rate at which this takes place is also dependent on the magnitude of the parameters included in nBK_0/V_{z0}^d.

Physically, this can be explained in terms of the increasing destructive mutual interference of the wake-induced perturbations at given radii. Equivalently, one can also interpret this effect in terms of the downstream development of the vorticity field described earlier. Specifically, as the vortex filaments forming the blade wakes are carried downstream, they are also turned and distorted into a spiral form around the axis;

this is depicted in Fig. I.6. As one proceeds downstream the number of such spirals at a given axial plane increases. At very large distances from the blade row, the distance between adjacent spirals becomes infinitesimally small. In this limit one can scarcely single out any of the distinct blade wakes even though originally (at the exit plane of the blade row, z = 0) they are as structured as the arrangement of the blades in the blade row itself. In other words, the circumferential non-uniformity due to the presence of the discrete blade wakes eventually becomes smeared out.

In consequence, the related perturbed flow field tends toward circumferential uniformity at large distances from the blade row. Thus, in taking account of the presence of the blade wakes as a source of circumferential non-uniformity, we find that the background free-vortex flow (assumed for simplicity in the present part of this study) acts to destroy this non-uniformity by twisting or "winding-up" the blade wakes. [From these considerations, one may well raise doubts as the to usefulness of a possible Trefftz-plane analysis, analogous with that of classical wing theory in computing the induced flow field at the blade row, even though this has been carried out successfully in related sutdies[16].]

Up to this point, we have not discussed the integrals in Eqs. (3.39) and (5.12) either on a numerical or analytical basis. Even after numerical evaluation of these integrals, their content is often difficult to interpret. We therefore attempt to understand certain features of the downstream flow by considering the asymptotic behavior of the above integrals for large z, or to be more precise, for large values of (nBK_0z/V^d_{z0}). Integrals of the type occurring in Eq. (3.39) and (5.123) can be evaluated asymptotically by the method stationary phase. In this procedure, one

ordinarily argues that for large $(nBK_0 z/V_{z0}^d)$, the dominant contribution to the integral is from the neighborhood of the stationary points of the arguement in the exponential; away from such points, the integrand oscillates rapidly and can be expected to make little net contribution to the final result. However, the arguemnts in the exponentials encountered here possess no such stationary points. Even so, one can examine the asymptotic behavior of the integrals by a related argument as described below.

In the interval from r = h to r = 1, the first derivative of $\{- nB/V_{z0}^d \ (K_0/r^2 - K_1)\}$ with respect to r is non-zero (in fact, positive) so that it is a monotonically increasing function of r on that interval. Therefore, the integrand can be put into a more tractable form by first transforming to the variable

$$\tau \equiv -\frac{nB}{V_{z0}^d}\left(\frac{K_0}{r^2} - K_1\right) , \tag{6.1}$$

whence

$$d\tau = d\tau \Big/ \frac{2K_0 nB}{V_{z0}^d r^3(\tau)} . \tag{6.2}$$

Then the integral becomes

$$Z_{np}(z) = \int_{-\frac{nB}{V_{z0}^d}\left(\frac{K_0}{h^2} - K_1\right)}^{-\frac{nB}{V_{z0}^d}(K_0 - K_1)} e^{iz\tau} \frac{F(r)\, d\tau}{\frac{2nBK_0}{V_{z0}^d r^3}} , \tag{6.3}$$

where from (6.1), r = r(τ) (see below). Here, for blade wakes in incompressible flow,

$$F(r)=\frac{inB\bar{\omega}_n(r)\left(\frac{K_0}{r^2}-K_1\right)r\,\Gamma_{np}(r)}{2\left[\lambda_{np}^2+n^2B^2\left(\frac{K_0}{r^2}-K_1\right)\right)} \quad , \tag{6.4}$$

while for blade wakes in compressible flow,

$$F(r)=\frac{inB\,G_{rn}(r)\,R^{I}_{np}(r)}{\Lambda_{np}\left(1-M^{d2}_{z_0}\right)_{av}\left\{\left[\frac{nB\left(\frac{M^{d}_{z_0}M_{\theta r}}{r}\right)_{av}}{\left(1-M^{d2}_{z_0}\right)_{av}}+\frac{nB}{V^{d}_{z_0}}\left(\frac{K_0}{r^2}-K_1\right)\right]^2+\left[\frac{\chi^{I2}_{np}\left(1-M^{d2}_{z_0}\right)_{av}-n^2B^2\left(\frac{M^{d}_{z_0}M_{\theta r}}{r}\right)_{av}}{\left(1-M^{d2}_{z_0}\right)^2_{av}}\right]\right\}} \tag{6.5}$$

Because of its monotonic feature, as already mentioned, it is clear that the inverse of $-nB(K_0/r^2 - K_1)$ exists in the interval from r = h to r = 1 and, therefore, that $r = r(\tau)$ can be obtained. In particular, on integrating Eq. (6.3) by parts, we find

$$Z_{np}(z)=\left[F(r)\frac{e^{iz\tau}}{iz\frac{2nBK_0}{V^{d}_{z_0}r^3}}\right]_{-\frac{nB}{V^{d}_{z_0}}\left(\frac{K_0}{h^2}-K_1\right)}^{-\frac{nB}{V^{d}_{z_0}}(K_0-K_1)}-\frac{1}{iz}\int_{-\frac{nB}{V^{d}_{z_0}}\left(\frac{K_0}{h^2}-K_1\right)}^{-\frac{nB}{V^{d}_{z_0}}(K_0-K_1)}e^{iz\tau}\frac{d}{d\tau}\left[F(r)\Big/\frac{2nBK_0}{V^{d}_{z_0}r^3}\right]d\tau \tag{6.6}$$

For large z, the first term on the RHS of Eq. (6.6) decays as z^{-1}; we show below that the integral on the right will drop off at least as fast as $1/z^2$. For that purpose, we note simply that

$$\frac{d}{d\tau}\left[\frac{F(r)}{\frac{2nBK_0}{V^{d}_{z_0}r^3(\tau)}}\right]=\frac{\frac{dF}{dr}+\frac{3}{r^2}F(r)}{\left(\frac{2nBK_0}{V^{d}_{z_0}r^3}\right)^2} \quad , \tag{6.7}$$

which is bounded in the interval from r = h to r = 1. Hence

$$\left|\frac{d}{d\tau}\left[\frac{F(r)}{\frac{2nBK_0}{V^{d}_{z_0}r^3(\tau)}}\right]\right|\leq M \quad , \tag{6.8}$$

where M is some positive constant, and, consequently, the integral exists. Further as stated, it can almost decay at least as rapidly as $1/z^2$. From the above analysis, we are able to conclude that the "persistent" parts

of the perturbations induced by the blade wakes should be expected to decay inversely with z at large distances from the blade row. In particular, for blade wakes in incompressible free-vortex mean flow,

$$Z_{np}(z) \sim \frac{1}{4k_0 z}\left\{\frac{\bar{\omega}_n(1)(k_0-k_1)\Gamma_{np}(1)}{\left[\lambda_{np}^2+n^2B^2(k_0-k_1)^2\right]}e^{-izn\beta(k_0-k_1)} - \frac{\bar{\omega}_n(h)h^4\left(\frac{k_0}{h^2}-k_1\right)\Gamma_{np}(h)}{\left[\lambda_{np}^2+n^2B^2\left(\frac{k_0}{h^2}-k_1\right)^2\right]}\right\} \tag{6.9}$$

far downstream, and for blade wakes in compressible flow,

$$Z_{np}(z) \sim \frac{V_{z_0}^d}{4k_0 z\lambda_{np}\left(1-M_{z_0}^{d2}\right)_{av}}\left\{\frac{G_n(1)R_{np}^I(1)\,e^{-iz\,n\beta(k_0-k_1)/V_{z_0}^d}}{\left[\frac{nB\left(M_{z_0}^d M_{\theta r}\right)_{av}}{r\left(1-M_{z_0}^{d2}\right)_{av}}+\frac{nB}{V_{z_0}^d}(k_0-k_1)\right]^2+\left[\frac{\chi_{np}^{I2}\left(1-M_{z_0}^{d2}\right)_{av}-n^2B^2\left(\frac{M_{z_0}^d M_{\theta r}}{r}\right)_{av}^2}{\left(1-M_{z_0}^{d2}\right)_{av}^2}\right]}\right.$$

$$\left. - \frac{G_n(h)h^3R_{np}^I(h)\,e^{-iz\,n\beta\left(\frac{k_0}{h^2}-k_1\right)/V_{z_0}^d}}{\left[\frac{nB\left(M_{z_0}^d M_{\theta r}\right)_{av}}{r\left(1-M_{z_0}^{d2}\right)_{av}}+\frac{nB}{V_{z_0}^d}\left(\frac{k_0}{h^2}-k_1\right)\right]^2+\left[\frac{\chi_{np}^{I2}\left(1-M_{z_0}^{d2}\right)_{av}-n^2B^2\left(\frac{M_{z_0}^d M_{\theta r}}{r}\right)_{av}^2}{\left(1-M_{z_0}^{d2}\right)_{av}^2}\right]}\right\} . \tag{6.10}$$

These results are in agreement with, and help provide interpretation of, the numerical evaluation of the subject integrals which are in turn used to obtain the results shown in Figs. I.9 - I.12.

Mathematically, these results are also in correspondence with the often-used Riemann-Lebesque Theorem, which states that integrals such as those occurring in Eqs. (3.39) and (5.123) approach zero as z approaches infinity, provided (cf. Eq. 6.5) the function F(r) (which here is to some extent related to the radial distribution of the losses) is Riemann-integral and provided also that the integral converges absolutely. The requirement of the Riemann-integrability condition requires simply that the radial distribution of the losses be sufficiently smooth at the exit plane of the blade row.

To provide a contrasting example, let us consider a simple model in which the stagnation pressure loss has a spike at some point $r = r_0$ along the blade span, such that $\bar{\omega}(r)$ assumes roughly the character

$$\bar{\omega}(r) \sim C_0 \delta(r - r_0) \quad , \tag{6.11}$$

where c_0 is some constant. In that case, we would have, in contrast with the above, a persistent term of the form

$$Z_{np}(z) \sim \frac{inB}{2} \frac{C_0 \left(\frac{K_0}{r_0^2} - K_1\right) r_0 \Gamma_{np}(r_0) e^{-inB\left(\frac{K_0}{r_0^2} - K_1\right) z}}{\left[\lambda_{np}^2 + n^2 B^2 \left(\frac{K_0}{r_0^2} - K_1\right)^2\right]} \quad , \tag{6.12}$$

which does not vanish for any value of z.

Hence, if for any reason, the stagnation pressure loss can be approximated using Eq. (6.11)(for instance, such an effect might arise as a result of three-dimensional boundary layer behavior on the blades), then the perturbation in fluid properties could effectively persist "forever" downstream of the blade row. There is some recently obtained evidence that an effect of roughly this type may well occur as a result of shock boundary layer interaction in transonic fans[35,36,21]

CHAPTER 7 - NUMERICAL EXAMPLES FOR AN ISOLATED TRANSONIC ROTOR

The numerical examples included here are intended only to illustrate the implications of the inclusion of viscous effects within the blade row represented here through a variation of entropy across stream surfaces (e.g., the effects of the presence of blade wakes). For this purpose, we will take the simplest available model, in which the presence of the blade wake can be approximately represented by

$$S = S_1 e^{iB\bar{\alpha}_0^d} \tag{7.1}$$

where the real part is implied. Of course in a more complete model of the blade wakes, we would wish to use an analytical representation such as that given by Eq. (5.27). The value of s_1 in (7.1) above can be estimated through Eq. (5.26), together with experimental cascade data of the type presented in Fig. I.4. Two extreme values of $\bar{\omega}$ (or s_1) will be considered here: - (i) The total pressure loss coefficient $\bar{\omega}$ is taken to be 0.025; this would correspond to the value of $\bar{\omega}$ when the rotor is operating under nominally design conditions; (ii) The value of $\bar{\omega}$ is taken to be 0.06, corresponding to a point near stall for a typical rotor. A brief outline of the numerical computation used is given in Appendix I.I. We have shown analytically in the preceding chapters that the blade wakes induce a persistent static pressure field when interacting with a downstream swirling flow. The actual magnitude of this blade-to-blade variation of the pressure is illustrated in Fig. I.9 for the case of a transonic rotor near "design" conditions (case i above) with a hub-to-tip ratio of 0.8, a tip Mach number of 1.3, an inlet Mach number of 0.65

and a pressure ratio of 1.8. The number of blades is taken to be 40. Each blade is positioned at $\theta = 2\pi/40\ (m-1)$, where m assumes integer values from 1 to 40. From the figure, we see that, for distances significantly away from the blade row, the pressure pattern associated with the wake-induced disturbances is indeed present, although fairly weak. This is to be expected: for B = 40 the factor (nBK_0/V^d_{z0}) is sufficiently large so that the integral describing the wake-induced disturbances has a small value unless z is itself very small. For a particular value of z, the value of the integral previously discussed increases with decreasing number of blades. The corresponding strength of the pressure field associated with the wake-induced disturbances would therefore increase as the number of blades is reduced with the total loading on the rotor kept constant.

The corresponding blade to blade variation of radial velocities is illustrated in Fig. I.10. The magnitude of the radial velocity due to the presence of the blade wakes increases steadily with z for some distance downstream; at about z = 0.75, it reaches a maximum and then decreases vanishing ultimately. This behavior of the radial velocity can be interpreted in terms of the downstream development of the vorticity field described in Chapters 5 and 6. Initially, as we have seen, the blade wakes are carried downstream and a corresponding "secondary" vorticity develops growing in strength as it proceeds downstream. Ultimately, however, the winding up of the vortex filaments forming the wakes around the axis destroys the coherence of the induced field and the radial velocity associated with this secondary vorticity decreases. It is important to note that the radial velocity predicted by the circumferentially averaged flow solution (shown by the broken line in Fig. I.11) would decay to a negligible level

at about z = 0.1. The axial variation of the blade to blade axial velocity and tangential velocity perturbations for the same case are shown in Fig. I.11 and Fig. I.12, respectively. As indicated earlier, the value of $\bar{\omega}$ used for obtaining these figures was chosen to be 0.025; the magnitude of the perturbations due to this effect owuld naturally increase in proportion to the total pressure loss coefficient $\bar{\omega}$.

We have already pointed out that, because of the (initially) cumulative effect of the wakes on the perturbation field, the incidence angle of the flow at the blade may be modified. This could be of importance since the knowledge of the distribution of the flow angle is necessary in the design of the blades.

The magnitude of this effect for blade wakes occurring downstream of transonic rotors is illustrated in Fig. I.14 to I.17, there, the flow angle deflections through the rotor (as defined in Fig. I.8) are computed according to three different theories. In all examples:

Curve 1 is obtained using the simple axisymmetric radial equilibrium analysis;

Curve 2 is obtained using the circumferentially-averaged flow solution

Curve 3 is obtained using the circumferentially non-uniform (three-dimensional) flow solution including the effects of the vorticity in the blade wakes discussed here (Part I).

From these examples, it is clear that the modification in the flow angle deflection caused by the presence of the vorticity in the wakes is quite significant. Curve 3 in Fig. I.13 and Fig. I.14 is computed using values of $\bar{\omega}$ equal to 0.025 and 0.06 respectively, but otherwise for the same rotor and operating conditions as those specified for Figs. I.9 -

I.12. The higher value of $\bar{\omega}$ results in a drastic change in the flow angle deflection; in this case, the difference in the flow angle deflection predicted by the present theory and the more conventional axisymmetric (actuator disc) theory varies from about 6° at the hub to about 4° at the tip.

The curves shown in Figs. I.15 and I.16 are for the corresponding case of a transonic rotor again with a hub to tip ratio of 0.8, a blade number of 40, but operating at a pressure ratio of 1.5, a tip Mach number of 1.1 and an inlet Mach number of 0.5. The modification in the flow angle deflection is smaller than in the previous case; for instance, the difference in flwo angle deflection predicted by the present theory and the actuator disc theory varies from about 1° at the hub to about 0.9° at the tip with a value of 0.025 for $\bar{\omega}$, as compared to the previous case of the transonic rotor with a pressure ratio of 0.8, where it varies from about 2.3° at the hub to about 1.5° at the tip. From these examples we see, as expected that the extent of the modification in the flow angle deflection increases not only with the loss coefficient but also with the loading on the rotor.

CHAPTER 8 - CONCLUSIONS: PART I

(i) Three-dimensional flow effects induced by the vorticity present in the viscous blade wakes, though usually of little importance in external aerodynamics (e.g., flow over an isolated wing) can be significant in the internal aerodynamics of axial turbomachinery operating at practical loading conditions. For highly-loaded rotors, for example, the presence of vorticity in such blade wakes modifies the flow angle deflection through a rotor significantly, even for (optimally) low values of the total pressure loss coefficient. This suggests that in determining or predicting the distribution of flow angles over the blade span, such effects ought to be included.

(ii) Blade-to-blade disturbances in the fluid flow induced by blade wakes interacting with swirling flow generally are not purely convected by the mean flow even approximately: (exceptions include entropy disturbances and the stagnation pressure perturbations). In consequence the vorticity in such wakes induces a persistent downstream static pressure pattern not convected along mean streamlines. Although this static pressure field is fairly weak for distances significantly away from typical blade rows, its downstream persistence, which is a uniquely three-dimensional feature, can make it of importance for a variety of purposes.

(iii) Disturbances predicted by the conventional axisymmetric actuator disc theory decay exponentially to a negligible level in a short distance away from the blade row. By contrast, as just mentioned, the present three-dimensional theory shows the disturbances associated with the blade wakes do persist for a moderate distance downstream of the blade row. Eventually, however, these perturbations decay inversely with the

axial distance, an effect due to the winding up arround the axis of the vortex filaments present in the blade wakes. This contortion of the wake system gives rise to a mutually destructive induced field. Correct prediction of these phenomena requires study of nature of the flow associated with the blade wakes.

(iv) In contrast with the case of non-swirling flows, the vorticity and pressure fields cannot be separated in incompressible swirling flow. Similarly, in the case of compressible swirling flows, the vorticity and pressure fields are further coupled to any entropy disturbances present. Thus, these various flow types cannot be separated into non-interacting disturbances as is usually possible for flows over isolated wings and bodies.

CHAPTER 9 - SUGGESTIONS FOR FUTURE WORK

In the development of the three-dimensional theory presented here, we have considered a free-vortex rotor which sheds viscous wakes into downstream flow field only. Among other resutls, we have found that the vorticity in these blade wakes induces a flow field which modifies the flow angle at the blade significantly. The extent of this modification is dependent upon the losses within the blade row as well as the loading on the rotor. In the general case, it is virtually unavoidable that such modifications of the flow angles at the blade row will cause a spanwise variation of the loading on the blades. This in turn will result in the shedding of vorticity from the trailing edge of the blades. This trailing vorticity, usually of the Beltrami type, has not been included in the blade wakes described here, but has been treated in separate basis elsewhere.[18,19]

It seems appropriate therefore to suggest that a possible next step in the logical development of the theory would be to treat these two types of vorticity in the blade wakes at the same time. The presence of trailing vorticity can be regarded as one of the consequences of the presence of viscous blade wakes in the actual downstream flow. In general, the strength of this trailing vorticity must be determined consistently from an appropriate set of physical boundary conditions at the blade row, including simultaneously the effects of losses at the blades of the type discussed in the preceeding chapters.

So far, we have only confined the variation of entropy across stream surfaces to be a consequence of the viscous interaction between the working fluid and blade surfaces. However, the general approach now does not exclude the possibility of including losses due to other mechanisms

within the blade row. For instance, shock waves, which provide another loss mechanism occur within the blade passages of transonic rotors; these shocks also can interact strongly with the boundary layers on the blading. Thus, the entropy of the working fluid is increased in a variety of ways on passage though the rotor. Estimation or measurement of these entropy changes would allow their inclusion in the present theory. In this framework the objective would be to be able to provide an eventual comparison of theory with experiment, including in a realistic way as many as possible of the effects important to the understanding, design, and operation of a practical rotor on ducted fan.

APPENDIX I.A

The solution of Eq. (3.27) of Part I:

On substituting Eq. (3.38) in Eq. (3.27), we obtain

$$\sum_{n=1}^{\infty}\sum_{p=1}^{\infty} e^{inB\theta}\left\{Z_{np}\left(\frac{d^2\Gamma_{np}}{dr^2}+\frac{1}{r}\frac{d\Gamma_{np}}{dr}-\frac{n^2B^2}{r^2}\Gamma_{np}\right)+\frac{d^2Z_{np}}{dz^2}\Gamma_{np}\right\}$$

$$=-i\sum_{n=1}^{\infty} nB\frac{\bar{\omega}_n}{2}\left(\frac{K_0}{r^2}-K_1\right)e^{inB\bar{\alpha}} \qquad (A.1)$$

Upon making use of Eq. (3.34), for each circumferential harmonic n, we have

$$\sum_{p=1}^{\infty}\Gamma_{np}(r)\left(\frac{d^2Z_{np}}{dz^2}-\lambda_{np}^2Z_{np}\right)=-inB\frac{\bar{\omega}_n}{2}\left(\frac{K_0}{r^2}-K_1\right)e^{-inBz\left(\frac{K_0}{r^2}-K_1\right)}. \qquad (A.2)$$

On multiplying Eq. (A.2) by $r\Gamma_{nj}$, and integrating over {h,1} we obtain, by virtue of the orthogonality of the normalized radial eigenfunction Γ_{nj},

$$\frac{d^2Z_{np}}{dz^2}-\lambda_{np}^2Z_{np}=-\frac{inB}{2}\int_h^1 r\Gamma_{np}(r)\,\bar{\omega}_n\left(\frac{K_0}{r^2}-K_1\right)e^{-inBz\left(\frac{K_0}{r^2}-K_1\right)}\,dr. \qquad (A.3)$$

On solving Eq. (A.3) by the method of variation of parameters, we obtain the particular solution of Eq. (3.27) as given in Eq. (3.39).

APPENDIX I.B

Derivation of Eq. (4.68) of Part I:

By substituting Eq. (4.67) into the LHS of Eq. (4.25), we have,

$$\underset{\sim}{V} \times \underset{\sim}{\Omega} = e^{S/C_p}(\underset{\sim}{V}_R \times \underset{\sim}{\Omega}_R) + \frac{V_R^2}{2}\nabla e^{S/C_p} \quad (B.1)$$

But

$$C_p T_t = C_p T + \frac{1}{2}V^2$$

$$= C_p T + \frac{1}{2}V_R^2 e^{S/C_p},$$

so that

$$T\nabla S = T_t \nabla S - \frac{V_R^2}{2}\nabla e^{S/C_p} \quad (B.2)$$

Thus the RHS of (4.25) becomes

$$H - T\nabla S = C_p \nabla T_t - T_t \nabla S + \frac{V_R^2}{2}\nabla e^{S/C_p} \quad (B.3)$$

Upon equating Eqs. (B.1) and (B.2), we obtain

$$\underset{\sim}{V}_R \times \underset{\sim}{\Omega}_R = C_p e^{-S/C_p}\nabla T_t + T_t \nabla C_p e^{-S/C_p} = \nabla(C_p T_t e^{-S/C_p})$$

Hence

$$\underset{\sim}{V}_R \times \underset{\sim}{\Omega}_R = \nabla H e^{-S/C_p}$$

$$= C_p \nabla (P_t)^{\frac{\gamma-1}{\gamma}} \quad (B.4)$$

where we have used the relation

$$P_t^{\frac{\gamma-1}{\gamma}} = T_t e^{-S/C_p}$$

for a perfect gas.

APPENDIX I.C

Derivation of Eqs. (4.87) and (4.88):

By making use of Eqs. (4.67), (4.89) and (4.90) in the continuity equation (4.15a), we obtain

$$\nabla\cdot\rho\underset{\sim}{W} = \nabla\cdot(\rho_R \underset{\sim}{W}_R e^{-s/c_p})$$

$$= \rho_R \underset{\sim}{W}_R\cdot\nabla e^{-s/c_p} + e^{-s/2c_p}\nabla\cdot(\rho_R\underset{\sim}{W}_R) = 0$$

Because entropy is conserved along the relative streamline, therefore

$$\nabla\cdot(\rho_R\underset{\sim}{W}_R) = 0 , \tag{C.1}$$

which is Eq. (4.87).

As for the equation of motion (4.16), its LHS becomes, on substitution

$$\underset{\sim}{W}_R \times \underset{\sim}{\Omega}_R = e^{-s/c_p}\nabla I + c_p T\nabla e^{-s/c_p} + \frac{\underset{\sim}{V}\cdot\underset{\sim}{W}}{2}\nabla e^{-s/c_p} \tag{C.2}$$

We note that

$$\underset{\sim}{V}\cdot\underset{\sim}{W} = V^2 - \underset{\sim}{V}\cdot(\underset{\sim}{\omega}\times\underset{\sim}{r}) \tag{C.3}$$

$$I = c_p T_t - \underset{\sim}{V}\cdot(\underset{\sim}{\omega}\times\underset{\sim}{r}) \tag{C.4}$$

Eq. (B.2) can be written in the form of

$$c_p T\nabla e^{-s/c_p} = c_p T_t\nabla e^{-s/c_p} - \frac{V^2}{2}\nabla e^{-s/c_p} . \tag{C.5}$$

Making use of Eqs. (C.3) to (C.5) in Eq. (C.2), we obtain

$$\underset{\sim}{W}_R \times \underset{\sim}{\Omega}_R = \nabla(I e^{-s/c_p}) + \frac{1}{2}\underset{\sim}{V}\cdot(\underset{\sim}{\omega}\times\underset{\sim}{r})\nabla e^{-s/c_p}$$

$$= \nabla(I e^{-s/c_p}) + \frac{1}{2}(H-I)\nabla e^{-s/c_p} . \tag{C.6}$$

APPENDIX I.D

Derivation of mass flux continuity condition for circumferential average flow at the actuator disc:

The continuity of mass flux across the actuator disc requires that in the immediate neighborhood of Z = 0,

$$\left(\bar{\rho}\bar{V}_z\right)_{Z=0^-} = \left(\bar{\rho}\bar{V}_z\right)_{Z=0^+} \tag{D.1}$$

where 0^- refers to a station immediately upstream of the blade row while 0^+ refers to one immediately downstream of the blade row. To $0(\varepsilon)$, we can write Eq. (D.1) as

$$\left[\rho_o^u V_{zo}^u\left(\frac{\delta V_z}{V_{zo}^u}+\frac{\delta\rho}{\rho_o^u}\right)\right]_{Z=0^-} - \left[\rho_o^d V_{zo}^d\left(\frac{\delta V_z}{V_{zo}^d}+\frac{\delta\rho}{\rho_o^d}\right)\right]_{Z=0^+} = \left(\rho_o^d V_{zo}^d\right)_{Z=0^+} - \left(\rho_o^u V_{zo}^u\right)_{Z=0^-} . \tag{D.2}$$

Using the definition,

$$\frac{\bar{\rho}}{\rho_t} \equiv \left[1-\frac{\gamma-1}{2}\frac{\bar{V}^2}{a_t^2}\right]^{1/\gamma-1} , \tag{D.3}$$

one obtains

$$\frac{\delta\rho}{\rho_t} = -\frac{\bar{V}_z\delta V}{a_t^2}\left[1-\frac{\gamma-1}{2}\frac{\bar{V}_z^2}{a_t^2}\right]^{\left(\frac{2-\gamma}{\gamma-1}\right)} .$$

Thus,

$$\frac{\delta\rho}{\rho_o} = \frac{\delta\rho}{\rho_t}\frac{\rho_t}{\rho_o} \simeq -\frac{V_{zo}\delta V_z}{a_o^2} . \tag{D.4}$$

Substituting for $\delta p/\rho_0$ in Eq. (D.2), we obtain

$$\left(1-M_{zo}^{u2}\right)\delta V_z\Big|_{o^-} - \frac{\rho_o^d}{\rho_o^u}\left(1-M_{zo}^{d2}\right)\delta V_z\Big|_{o^+} = \frac{\rho_o^d}{\rho_o^u}V_{zo}^d - V_{zo}^u , \tag{D.5}$$

or

$$(1-M_{z0}^{u2})\frac{\partial \bar{\Phi}^u}{\partial z}\bigg|_{0^-} - \rho_0^d(1-M_{z0}^{d2})\frac{\partial \bar{\Phi}^d}{\partial z}\bigg|_{0^+} = (\rho_0^d V_{z0}^d - 1). \qquad \text{(D.6)}$$

(dimensionless)

APPENDIX I.E

Relationship between the transformed vorticity field and the actual vorticity field:

For flow steady in absolute frame the stagnation density ρ_t remains constant along the stream line, so that the continuity equation can be written as

$$\nabla\cdot\underset{\sim}{V} + \underset{\sim}{V}\cdot\nabla \ln\frac{\rho}{\rho_t} = 0 \tag{E.1}$$

Using the thermodynamic relation

$$T_t\nabla S = \nabla H - \frac{1}{\rho_t}\nabla P_t \,, \tag{E.2}$$

in the Euler equations of motion, we have

$$\underset{\sim}{V}\times\nabla\times\underset{\sim}{V} = -RT\nabla \ln P_t \tag{E.3}$$

To $0(\varepsilon)$,

$$\nabla\cdot\tilde{\underset{\sim}{V}} = -(\bar{\underline{V}} + \tilde{\underset{\sim}{V}})\cdot\nabla\ln\frac{\rho}{\rho_t} \tag{E.4}$$

$$\bar{\underline{V}}\times(\nabla\times\tilde{\underset{\sim}{V}}) = -R\bar{T}\nabla\ln P_t \tag{E.5}$$

The curl of Eq. (E.5) is

$$\left(\frac{\bar{V}_\theta}{r}\frac{\partial}{\partial\theta} + \bar{V}_z\frac{\partial}{\partial z}\right)\xi = 0 \tag{E.6a}$$

$$\left(\frac{\bar{V}_\theta}{r}\frac{\partial}{\partial\theta} + \bar{V}_z\frac{\partial}{\partial z}\right)\eta + \frac{2\bar{V}_\theta}{r}\xi = -\frac{dR\bar{T}}{dr}\frac{\partial\ln P_t}{\partial z} \tag{E.6b}$$

$$\left(\frac{\bar{V}_\theta}{r}\frac{\partial}{\partial\theta} + \bar{V}_z\frac{\partial}{\partial z}\right)\zeta = \frac{dR\bar{T}}{dr}\frac{\partial\ln P_t}{r\partial\theta} \tag{E.6c}$$

The components of Eq. (E.5) are:

$$\bar{V}_\theta \zeta - \bar{V}_z \eta = -R\bar{T}\frac{\partial \ln P_t}{\partial r} \tag{E.7a}$$

$$\bar{V}_z \xi = -R\bar{T}\frac{1}{r}\frac{\partial \ln P_t}{\partial \theta} \tag{E.7b}$$

$$\bar{V}_\theta \xi = R\bar{T}\frac{\partial \ln P_t}{\partial z} \tag{E.7c}$$

The last two equations may be combined to give

$$\left(\frac{\bar{V}_\theta}{r}\frac{\partial}{\partial \theta} + \bar{V}_z \frac{\partial}{\partial z}\right) \ln P_t = 0, \tag{E.8}$$

giving

$$\ln P_t = F\left(\theta - \frac{\bar{V}_\theta}{r^2} z\right). \tag{E.9}$$

Eqs. (E.7a) and (E.7b) give

$$\xi = -\frac{R\bar{T}}{r\bar{V}_z} F' \tag{E.10a}$$

$$\bar{V}_\theta \zeta - \bar{V}_z \eta = -\frac{2\bar{V}_\theta z}{r}\frac{R\bar{T}}{r\bar{V}_z} F' \tag{E.10b}$$

The solenoidality of the vorticity vector gives

$$\eta = \frac{\bar{V}_\theta}{\bar{V}_z}\left(\frac{2z}{r^2}\frac{R\bar{T}}{\bar{V}_z} F' + \zeta\right) \tag{E.11}$$

and

$$\frac{1}{r}\frac{\partial \eta}{\partial \theta} = \frac{\bar{V}_\theta}{\bar{V}_z}\left(\frac{2z}{r^2}\frac{R\bar{T}}{r\bar{V}_z} F'' + \frac{1}{r}\frac{\partial \zeta}{\partial \theta}\right). \tag{E.12}$$

From Eqs. (E.10a) and (E.12), one obtains

$$\left(\frac{\bar{V}_\theta}{r}\frac{\partial}{\partial \theta} + \bar{V}_z \frac{\partial}{\partial z}\right)\zeta = \frac{1}{r}\frac{dR\bar{T}}{dr} F' \tag{E.13}$$

Let $\zeta = f(r)\, F'(\theta - K_0 Z/r^2)Z$ so that $\zeta = 0$ at $Z = 0$ (ζ can be made non-zero at $Z = 0$ by adding a constant). Therefore,

$$\left(\frac{\bar{V}_\theta}{r}\frac{\partial}{\partial\theta} + \bar{V}_z\frac{\partial}{\partial z}\right)\zeta = f(r)\,F' . \tag{E.14}$$

Comparing Eq. (E.14) with (E.13), we identify f(r) to be

$$f(r) = \frac{1}{r}\frac{d\bar{RT}}{dr} .$$

Hence,

$$\zeta = \frac{z}{r\bar{V}_z}\frac{d\bar{RT}}{dr}F'\left(\theta - \frac{K_0 z}{r^2}\right) \tag{E.15}$$

The tangential vorticity component η is now obtainable from Eq. (E.10b); it is given by

$$\eta = \frac{\bar{V}_\theta z}{\bar{V}_z r^2}\frac{1}{r\bar{V}_z}\frac{d(r^2\bar{RT})}{dr}F' . \tag{E.16}$$

For flow with constant stagnation enthalpy,

$$C_p T_t = C_p\bar{T} + \frac{1}{2}\bar{V}_\theta^2 + \frac{1}{2}\bar{V}_z^2 = \text{constant} , \tag{E.17a}$$

so that

$$\frac{d\bar{RT}}{dr} = \frac{\gamma-1}{\gamma}\frac{\bar{V}_\theta^2}{r} \tag{E.17b}$$

and

$$\frac{dr^2\bar{RT}}{dr} = \left(\frac{\gamma-1}{\gamma}\right)r\bar{V}_\theta^2 + 2r\bar{RT} \tag{E.17c}$$

From the above, one readily sees that there is indeed an axial vorticity component which grows with Z whenever there is a swirl; the strength of the growth is proportional to the strength of the swirl. By allowing

the specific heat ratio γ to approach infinity, the incompressible limit is obtained. In that limit,

$$\frac{d\bar{R}\bar{T}}{dr} = 0 \quad , \quad \frac{dr^2\bar{R}\bar{T}}{dr} = 2r\bar{R}\bar{T} \, , \qquad \zeta = 0$$

i.e., axial vorticity componetn ζ is zero in the incompressible limit.

APPENDIX I.F

The solution for $\phi_I^d(r,\theta,z)$:

On substituting Eq. (5.122) in Eq. (5.95), we obtain

$$\sum_{n=1}^{\infty}\sum_{p=1}^{\infty}\left\{\left[(1-M_{zo}^{d2})_{av}\frac{d^2Z_{np}}{dz^2}-2inB\left(\frac{M_{zo}^{d}M_{\theta r}}{r}\right)_{av}\frac{dZ_{np}}{dz}\right]R_{np}^{I}e^{inB\theta}+e^{inB\theta}\cdot\right.$$
$$\left.\left[\frac{d^2R_{np}^{I}}{dr^2}+\frac{(1+M_{\theta a}^{2})}{r}\frac{dR_{np}^{I}}{dr}-\frac{n^2B^2}{r^2}(1-M_{\theta r}^{2})R_{np}^{I}\right]Z_{np}\right\}=-\sum_{n=1}^{\infty}inBG_{n(r)}e^{inB\left[\theta-\frac{z}{V_{zo}^{d}}\left(\frac{K_o}{r^2}-K_1\right)\right]} \quad (F.1)$$

with $G_n(r)$ given in Eq. (5.126).

On making use of Eq. (5.118), for each circumferential harmonic n, we have

$$\sum_{p=1}^{\infty}\left\{(1-M_{zo}^{d2})_{av}\frac{d^2Z_{np}}{dz^2}-2inB\left(\frac{M_{zo}^{d}M_{\theta r}}{r}\right)_{av}\frac{dZ_{np}}{dz}+\left[K_{np}^{2}(1-M_{zo}^{d2})_{av}-2nBK_{np}\left(\frac{M_{zo}^{d}M_{\theta r}}{r}\right)_{av}\right]Z_{np}\right\}R_{np}^{I}$$
$$=-inG_{n(r)}e^{-inB\frac{z}{V_{zo}^{d}}\left(\frac{K_o}{r^2}-K_1\right)} \quad (F.2)$$

Multiplying Eq. (F.2) by $e^{\int 1+M_{\theta a}/r\,dr}\,R_{nj}^{I}(r)$ and integrating {h,1}, we obtain, by virtue of the orthogonality of the set of eigenfunctions $\{R_{nj}^{I}(r)\}$,

$$(1-M_{zo}^{d2})_{av}\frac{d^2Z_{np}}{dz^2}-2inB\left(\frac{M_{zo}^{d}M_{\theta r}}{r}\right)_{av}\frac{dZ_{np}}{dz}+\left[K_{np}^{2}(1-M_{zo}^{d2})_{av}-2nBK_{np}\left(\frac{M_{zo}^{d}M_{\theta r}}{r}\right)_{av}\right]Z_{np}$$
$$=-\frac{1}{\Delta_{nn}}\int_{h}^{1}inBG_{n(r)}R_{np}^{I}e^{\int\frac{1+M_{\theta a}^{2}}{r}}e^{-inB\left(\frac{K_o}{r^2}-K_1\right)\frac{z}{V_{zo}^{d}}} \quad (F.3)$$

On solving Eq. (F.3) by the method of variation of parameters, we obtain the particular solution of $Z_{np}(z)$ as given in Eq. (5.123).

APPENDIX I.G

The derivation of mass flux continuity condition at the blade row for the circumferentially non-uniform flow:

The mass flux, continuity condition demands that the local change in the mass flux across the plane Z = 0 be given by

$$\Delta \dot{m} = \Delta(\rho V_z) = (\rho V_z)^d - (\rho V_z)^u = 0 \tag{G.1}$$

Here, we will use the superscripts "u" and "d" to denote stations immediately upstream and downstream of the blade row.

The energy equation for the flow relative to the rotor coordinates is

$$C_p T_{-\infty} + \frac{1}{2} V_{-\infty}^2 + \frac{1}{2}\omega^2 r^2 = C_p T^u + \frac{1}{2} V_z^{u2} + \frac{1}{2} V_r^{u2} + \frac{1}{2}(V_\theta^u - \omega r)^2$$

$$= C_p T^d + \frac{1}{2} V_z^{d2} + \frac{1}{2} V_r^{d2} + \frac{1}{2}(V_\theta^d - \omega r)^2 \ . \tag{G.2}$$

The subscript "$-\infty$" refers to a station far upstream (i.e., the upstream radial equilibrium value). Eq. (G.2) is equivalent to the statement of constancy of rothalpy.

To $O(\varepsilon)$, we obtain from Eq. (G.2)

$$\frac{T^d}{T_{-\infty}} = 1 + \frac{1}{2C_p T_{-\infty}}\left[V_{-\infty}^2 - \bar{V}_z^{d2} - 2\bar{V}_\theta^d \omega r - \bar{V}_\theta^{d2}\right] - \frac{V_{z0}^d \tilde{V}_z^d + V_{\theta 0}^d \tilde{V}_\theta^d - \omega r \tilde{V}_\theta^d}{C_p T_{-\infty}} \ , \tag{G.3a}$$

and

$$\frac{T^u}{T_{-\infty}} = 1 + \frac{1}{2C_p T_{-\infty}}\left[V_{-\infty}^2 - \bar{V}_z^{u2}\right] - \frac{V_{z0}^u \tilde{V}_z^u - \omega r \tilde{V}_\theta^u}{C_p T_{-\infty}} \ . \tag{G.3b}$$

The circumferential mean of the above two equations gives

$$\frac{\bar{T}^d}{T_{-\infty}} = 1 + \frac{1}{2C_p T_{-\infty}}\left[V_{-\infty}^2 - \bar{V}_z^{d2} - \bar{V}_\theta^{d2} + 2\bar{V}_\theta^d \omega r\right] \ , \tag{G.4a}$$

and

$$\frac{\bar{T}^u}{T_{-\infty}} = 1 + \frac{1}{2C_p T_{-\infty}}\left[V_{-\infty}^2 - \bar{V}_z^{u2}\right] . \tag{G.4b}$$

The viscous interaction within the blade row introduces an entropy jump of the fluid across the blade row. As such, one must not relate the thermodynamic properties of the fluid downstream to those of the upstream by means of any thermodyanmic relation which bears any implication of isentropic process.

For a calorically perfect gas,

$$\frac{\rho^d}{\rho_{-\infty}} = \left(\frac{T^d}{T_{-\infty}}\right)^{\frac{1}{\gamma-1}} e^{-\Delta S/R} \tag{G.5}$$

Upon making use of Eqs. (G.4a) and (G.5) in Eq. (G.3a), we obtain to $O(\varepsilon)$

$$\frac{\rho^d}{\rho_{-\infty}} \simeq \left(\frac{\bar{T}^d}{T_{-\infty}}\right)^{\frac{1}{\gamma-1}}\left[1 - \frac{(V_{z0}^d \tilde{V}_z^d + V_{\theta 0}^d \tilde{V}_\theta^d - \omega r \tilde{V}_\theta^d)}{C_p \bar{T}^d (\gamma-1)} - \frac{\Delta S}{R}\right] \tag{G.6}$$

Similarly, we can write

$$\frac{\rho^u}{\rho_{-\infty}} \simeq \left(\frac{\bar{T}^u}{T_{-\infty}}\right)^{\frac{1}{\gamma-1}}\left[1 - \frac{V_{z0}^u \tilde{V}_z^u - \omega r \tilde{V}_\theta^u}{C_p \bar{T}^u (\gamma-1)}\right] . \tag{G.7}$$

Eq. (G.1) may be rewritten as [to $O(\varepsilon)$]

$$\left(\bar{\rho}^d \bar{V}_z^d - \bar{\rho}^u \bar{V}_z^u\right) + \rho_0^d \tilde{V}_z^d + \tilde{\rho}^d V_{z0}^d - \rho_0^u \tilde{V}_z^u - \tilde{\rho}^u V_{z0}^u = 0 . \tag{G.8}$$

But the mass flux continuity condition for the circumferential averaged flow is

$$\bar{\rho}^d \bar{V}_z^d = \bar{\rho}^u \bar{V}_z^u .$$

so that Eq. (G.8) becomes

$$\rho_0^d \tilde{V}_z^d + \tilde{\rho}^d V_{z0}^d - \rho_0^u \tilde{V}_z^u - \tilde{\rho}^u V_{z0}^u = 0 . \tag{G.9}$$

Because $\bar{\rho}^u/\rho_{-\infty} = (\bar{T}^u/T_{-\infty})^{1/\gamma-1}$ and $\bar{\rho}^d/\rho_{-\infty} = (\bar{T}^d/T_{-\infty})^{1/\gamma-1}$, we deduce from Eqs. (G.6) and (G.7) that

$$\frac{\tilde{\rho}^d}{\rho_{-\infty}} \simeq -\left(\frac{T_0^d}{T_{-\infty}}\right)^{\frac{1}{\gamma-1}} \frac{\left(V_{z0}^d \tilde{V}_z^d + V_{\theta 0}^d \tilde{V}_\theta^d - \omega r \tilde{V}_\theta^d\right)}{c_p T_0^d (\gamma-1)} - \left(\frac{T_0}{T_{-\infty}}\right)^{\frac{1}{\gamma-1}} \frac{\Delta S}{R} , \tag{G.10}$$

and

$$\frac{\tilde{\rho}^u}{\rho_{-\infty}} = -\frac{V_{z0}^u \tilde{V}_z^u - \omega r \tilde{V}_\theta^u}{c_p T_0^u (\gamma-1)} \tag{G.11}$$

Substituting for $\tilde{\rho}^d$ and $\tilde{\rho}^u$ in Eq. (G.9) and noting that $a_0^{u\,2} = c_p T_0^u (\gamma-1)$, $a_0^{d\,2} = c_p T_0^d (\gamma-1)$, we have, in appropriate dimensionless form,

$$\rho_0^d (1-M_{z0}^{d2}) \tilde{V}_z^d - \rho_0^d M_{z0}^d M_{\theta r} \tilde{V}_\theta^u - \left(\frac{\gamma}{\gamma-1}\right) \Delta S - (1-M_{z0}^{u2}) \tilde{V}_z^u - \omega r M_{z0}^{u2} \tilde{V}_\theta^u = 0 . \tag{G.12}$$

From Eqs. (5.36), we have

$$\tilde{\underset{\sim}{V}}^d = \nabla \phi^d + V_{z0}^d \frac{S}{2} \hat{e}_z - \frac{(I + \frac{1}{2}\omega k_0)}{V_{z0}^d} S \hat{e}_z + V_{0\theta}^d \frac{S}{2} \hat{e}_\theta . \tag{G.13}$$

If Beltrami component of vorticity were present, it is then necessary to add $(G\hat{e}_r)$ to Eq. (G.13). Substituting for the various components of velocity in Eq. (G.12), we finally obtain the mass flux continuity condition at the blade row to be,

$$\rho_0^d (1-M_{z0}^{d2}) \left.\frac{\partial \phi^d}{\partial z}\right|_{z=0^+} - \rho_0^d \frac{M_{z0}^d M_{\theta r}}{r} \left.\frac{\partial \phi^d}{\partial \theta}\right|_{z=0^+} - (1-M_{z0}^{u2}) \left.\frac{\partial \phi^u}{\partial z}\right|_{z=0^-} - \omega M_{z0}^{u2} \left.\frac{\partial \phi^u}{\partial \theta}\right|_{z=0^-}$$

$$= \left\{ \left(\frac{\gamma}{\gamma-1}\right) + \rho_0^d (1-M_{z0}^{d2}) \left[\frac{(I + \frac{1}{2}\omega k_0)}{V_{z0}^d} - \frac{V_{z0}^d}{2} \right] + \rho_0^d K_0 \frac{M_{z0}^d M_{\theta r}}{2r} \right\} S . \tag{G.14}$$

APPENDIX I.H

Variational method for the determination of characteristic values and functions:

Mathematically, the problem of solving a boundary value problem for a differential equation is similar to the minimizing of the integral for which the given differential equation is the Euler-Lagrange equation in the calculus of variation. The methods employed for the solution of problems in the calculus of variations are also the methods for the solution of the boundary value problems for the differential equations. Examples of such methods are the Raleigh-Ritz's method and the Galerkin's method. We shall confine ourselves to the method of B. G. Galerkin since it is being used for the solution of Eqs. (5.71), (5.113) and (5.118).

Method of B. G. Galerkin[61]

Basically, by the method of B. G. Galerkin, the solution of the equation

$$L(u) = 0. \tag{H.1}$$

can be sought in the approximate form of

$$\bar{u} = \sum_{i=1}^{m} a_i \psi_i \tag{H.2}$$

Here, L is the differential operator (which may involve two variables), the solution of which satisfies a set of homogeneous boundary conditions. The set of functions $\{\psi_i\}$ are chosen to satisfy the given boundary conditions and the a_i are the yet undetermined coefficients. The functions ψ_i are assumed to be linearly independent. In order that $\bar{u}$ be an exact solution of Eq. (H.1), it is necessary that

$$L(\bar{u}) = 0 . \tag{H.3}$$

Eq. (H.3) together with the fact that $L(\bar{u})$ be continuous, ensures that the expression $L(\bar{u})$ is orthogonal to all the functions ψ_i. So if i runs from 1 to m, then there are m conditions of orthogonality sufficient for the determination of the coefficients a_i; i.e., the system of equations

$$\iint_R L(\bar{u})\psi_i \, dX = \iint_R L\left(\sum_{j=1}^{m} a_j \psi_j\right)\psi_i \, dX = 0 , \tag{H.4}$$

where i runs from 1 to m. The set of equations in (H.4) is sufficent for the determination of the coefficients a_i.

In what follows, we outline briefly how the characteristic values and functions of Eqs. (5.71), (5.113), and (5.118) may be determined.

Seeking the solution of Eq. (5.71) in the form of

$$\bar{R}_p^d(r) = \sum_i a_i \psi_i(r) \tag{H.5}$$

where $\{\psi_i(r)\}$ is a complete set of functions satisfying the boundary conditions in (5.72).

Substituting for $\bar{R}_p^d$ and $d\bar{R}_p^d/dr$ in Eqs. (5.71), we obtain

$$\frac{d}{dr}\left\{e^{\int \frac{1+M_{\theta a}^2}{r} dr} \sum_{j=1}^{p} a_j \psi_j'(r)\right\} + \lambda_p^{d^2}\left(1-M_{za}^{d^2}\right) e^{\int \frac{1+M_{\theta a}^2}{r} dr} \sum_{j=1}^{p} a_j \psi_j = 0 \tag{H.6}$$

But the othogonality of the LHS of Eq. (H.6) to the set of functions $\{\psi_i(r)\}$ (where i runs from 1 to p) leads to

$$\int_h^1 \frac{d}{dr}\left\{e^{\int \frac{1+M_{\theta a}^2}{r} dr} \sum_{j=1}^{p} a_j \psi_j'\right\}\psi_i \, dr + \lambda_p^{d^2} \int_h^1 \left(1-M_{za}^{d^2}\right) e^{\int \frac{1+M_{\theta a}^2}{r} dr} \psi_i \sum_{j=1}^{p} a_j \psi_j \, dr = 0 . \tag{H.7}$$

On integrating the first integral of Eq. (H.7) by parts and noting

that

$$\left.\frac{d\psi_i}{dr}\right|_{r=h} = \left.\frac{d\psi_i}{dr}\right|_{r=1} = 0 , \tag{H.8}$$

we obtain

$$\sum_{j=1}^{p} \left(-\alpha_{ij} + \lambda_p^{d^2}\beta_{ij}\right) a_j = 0 , \tag{H.9}$$

where

$$\alpha_{ij} = \int_h^1 e^{\int \frac{1+M_{\theta a}^2}{r} dr} \psi_i' \psi_j' \, dr \tag{H.10a}$$

and

$$\beta_{ij} = \int_h^1 e^{\int \frac{1+M_{\theta a}^2}{r} dr} \left(1 - M_{z0}^{d^2}\right) \psi_i \psi_j \, dr . \tag{H.10b}$$

It is seen that the system of equations in (H.9) is a homogeneous system of equations in p unknowns; therfore it has a non-trivial solution only in the case where the determinant of this system vanishes; i.e.,

$$\left|\left(-\alpha_{ij} + \lambda_p^{d^2}\beta_{ij}\right)\right| = 0 . \tag{H.11}$$

Eq. (H.11) will result in a polynomial of p^{th} degree in $\lambda_p^{d^2}$ and therfore will give p roots of $\lambda_p^{d^2}$ which are the characteristic values. For each $\lambda_p^{d^2}$, the system of Eqs. (H.9) will have a non-zero solution a_i which will give the approximate characteristic function $\bar{R}_p^d(r)$ for that particular $\lambda_p^{d^2}$. We note that these functions are determined up to an arbitrary factor only. Since the system of Eqs. (H.9) is only an approximation to Eq. (5.71), therefore, it is expected that the determined values of $\lambda_p^{d^2}$ will be approximations to the actual characteristic values.

Similarly, the functions $\bar{R}_p^d(r)$ will be approximations to the respective characteristic functions $R_p^d(r)$. However, they are sufficiently accurate for all practical purposes.

Written in matrix form, Eq. (H.9) becomes p by p matrix equation:

$$[\alpha_{ij}][a_i] = \lambda_p^{d^2}[\beta_{ij}][a_i] \tag{H.12}$$

where $[a_{ij}]$ is a matrix with elements a_{ij} and the subscripts i and j runs from 1 to p. The solution then simply involves the determination of the eigenvalues and the eigenvectors of a p by p matrix given by the following:

$$[\alpha_{ij}] = \lambda_p^{d^2}[\beta_{ij}] , \tag{H.13}$$

or

$$[\alpha_{ij}][\beta_{ij}]^{-1} = \lambda_p^{d^2}[\delta_{ij}] . \tag{H.14}$$

The procedure for the solution to Eq. (5.118) is quite similar to that of Eq. (5.71) but with

$$\alpha_{ij} = \int_h^1 e^{\int \frac{1+M_{\theta a}^2}{r} dr} \left[\psi_i' \psi_j' + \frac{n^2 B^2}{r^2}(1-M_{\theta r}^2)\psi_i \psi_j\right] dr ,$$

$$\beta_{ij} = \int_h^1 e^{\int \frac{1+M_{\theta a}^2}{r} dr} \psi_i \psi_j \, dr ,$$

and $\chi_{np}^{I^2}$ defined by Eq. (5.125) replacing $\lambda_p^{d^2}$.

As for Eq. (5.113), we would have the following corresponding matrix equation:

$$[A_{ij}][a_i] = \lambda_{np}^d [B_{ij} + \lambda_{np}^d C_{ij}][a_i] , \tag{H.15}$$

where

$$A_{ij} = \int_h^1 e^{\int \frac{1+M_{\theta a}^2}{r} dr} \left[\psi_i' \psi_j' + \frac{n^2 B^2}{r^2}(1-M_{\theta r}^2)\psi_i \psi_j\right] dr \tag{H.16}$$

$$B_{ij} = \int_h^1 e^{\int \frac{1+M_{\theta a}^2}{r} dr} \frac{2M_{z0}^d M_{\theta r}}{r} nB \psi_i \psi_j \, dr, \tag{H.17}$$

$$C_{ij} = \int_h^1 e^{\int \frac{1+M_{\theta a}^2}{r} dr} (M_{z0}^{d2} - 1)\psi_i \psi_j \, dr. \tag{H.18}$$

However, the matrix equation (H.15) can be reexpanded into the following equivalent form,

$$\begin{bmatrix} [A_{ij}] & [0] \\ [0] & [\delta_{ij}] \end{bmatrix} \begin{bmatrix} [a_i] \\ [\lambda_{np}^d a_i] \end{bmatrix} = \lambda_{np}^d \begin{bmatrix} [B_{ij}] & [C_{ij}] \\ [\delta_{ij}] & [0] \end{bmatrix} \begin{bmatrix} [a_i] \\ [\lambda_{np}^d a_i] \end{bmatrix}, \tag{H.19}$$

so that the corresponding matrix equation for the determination of the eigenvalues and eigenvectors become

$$\begin{bmatrix} [A_{ij}] & [0] \\ [0] & [\delta_{ij}] \end{bmatrix} = \lambda_{np}^d \begin{bmatrix} [B_{ij}] & [C_{ij}] \\ [\delta_{ij}] & [0] \end{bmatrix}. \tag{H.20}$$

A convenient set of functions $\psi_i(r)$ used in the solution of equations (5.71), (5.113), and (5.118) would be the set of orthogonal functions $\{R_{0i}(r)\}$ for the solution of a Sturm-Lioville type of equation:

$$\frac{d^2 R_{oi}}{dr^2} + \frac{1}{r}\frac{dR_{oi}}{dr} + \lambda_{oi}^2 R_{oi} = 0, \tag{H.21}$$

which is a zeroth order Bessel equation.

The boundary conditions to be satisfied are:

$$\left.\frac{dR_{oi}}{dr}\right|_{r=h} = \left.\frac{dR_{oi}}{dr}\right|_{r=1} = 0. \tag{H.22}$$

Then the orthonormal function $R_{0i}(r)$ would be a linear combination of zeroth order Bessel function of the first kind and second kind and is given by

$$R_{oi}(r)=\frac{1}{\sqrt{N_{oi}}}\left\{J_o(\lambda_{oi}r)-\frac{J_o'(\lambda_{oi})}{Y_o'(\lambda_{oi})}Y_o(\lambda_{oi}r)\right\} \tag{H.24}$$

where

$$N_{oi}=\int_h^1 r\left\{J_o(\lambda_i r)-\frac{J_o'(\lambda_{oi})}{Y_o'(\lambda_{oi})}Y_o(\lambda_{oi}r)\right\}^2 dr \cdot \tag{H.25}$$

By taking λ_{0i} to be the roots of

$$J_1(\lambda_{oi})Y_1(\lambda_{oi}h)-Y_1(\lambda_{oi})J_1(\lambda_{oi}h)=0 \cdot \tag{H.26}$$

Eq. (H.22) satisfies.

Hence the characteristic function can be approximated by

$$\sum_{i=1}^{p} a_{i-1}R_{oi-1}(r) \tag{H.27}$$

Here $\lambda_{00} = 0$, and $R_{00} = \sqrt{2/(1-h)}$ are included in the sets of $\lambda_{0(i-1)}$ and $R_{0(i-1)}(r)$ (i=1,2,...p) in order for the latter to be a complete set of orthonormal functions.

However, a much simpler set for $\{\psi_i(r)\}$ would be given by

$$\psi_i(r)=\cos\left[\frac{(i-1)\pi(r-h)}{(1-h)}\right] \cdot \tag{H.28}$$

Finally, we note that the orthogonality of the eigenfunctions satisfying Eq. (5.71) and (5.118) may be slightly modified through the use of Galerkin scheme. However, this modification is usually negligible.

APPENDIX I.I

A note on numerical computation:

The Bessel functions of high order and their derivatives encountered here are evaluated using the asymptotic expansions given in Ref. 62. The computer subroutines used for their numerical evaluation are those developed by W. K. Cheng[18] and L. T. Chen[34].

The numerical evaluation of the eigenvalues and eigenvectors of matricies, and the numerical solution of matrix equations are all done using the IMSL subroutines.

We note that in the construction of the integral in Eq. (5.127), use is made of the orthogonality of the functions $\{R^I_{np}\}$. But the function $R^I_{np}(r)$ is determined from Eq. (5.118) using the Galerkin Method. It is approximated by

$$R^I_{np}(r) = \sum_{i=1}^{P} a_{ni} \cos\left[\frac{(i-1)\pi(r-h)}{(1-h)}\right] . \tag{I.1}$$

Such a way of seeking a solution for $R^I_{up}(r)$ may destroy the orthogonality of $\{R^I_{np}(r)\}$and may therefore not justify out way of constructing $\phi^d(r,\theta,z)$. However, numerical results indicate that the orthogonality of $\{R^I_{np}(r)\}$ is still being maintained through the use of Galerkin's Scheme of solution and the representation in Eq. (I.1). Some of the numerical values of the integral

$$\int_h^1 e^{\int \frac{1+M_{\theta a}^2}{r} dr} R^I_{np} R^I_{nq} \, dr$$

are shown in TABLE I. It is seen that the value of the integral is nearly zero if p=q.

The set of functions used for the solution of Eqs. (5.71) and (5.113)

is

$$\left\{\cos\left[\frac{(i-1)\pi(r-h)}{(1-h)}\right]\right\}$$

too.

Finally, we would like to point out that in matching the upstream flow to the downstream one it is necessary to expand the radial dependence of the viscous losses within the blade row as a Fourier Bessel Series. This would have the implication that the viscous losses must have zero radial derivative at the hub and the tip. However, in some cases, the loss function used may not have zero radial derivative at the hub and the tip as requires, then one can always argue that the function may slightly be modified there so that its radial derivative vanishes there while leaving the function itself unchanged at all other points. Since this can be done in an infinite number of ways, consequently in such cases there would be some uncertianty as to the accuracy of the numerical results at the hub and the tip in such cases.

p \ q	1	2	3	4	5	6	7	8	9	10
1	3.76057	-0.00001	0.00001	-0.00001	0.00001	-0.00001	0.00001	-0.00000	0.00001	-0.00000
2	-0.00001	2.45615	0.00001	0.00002	0.00002	0.00001	0.00001	0.00001	0.00002	0.00002
3	0.00001	0.0001	1.55693	0.00002	0.00001	0.00002	0.00002	0.00002	0.00001	0.00002
4	-0.00001	0.00002	0.00002	1.31732	0.00001	0.00002	0.00002	0.00001	0.00001	-0.00000
5	0.00001	0.00002	0.00001	0.00001	1.26865	0.00002	0.00001	0.00002	0.00000	0.00002
6	-0.00001	0.00001	0.00002	0.00002	0.00002	1.24984	0.00001	0.00000	0.00002	0.00001
7	0.00001	0.00001	0.00002	0.00002	0.00001	0.00001	1.24037	0.00001	0.00001	0.00002
8	0.00000	0.00001	0.00002	0.00001	0.00002	0.00000	0.00001	1.23487	0.00002	0.00002
9	-0.00001	0.00002	0.00001	0.00001	0.00000	0.00002	0.00001	0.00002	1.23140	0.00001
10	-0.00000	0.00002	0.00002	-0.00000	0.00002	0.00001	0.00002	0.00002	0.00001	1.22903

TABLE I

Values of the integral $\int_h^1 e^{\int 1+M_{0a}^2/r\, dr} R_{np}^I R_{nq}^I dr$ where p and q each runs from 1 to 10.

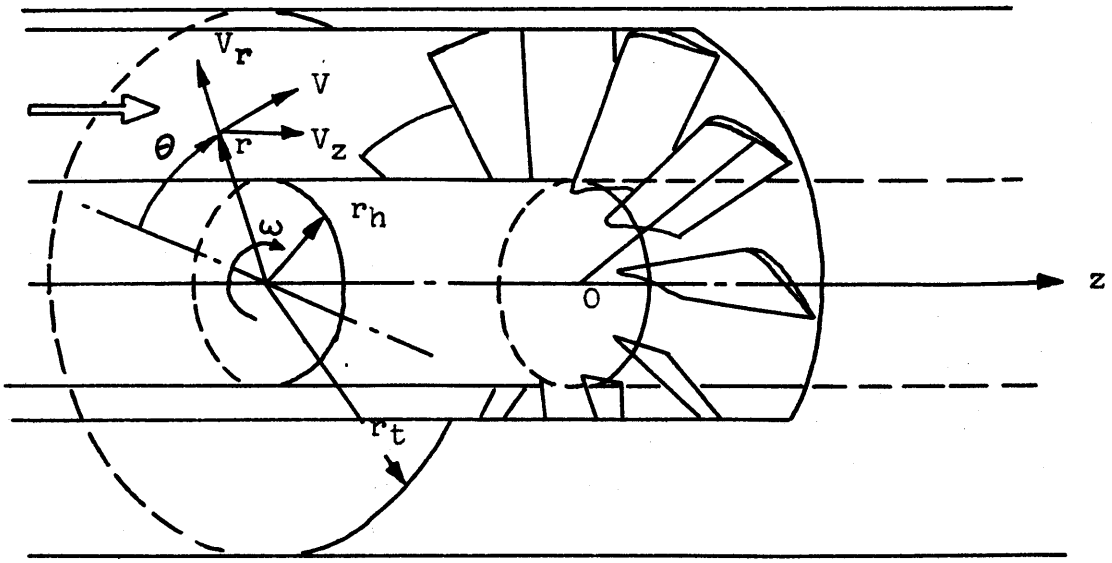

FIG. I.1a: CYLINDRICAL COORDINATE SYSTEM FOR THE FLOW THROUGH A BLADE ROW ENCASED IN AN INFINITE ANNULUS.

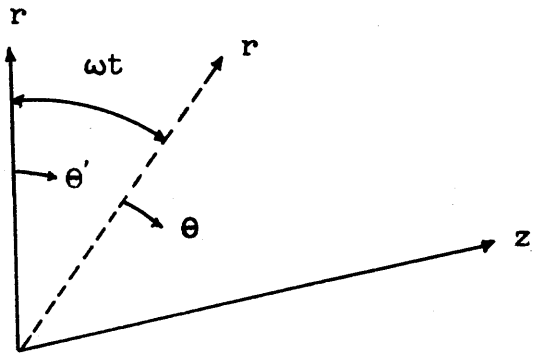

$$\theta' = \theta + \omega t$$

FIG. I.1b: THE ROTATING AND STATIONARY COORDINATE SYSTEMS.

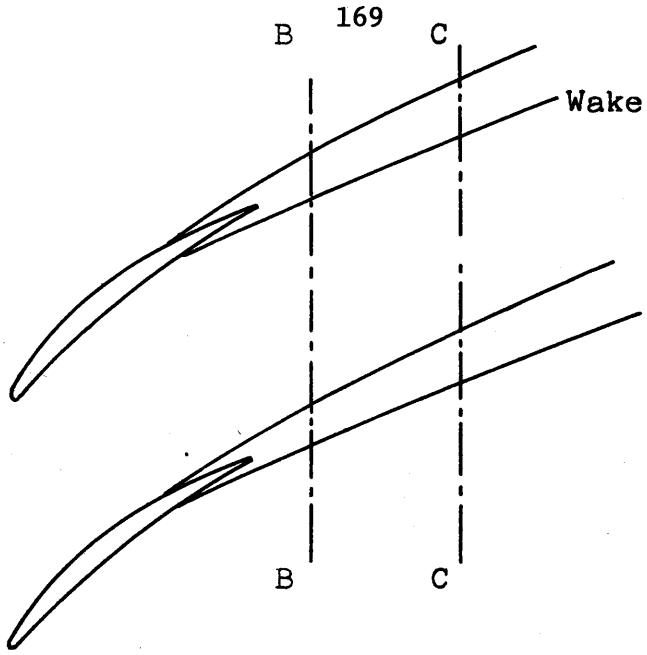

FIG. I.2a: SKETCH OF WAKES FORMED BY CASCADE ELEMENTS.

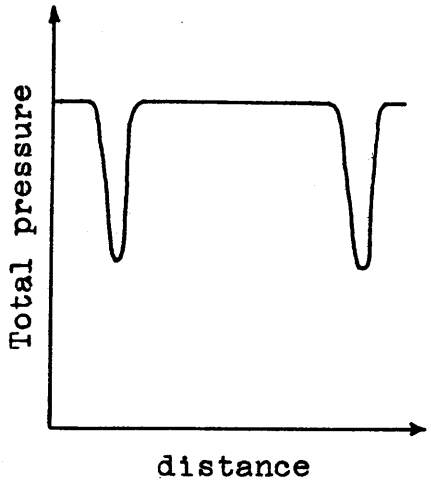

FIG. I.2b: TOTAL PRESSURE DISTRIBUTION ALONG B - B.

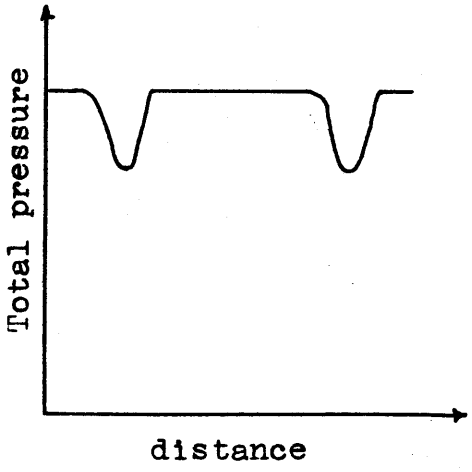

FIG. I.2c: TOTAL PRESSURE DISTRIBUTION ALONG C - C.

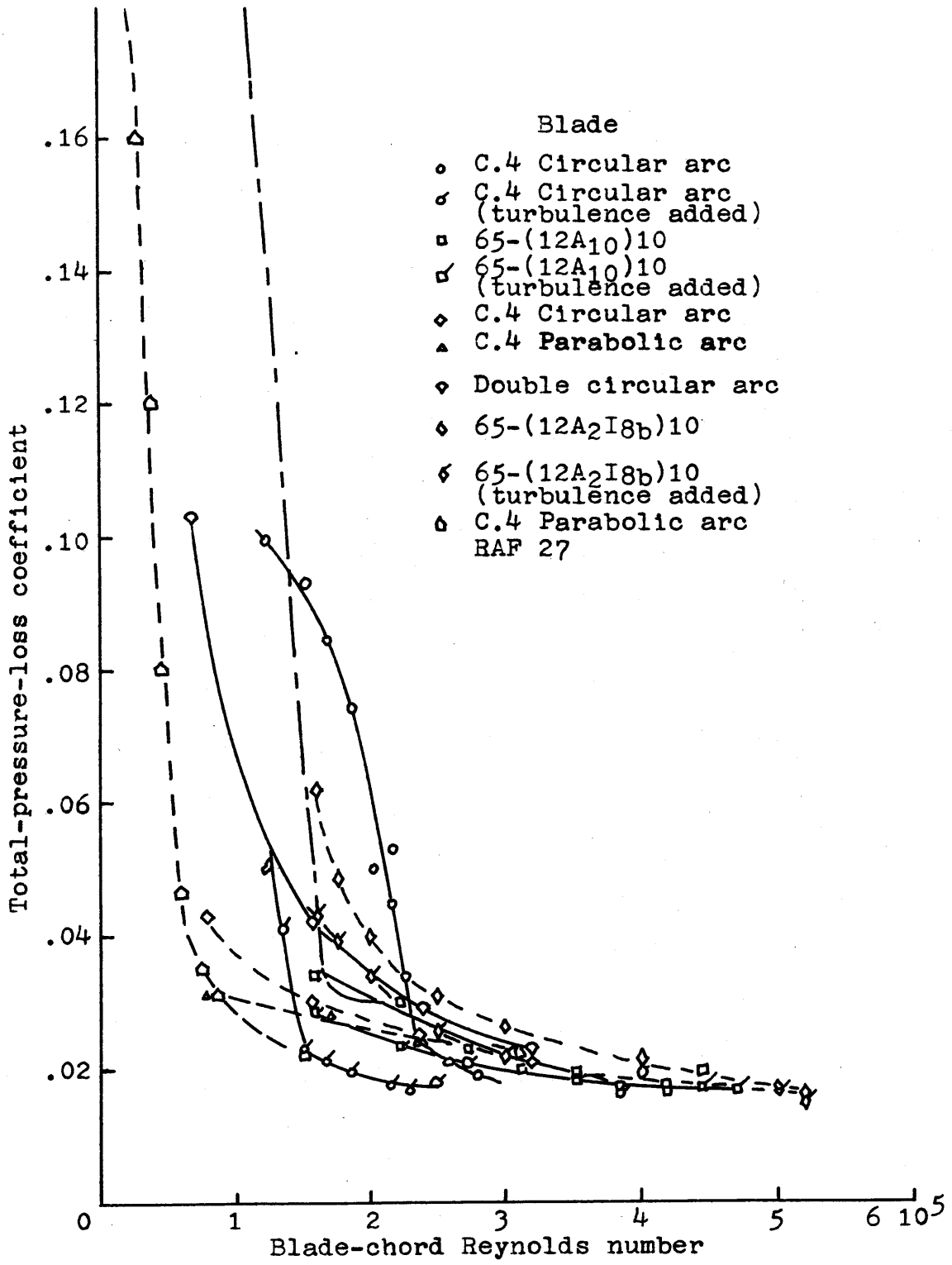

FIG. I.3: COMPOSITE PLOT OF LOSS COEFFICIENT AGAINST BLADE-CHORD REYNOLDS NUMBER IN REGION OF MINIMUM LOSS FOR TWO-DIMENSIONAL CASCADE BLADE SECTIONS AT LOW SPEED.

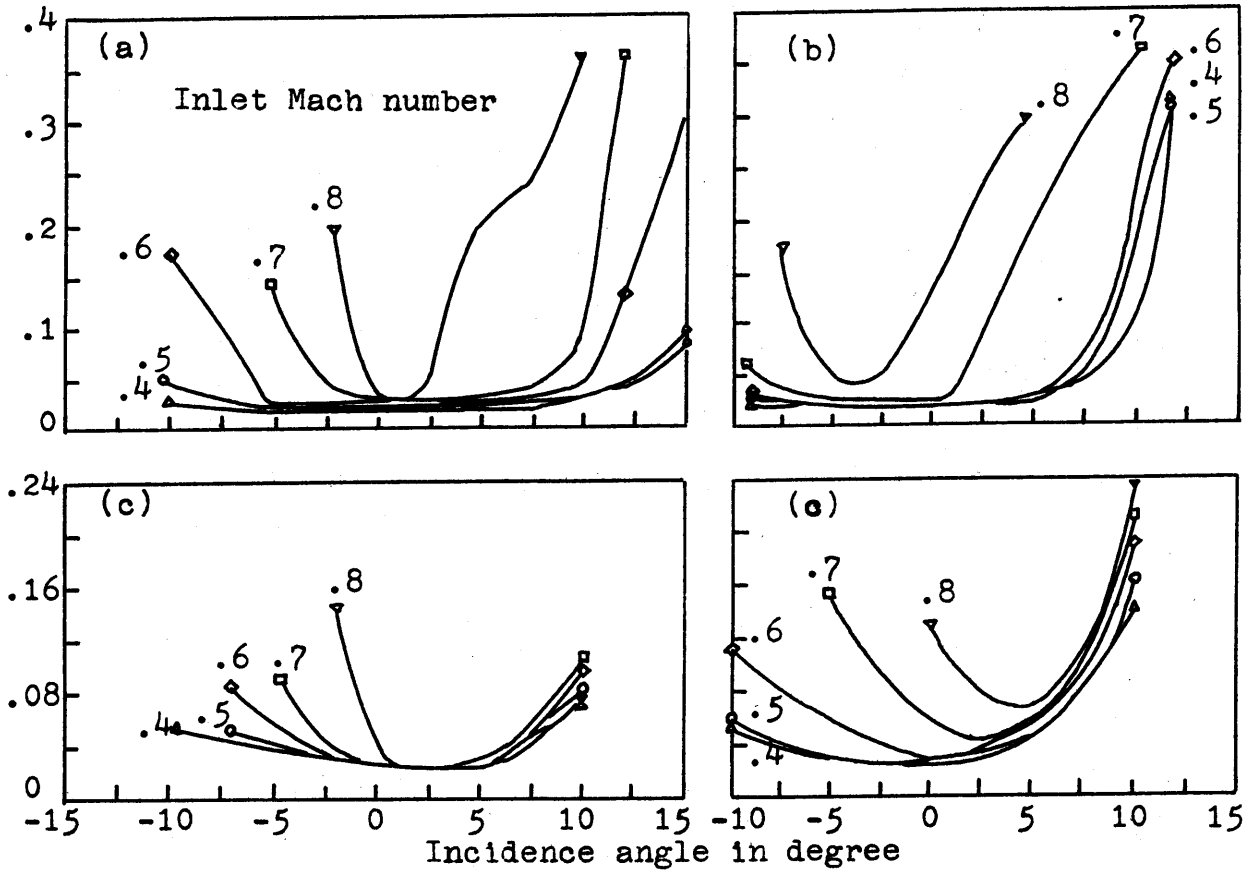

(a) C.4 Circular-arc blade. (b) C.4 Parabolic-arc blade.
(c) Double-circular-arc blade. (d) Sharp-nose blade.

FIG. I.4: EFFECT OF INLET MACH NUMBER ON LOSS CHARACTERISTICS OF CASCADE BLADE SECTIONS.

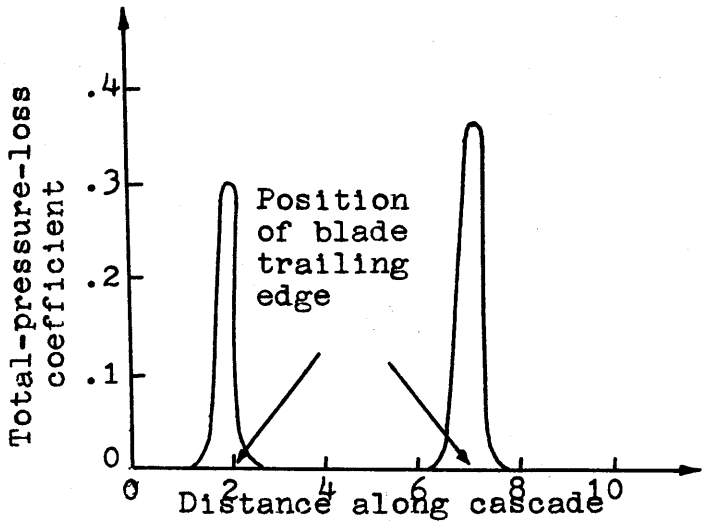

FIG. I.5: VARIATIONS OF TOTAL PRESSURE LOSS FOR CASCADE AT FIXED INCIDENCE.

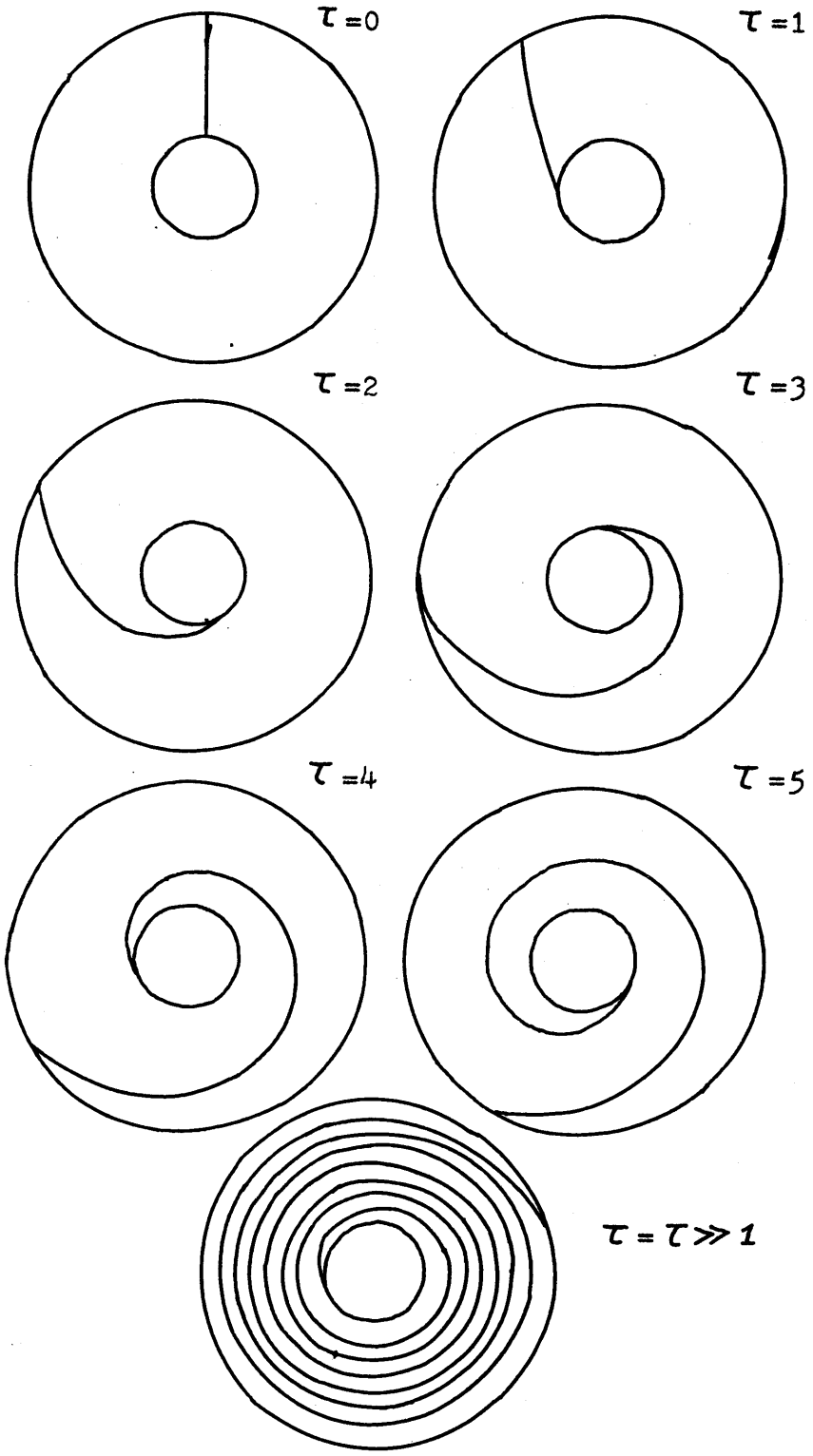

FIG. I.6: DOWNSTREAM DEVELOPMENT OF A RADIAL VORTEX FILAMENT SHOWN ON VARIOUS AXIAL PLANES.

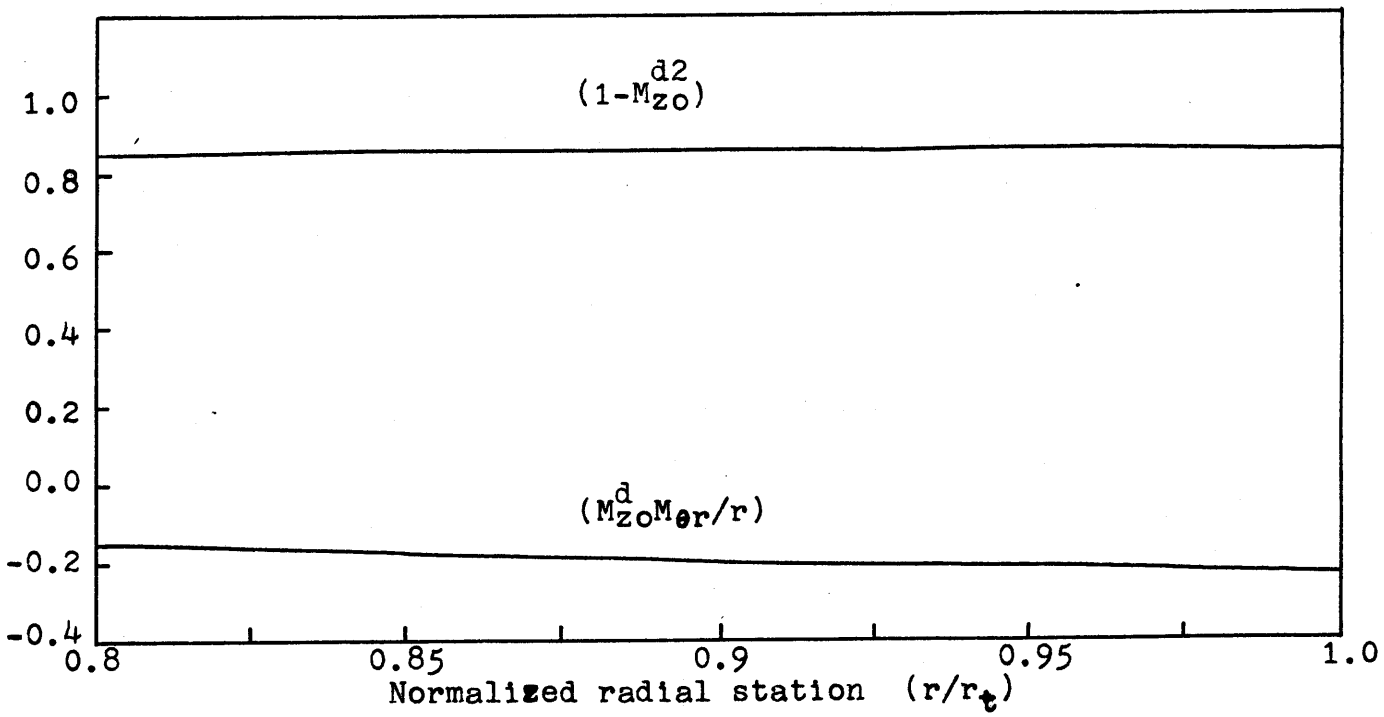

FIG. I.7: RADIAL VARIATION OF $(1-M_{zo}^{d2})$ AND $(M_{zo}^{d}M_{\theta r}/r)$ FOR A TRANSONIC ROTOR WITH AN INLET MACH NUMBER OF 0.65, A TIP MACH NUMBER OF 1.3 AND A PRESSURE RATIO OF 1.8.

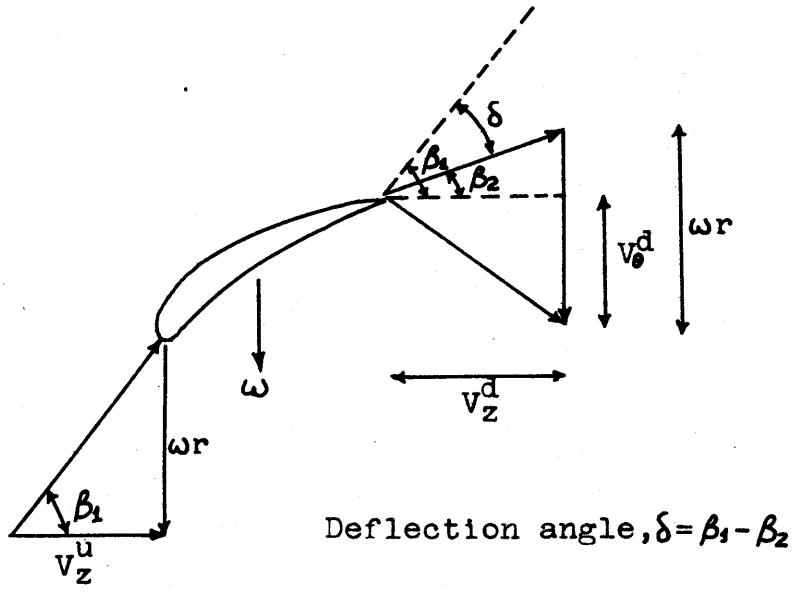

FIG. I.8: DEFINITION OF FLOW DEFLECTION ANGLE.

Full line - three-dimensional solution with wakes present.
Broken line - Actuator disc solution.

Inlet Mach number=0.65
Relative tip Mach number=1.3
Pressure ratio=1.8

Wake Model $\frac{s}{c_p}=0.025\, f\, \cos(B\theta)$

where $f=\frac{\gamma-1}{\gamma}\left[1-\left(1+\frac{\gamma-1}{2}M^2\right)^{\frac{\gamma}{\gamma-1}}\right]$

Number of blades B=40
Hub-to tip ratio=0.8

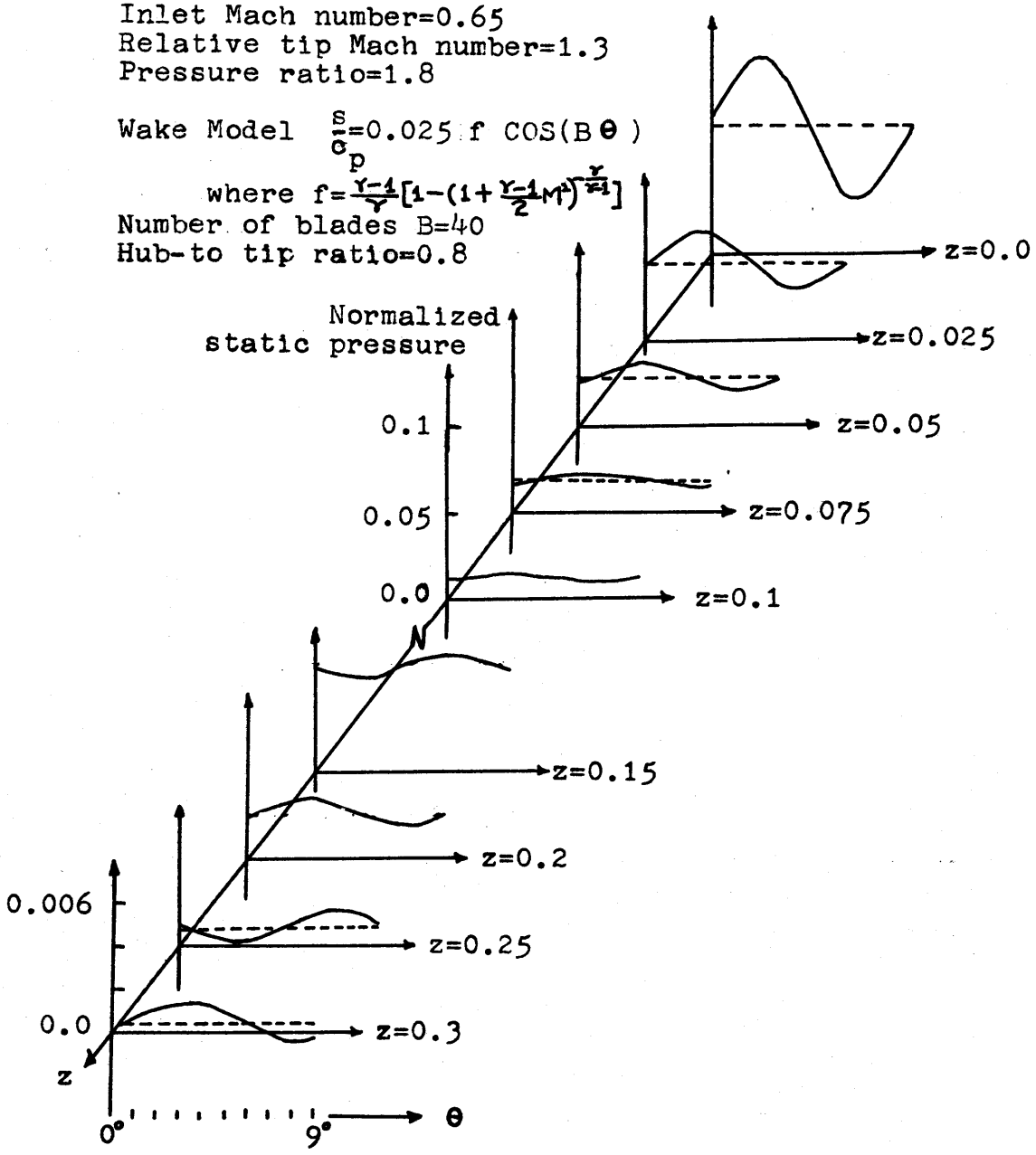

FIG. I.9: DOWNSTREAM BLADE-TO-BLADE VARIATION OF STATIC PRESSURE PERTURBATION AT $r/r_t=0.95$.

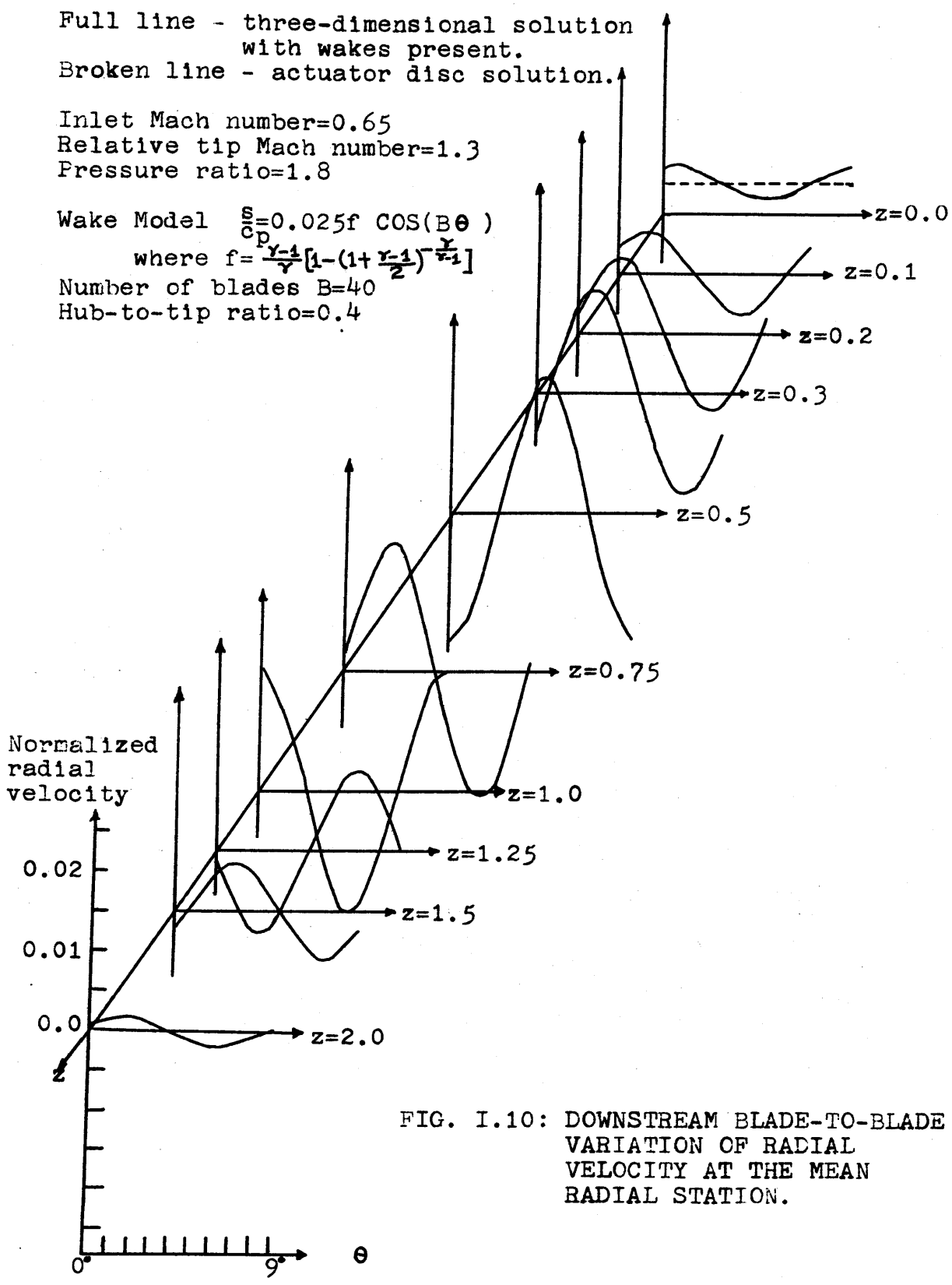

FIG. I.10: DOWNSTREAM BLADE-TO-BLADE VARIATION OF RADIAL VELOCITY AT THE MEAN RADIAL STATION.

Full line - three-dimensional solution
with wakes present.
Broken line - actuator disc solution.

Inlet Mach number=0.65
Relative tip Mach number=1.3
Pressure ratio=1.8

Wake Model $\frac{s}{c_p}$ =0.025f COS(B θ)

where $f=\frac{\gamma-1}{\gamma}\left[1-\left(1+\frac{\gamma-1}{2}M^2\right)^{-\frac{\gamma}{\gamma-1}}\right]$

Number of blades B=40
Hub-to-tip ratio=0.8

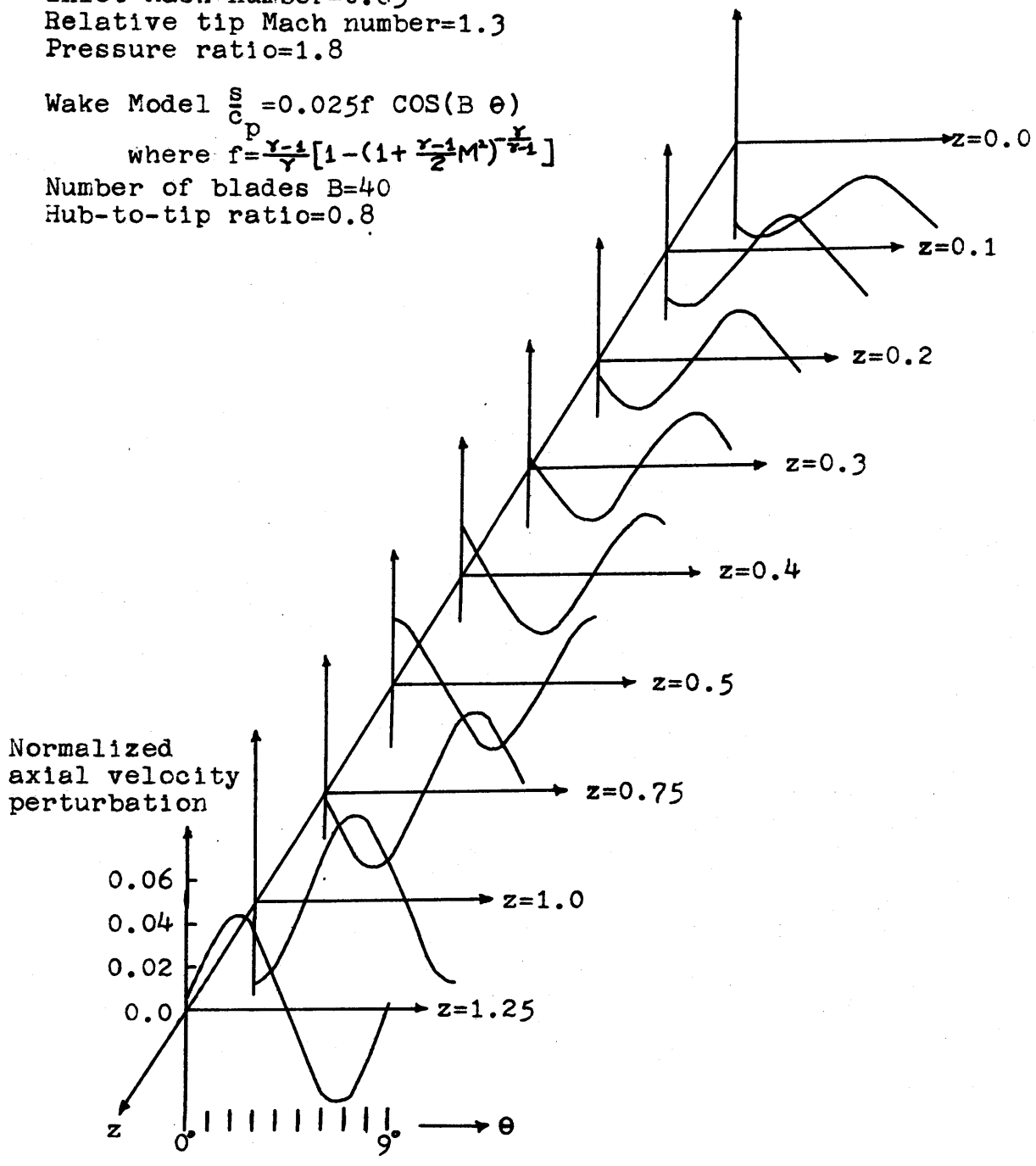

FIG. I.11: DOWNSTREAM BLADE-TO-BLADE VARIATION OF AXIAL VELOCITY PERTURBATION AT THE MEAN RADIAL STATION.

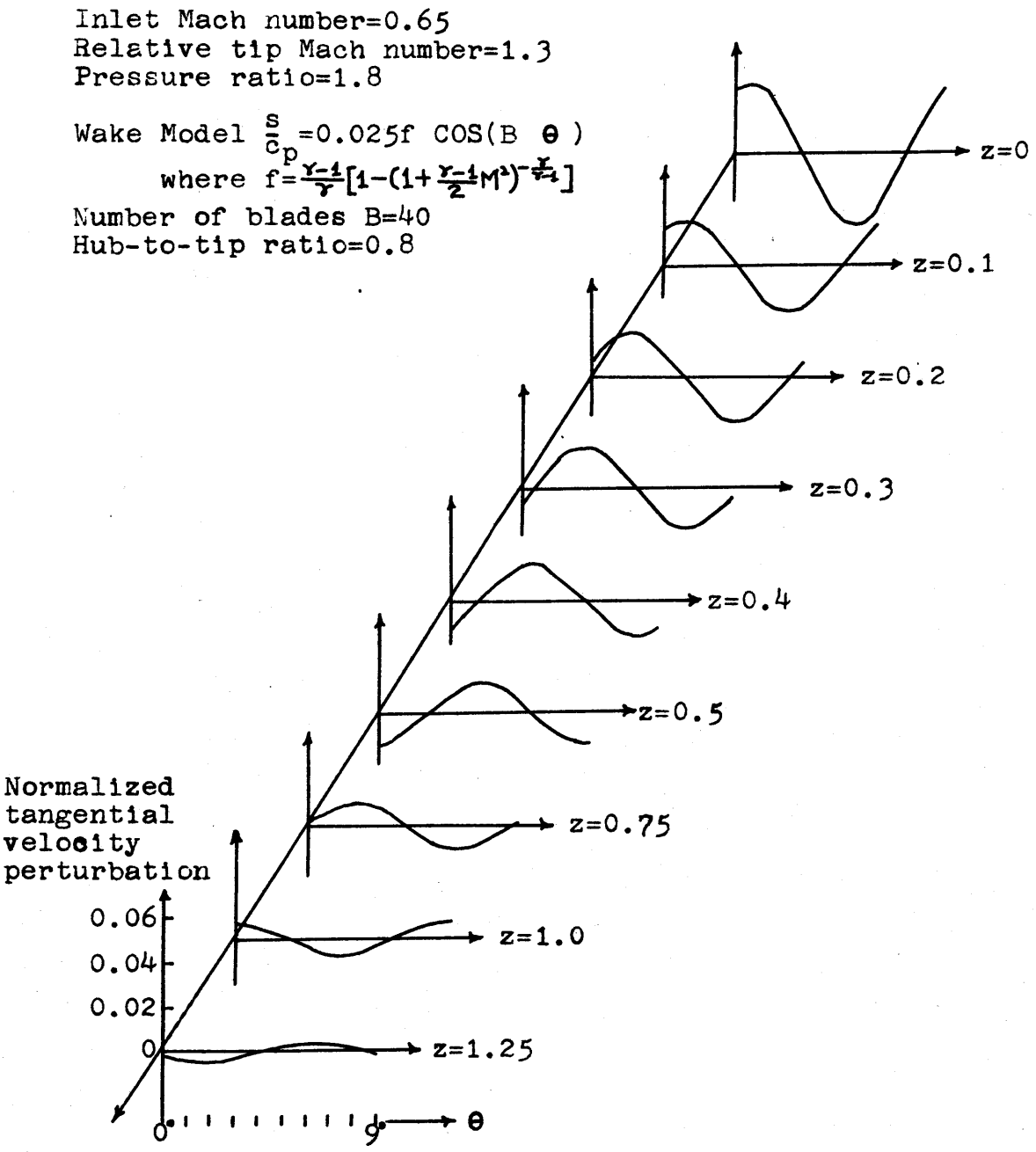

FIG. I.12: DOWNSTREAM BLADE-TO-BLADE VARIATION OF TANGENTIAL VELOCITY PERTURBATION.

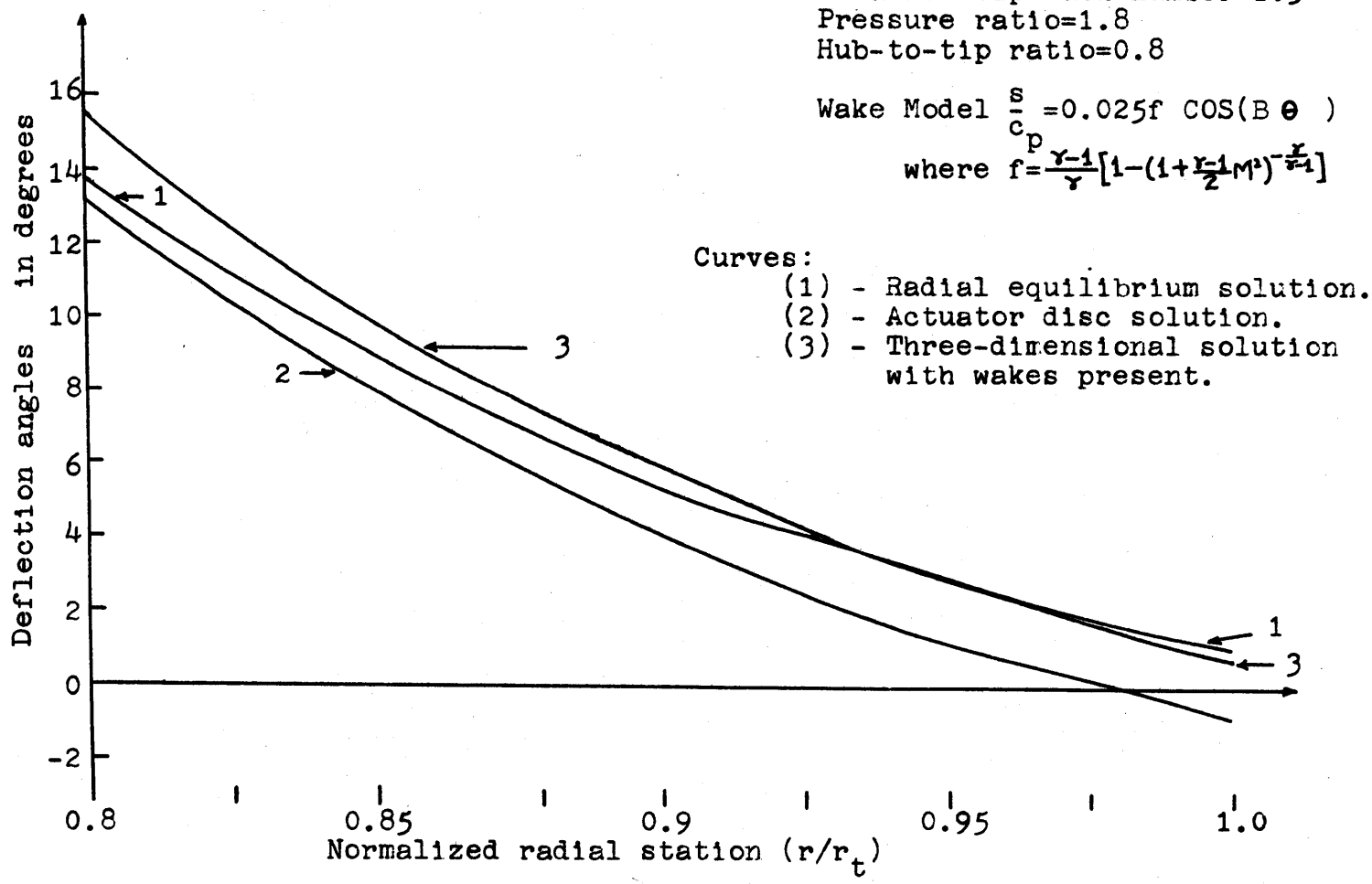

FIG. I.13: RADIAL VARIATION OF FLOW DEFLECTION ANGLES.

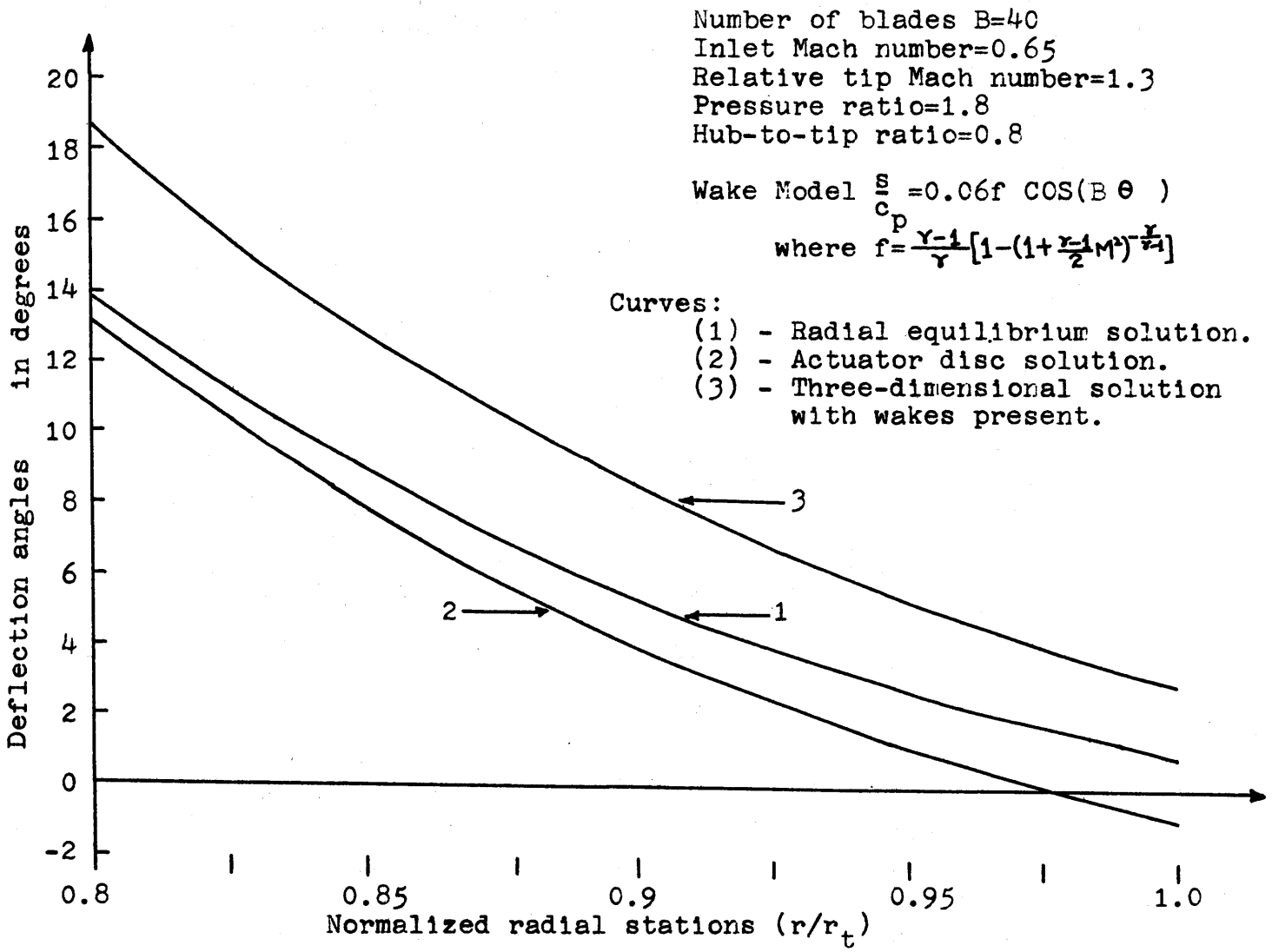

FIG. I.14: RADIAL VARIATION OF FLOW DEFLECTION ANGLES.

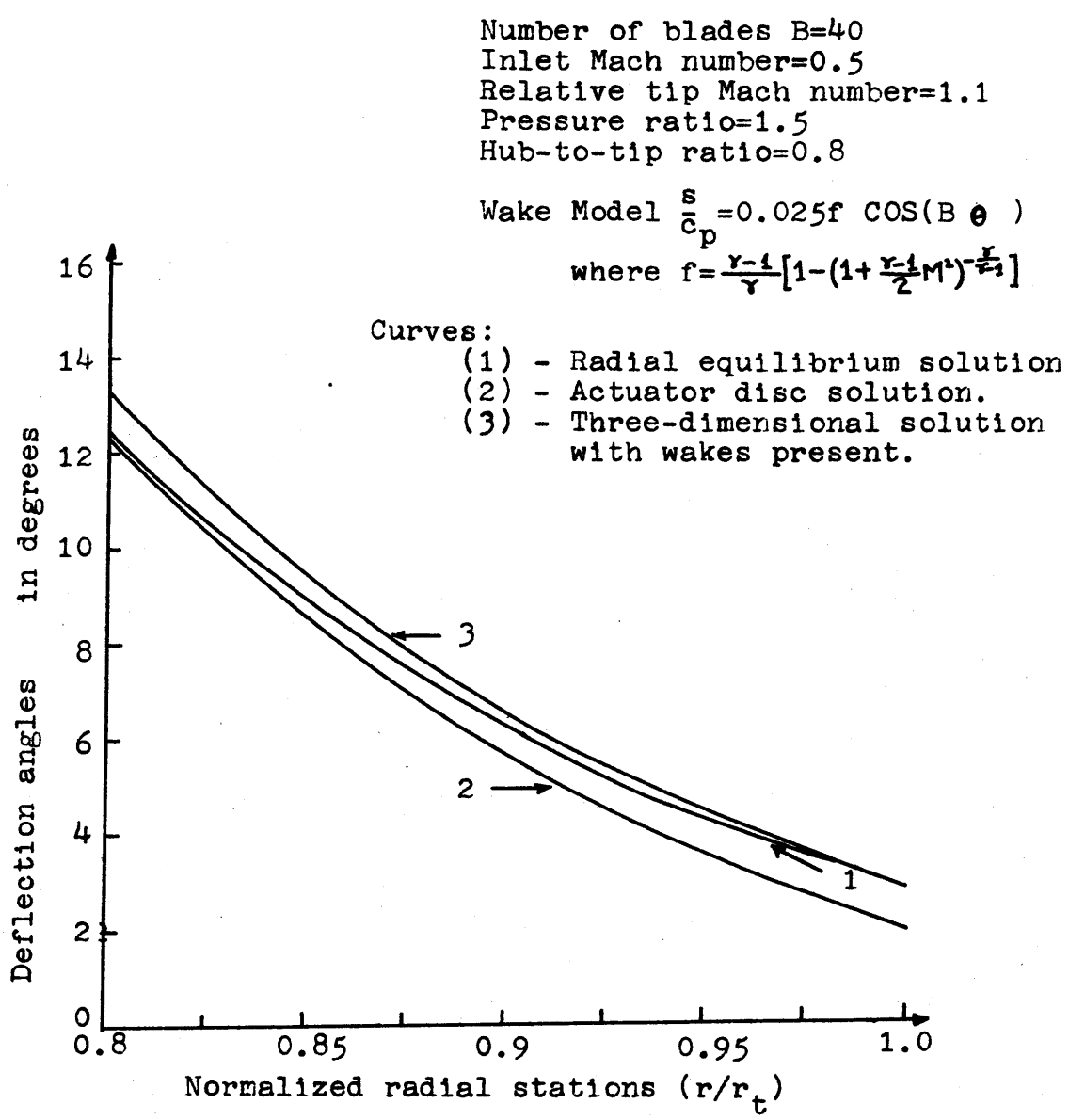

FIG. I.15: RADIAL VARIATION OF FLOW DEFLECTION ANGLES.

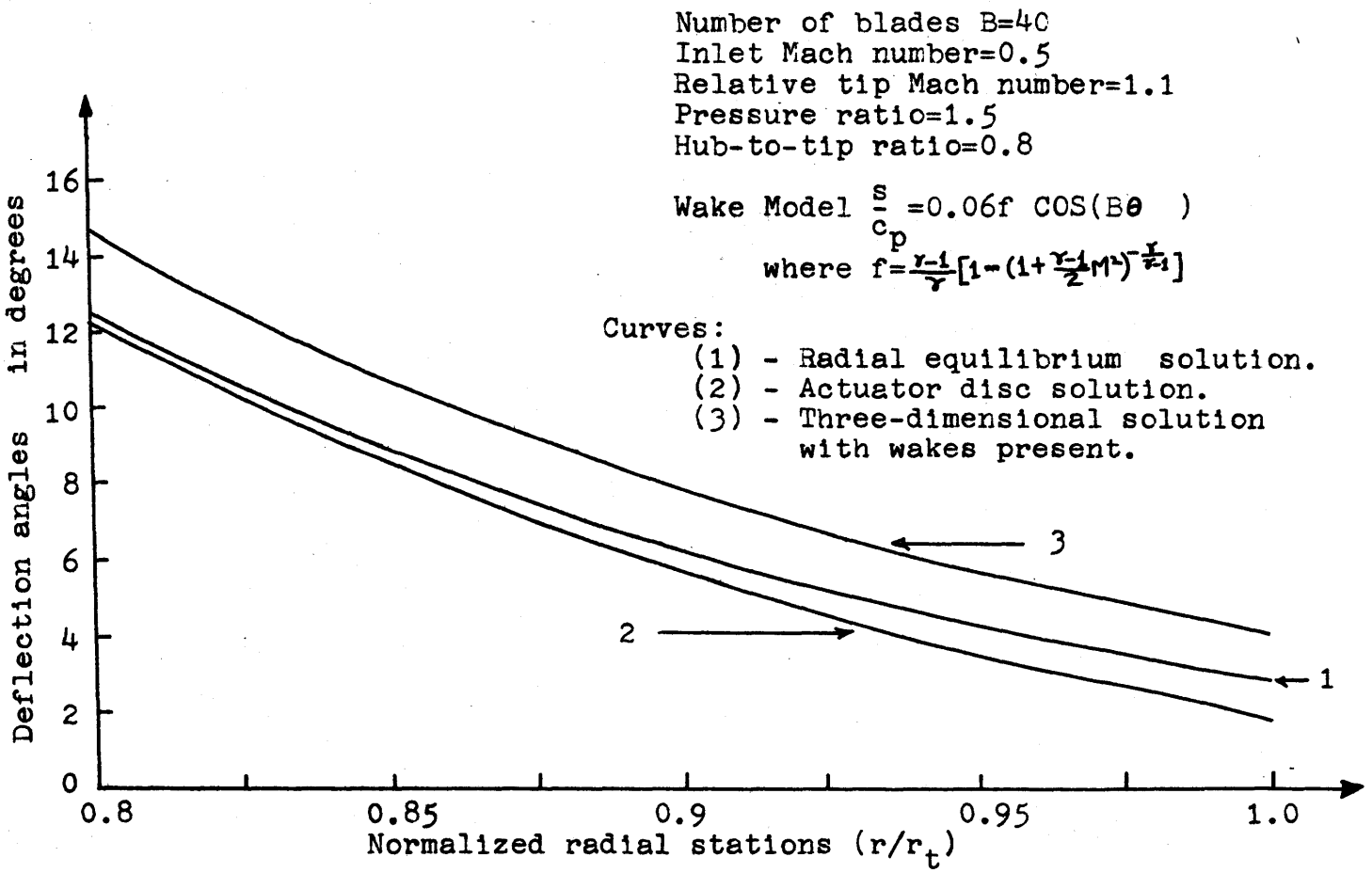

FIG. I.16: RADIAL VARIATION OF FLOW DEFLECTION ANGLES.

REFERENCES

1. Marble, F. E., "Three-Dimensional Flow in Turbomachines," High Speed Aerodynamics and Jet Propulsion, 10, Sec. C, Princeton, 1964.

2. Hawthorne, W.R., "Rotational Flow Through Cascades," Parts I & II, Philosophical Transactions of the Royal Society, June, 1954.

3. Hawthorne, W.R., Novak, R.A., "The Aerodynamics of Turbomachinery," Annual Review of Fluid Mechanics, Vol. 1, 1969.

4. Hawthorne, W.R., "On the Theory of Shear Flow," MIT GTL Report #88, MIT, 1966.

5. Horlock, J.H., and B. Lakshminarayana, "Secondary Flow," Annual Review of Fluid Mechanics, 5, 247, 1973.

6. Wu, C.H., "A General Theory of Three-Dimensional Flow in Subsonic and Supersonic Turbomachines of Axial, Radial and Mixed Flow Types," NACA TN 2604, 1952.

7. McCune, J.E., "A Three-Dimensional Theory of Axial Compressor Blade Rows--Application in Subsonic and Supersonic Flows," J. of Aerospace Sci., 25, 9, Sept. 1958.

8. McCune, J.E., "The Transonic Fluid of an Axial Compressor Blade Row," J. of Aerospace Sci, 25, 10, Oct. 1958.

9. Davidson, R.E., "Linearized Potential Theory of Propeller Induction In A Compressible Flow," NACA TN 2983, 1953.

10. Okuroumu, O., and McCune, J.E., "Three-Dimensional Vortex Theory of Axial Compressor Blade Rows at Subsonic and Transonic Speeds," AIAA J., 8, 7, July 1970.

11. Okuroumu, O., and McCune, J.E., "The Lifting Surface Theory of Axial Compressor Blade Rows, Part I - Subsonic Compressor," AIAA J., 12, 10, 1974.

12. Okuroumu, O., and McCune, J.E., "The Lifting Surface Theory of Axial Compressor Blade Rows, Part II - Transonic Compressor," AIAA J., 12,10 1974.

13. McCune, J.E., and Dharwadkar, S.P., "Lifting Line Theory for Subsonic Axial Compressor Rotors," MIT GTL Report #110, 1972.

14. Falcão, A.F., "Three-Dimensional Flow Analysis in Axial Turbomachines," Ph.D. Thesis, Cambridge, University, 1970.

15. Namba, M., "Lifting Surface Theory ofr a Rotating Subsonic or Transonic Blade Row," ARC R&M, #3740, 1974.

16. McCune, J.E., and Hawthorne, W.R., "The Effects of Trailing Vorticity on the Flow Through Highly-Loaded Cascades," J. of Fluid Mech., 74, Part 4, April 1976.

17. Morton, K.B., "Three-Dimensional Compressible Flow Through Highly Loaded Rectilinear Cascasdes," S.M. Thesis, Dept. of Aero & Astro, 1974.

18. Cheng, W.K., "A Three-Dimensional Theory of the Velocity Induced by a Heavily-Loaded Annular Cascade of Blades," M.S.Thesis, Dept. of Aero & Astro, MIT, June 1975.

19. Adebayo, A.O. and McCune, J.E., "Three-Dimensional Beltrami Flow in Turbomachinery with Strong Arbitrary Swirl," MIT GTL Report #132, 1977.

20. Cheng, W.K., "Uniform Inlet Three-Dimensional Transonic Beltrami Flow Through a Ducted Fan," MIT GTL Report #130, 1977.

21. Kerrebrock, J.L., "Small Disturbances in Turbomachine Annuli With Swirl," GTL Report #125, MIT, 1975. Also AIAA J, 15, 6, June 1977.

22. Lamb, H., "Hydrodynamics," Sixth Ed., Cambridge, Univ. Press, 1932.

23. Darwin, C., "Note on Hydrodynamics," Proc. Cambridge Phil. Soc., 49 342-254, 1953.

24. Lighthill, M.J., "Drift," J. Fluid Mech., 1, 31-53 (1956); note also "Corregenda to Drift", J. Fluid. Mech., 2, 311-2 (1957).

25. Hawthorne, W.R., "Engineering Aspects," Chapter 1, Research Frontiers in Fluid Dynamics, R.T. Seeger and G. Temple Eds., Interscience, NY, 1965.

26. McCune, J.E., "Three-Dimensional Flow in Highly-Loaded Axial Turbomachines," M.S. No. 56180(22S2), ZAMP, Nov. 1977.

27. Johnson, I., and Bullock, R., Eds., "Aerodynamic Design of Axial Flow Compressors," NASA SP-36, NASA 1965.

28. Sears, W.R., "Some Recent Developments in Airfoil Theory," J. of Aero. Sci., 23, 5, May 1956.

29. McCune, J.E., "Three-Dimensional Inviscid Flow Through a Highly-Loaded Transonic Compressor Rotor," Proc. Workshop of Transonic Flow Through Turbomachinery, T.C. Adamson, Ed., 1977.

30. Munk, M., and Prin, R.C., "On the Multiplicity of Steady Gas Flows Having the Same Streamline Pattern," Proc. Nat. Acad. Sci., U.S., 33, 5, 1947.

31. Nemenyi and R. Prim, "Some Geometric Properties of Plane Gas Flow,"

J. of Math & Phys., 27, 1948.

32. Yih, C.S., "Dynamics of Non-Homogeneous Fluids," Macmillan, NY, 1965.

33. Hawthorne, W.R., Ringrose, J., "Actuator Disc Theory of the Compressible Flow in Free Vortex Turbomachinery," Proc. Inst. Mech. Engrs. Feb. 1963.

34. Chen, L.T., and McCune, J.E., "Comparison of Three-Dimensional Quasi-Linear Large Swirl Theory with Measured Outflow from a High Work Compressor Rotor," MIT GTL Report #128.

35. Epstein, A.H., "Quantitative Density Visualization in a Transonic Compressor Rotor," Ph.D. Thesis, MIT, Sept. 1975.

36. Thompkins, Jr., W.T., "An Experimental and Computational Study of the Flow in a Transonic Compressor Rotor," Ph.D. Thesis, MIT June 1976.

37. Bellman, D.R., & D.L. Hughes, "The Flight Investigation of Pressure Phenomena in the Air Intake of an F-11A Airplane, AIAA Paper 69-488, presented at the Fifth Propulsion Joint Specialist Conf. Colorado, 9-13 June, 1969.

38. Burcham,F.W., Jr., and D.R. Bellman, "A Flight Investigation of Steady State and Dynamic Pressure Phenomena in the Air Inlets of Supersonic Aircrafts," Paper #24, AGARD, Propulsion and Energetics Panel 38th Meeting, Sandefjord, Norway, Sept. 1971.

39. Valentine, H.H., and W.T. Beale, "Experimental Investigation of Distortion Removal Characteristics of Several Free Wheeling Fans," NACA RM 57 112, 1958.

40. Walker, C.L., J.N. Sivo, and E.T. Jansen, "Effect of Unequal Airflow Distribution From Twin Inlet Ducts on Performance of an Axial-Flow Turbojet Engine," NACA RM E54E13, 1954.

41. Wenzel, L.M., Experimental Investigation of the Effects of Pulse Pressure Distortions Imposed on the Inlet of a Turbofan Engine," NASA TMX-1928, Nov. 1969.

42. Wallner, L.E., Conrad, E.W., and Prince W.R., "Effect of Uneven Air-Flow Distribution to the Twin Inlets of an Axial Flow Turbojet Engine," NACA RM E 52 K 06, 1953.

43. Turner, R.C., Ritchie, J., and Moss G.E., "The Effect of Inlet Circumferential Maldistribution on Axial Compressor Stage," ARC R&M 3066, 1957.

44. Harry, D.P, and Lubick, R.J., "Inlet Air Distortion Effects on Stall, Surge, and Acceleration Margin of a Turbojet Engine Equipped with Variable Compessor Inlet Guide Vanes," NACA RM E54K26, 1955.

45. Whitehead, D.S., Vibration of Cascade Blades Treated by Actuator Disc Methods," Proc. I. Mech. E., 173, 21, 255.

46. Ehrich, F., "Circumferential Inlet Distortion in Axial Flow Turbomachinery, " Jnl. Aero. Soc., 24, 6, 413-17, June 1957.

47. Katz, R., "Performance of Axial Compressors with Asymmetric Inlet Flows," Daniel and Guggenheim Jet Propulsion Centre, Cal. Inst. of Tech, Report, June 1958 (AFOSR-TR-58-59 AD 162-112).

48. Rannie, W.D., and Marble, F.E., "Unsteady Flows in Axial Turbomachines," ONERA, Comptes Rendus des Journes Internationales de Sciences Aeronautiques, Part 2, pp. 1-21, Paris, May 27-29, 1957. Also Daniel and Florence Guggenheim Jet Propulsion Centre, Cal. Inst. Tech., USA Report, May 1957.

49. Doyle, M.D.C., Dixon, S.L., and Horlock, J.H., "Circumferential Asymmetry in Axial Compressors," J. R. Aero. Sci., 70, 956-957, Oct. 1966.

50. Hsuan Yeh, "An Actuator Disc Analysis of Inlet Distortion and Rotating Stall in Axial Flow Turbomachines," J. Aero/Space Sci., 26, 11, 739-753, Nov. 1959.

51. Krzywoblocki, M.Z., "Compressibility Effects in Circumferential Inlet Distortion in Axial Compressors," Ost. Ing-Arch: Pt. I: 13, 4, 214 (1959-1960); Pt. II., 14, 2, 79.

52. Dixon, S.L., "Rotating Stall in Compressor Blade Rows of Low Hub Tip Ratio," Ph.D. Thesis, Liverpool University, 1968.

53. Dunham, J., "Non-Axisymmetric Flows in Axial Compressors," Ph.D. Thesis, Cambridge Univ. Eng. Dept. 1962.

54. Dunham, J., "Non-Axisymmetric Flows in Axial Compressors," Mech. Eng. Sci., Monograph #3, 1965.

55. Dunham, J., "Observation of Stall Cells in a Single Stage Compressor," Aero Res. Council, London, CP 589, 1962.

56. Dunham, J., "Comment on an Acutator Disc Analysis of Inlet Distortion and Rotating Stall in Axial- Flow Turbomachines," Jnl. Aero. Sci., 29 362, 1962.

57. Greitzer, E.M., and Strand, T., "Asymmetric Swirling Flows in Turbomachine Annuli," ASME meeting, London, 1978.

58. Sears, W.R, "On Asymmetric Flow in an Axial Flow Compressor Stage," J. Appl. Mech., March 1953.

59. Hawthorne, W.R., McCune, J.E., Mitchell, N.A., and Tan, C.S., "Non-Axisymetric Flow Through an Annular Actuator Disc; Inlet Distortion

Problem," prepared for ASME meeting, London, April 1978.

60. Rizvi, S.A.H., "Inlet Maldistribution Effects in Axial-Compressor Rotors," Ph.D. Dissertation, Cambridge University, 1977.

61. Kantorovich, L.V., and V.I. Krylov, "Approximate Methods of Higher Analysis," Interscience Publishers, Inc., 1958.